5-21-2005

Environmental Remediation with Fenton Reagents and Synthesis of a Novel Halide Fluorescence Sensor

Guoxiang Xu
University of New Orleans

ENVIRONMENTAL REMEDIATION WITH FENTON REAGENTS AND SYNTHESIS OF A NOVEL HALIDE FLUORESCENCE SENSOR

A Dissertation

Submitted to the Graduate Faculty of the
University of New Orleans
in partial fulfillment of the
requirements for the degree of

Doctor of Philosophy
in
The Department of Chemistry

by

Guoxiang Xu

B.S. Nankai University, 1997
M.S. University of New Orleans, 2001

May 2004

To my father's father, who always reminds me of

him and myself

ACKNOWLEDGEMENTS

The author is fully indebted to Professor Matthew A. Tarr for his years-long patient guidance, encouragement and support throughout research projects as well as his help in the preparation of this dissertation. The author also thanks his coworkers, Weixi Zheng, Chanel Fortier and Anindya Pradhan for their daily assistance and collaboration for the past years.

The author also fully acknowledges Professor Ronald F. Evilia, Zeev Rosenzweig, Guijun Wang and John B. Wiley for serving on the advisory committee and valuable suggestions. Acknowledgment also goes to Dr. Yan Cai and Professor Richard B. Cole for their collaboration and assistance on Mass Spectrometry experiments. In addition, gratefulness goes to Professors Bruce C. Gibb, Scott Whittenburg, Zeev Rosenzweig, Mark L. Trudell and Guijun Wang for their help in related experiments and/or discussion. The author also thanks Dr. XueHe Li and Dr. YongFen Chen for their helpful discussion and Corinne Gibb for help in NMR experiments.

Table of Contents

List of Tables

List of Figures

ABSTRACT

Suwannee River fulvic acid (SRFA) and humic acid (SRHA) were used as dissolved organic matter (DOM) and were applied to probe the effect of DOM. Addition of DOM resulted in decreased first order rate constants for all species selected. The inhibition became more significant as the hydrophobicity of the species increased. The decrease could not be simply attributed to the binding of hydrophobic species to DOM. This can be explained by the physical isolation of iron (II), which binds to hydrophilic sites of DOM and is the hydroxyl radical generation site, from hydrophobic pollutants which bind to hydrophobic sites of DOM.

Accordingly, species which could compete against this physical isolation by DOM and bring iron (II) closer to target species could increase the degradation rates. This was observed with application of carboxymethyl-ß-cyclodextrin (CMßCD). Effects from concentration, structure of the target species and acidity etc., were studied. The increased degradation rates were observed even in the presence of DOM. Studies on ternary complexes of hydrophobic pollutants, iron (II) and CMßCD were carried with ES-MS, UV and Fluorescence experiments and further calix[6]arene derivatives. Along with the fact that CMßCD can increase the solubility of hydrophobic species and remove them from contaminated sites, this indicates a potential application to in-situ degradation systems. Initial two-phase studies were carried out with quartz sand

deposited with polycholobiphenyl (PCBs) and polycyclic aromatic hydrocarbons (PAHs). Successful degradations were observed with PCBs but not PAHs. The difference is attributed to the slow equilibrium of sorbed PAHs with dissolved CMßCD and the higher PAH loading used in these experiments.

A halide sensor-molecule (1,8-diphenylureaylnaphthalene), which performs with increasing fluorescence in the presence of fluoride and decreasing fluorescence with all other halides, was synthesized and reported. Studies using NMR and computer modeling with SPARTAN were carried out to compare the sensor-molecule with an analog, 2,3-diphenylureaylnaphthalene. Both studies indicated that only fluoride can be accommodated in the space between the urea group protons to form a strong interaction. The sensor-molecule could to lead to improved sensors that overcome limitations with current fluorescence-quenching based anion sensors.

Chapter I Introduction

Chemical, pharmaceutical and petroleum industries generate waste products and contaminated soil at hundreds of thousands of application sites. Many of the pollutants concern people since they have been shown to be toxic and carcinogenic and could have harmful effects to man and other living organisms.

While there are quite a few treatments, many have significant limitations in practice. For example, photo-degradation/sono-degradation is limited since light/ultrasound can only penetrate a limited depth into real water and soil systems due to energy loss by absorption or blockage. Land disposal threatens water supplies and incineration is costly because of the large volume of water accompanying the waste and the high transport costs. Meanwhile incineration may result in the formation of polychlorinated dibenzo-p-dioxins (PCDDs) and polychlorinated dibenzofurans (PCDFs)[1], which are related to a variety of diseases and birth defects. Though biological treatment has been developed and has shown significant potential, bioremediation methods have a limited ability for treating components that are biorefractory or toxic to microorganisms[2]. Another major limitation of biological treatment is that, although many biological treatments are environmentally benign, biological treatment requires a relatively long time period; typically much longer than chemical treatment methods. In many circumstances, pollution remediation requires rapid results, for example, water contamination in civil residential areas. Consequently,

chemical degradation methods pose a viable option for such treatment. Among chemical methods, Fenton chemistry shows good potential for pollutant remediation.

Fenton Chemistry

In Fenton chemistry, iron works as a catalyst with hydrogen peroxide to generate hydroxyl radical. Hydroxyl radical is one of the strongest oxidants known, second only to fluorine (HO?, E°=-2.8V vs. Fluorine, E°=-3.0V), and reacts rapidly with a wide spectrum of compounds. It is the key oxidant in the degradation of pollutants by ultraviolet/ozone treatment, ultraviolet/peroxide treatment, titanium dioxide photo-catalysis and sonolysis. The highly reactive and nonselective nature of the radical makes it useful in degradation of a wide variety of species[3]. Another advantage of Fenton chemistry is that it is in aqueous system and does not have the penetration depth limitations of optical/sonic treatments.

While the mechanism of Fenton Chemistry is still not well agreed on, it is widely regarded that the reaction between Fe^{2+} and H_2O_2 generates an intermediate, hydroxyl radical, capable of oxidizing other species. In the process, Fe^{2+} first cycles to Fe^{3+} and then back to Fe^{2+} and so on in the catalytic cycle[4]. The first step in this cycle is given in reaction 1-1.

$$H_2O_2 + Fe^{2+} \rightarrow Fe^{3+} + HO^- + HO\cdot \qquad (1\text{-}1)$$

Ferric species are also capable of producing radicals in the Haber-Weiss process[5]

$$H_2O_2 + Fe^{3+} \rightarrow Fe^{2+} + H^+ + HO_2\cdot \qquad (1\text{-}2)$$

$$HO_2\cdot + Fe^{2+} \rightarrow Fe^{3+} + HO_2^- \qquad (1\text{-}3)$$

$$H_2O_2 + HO^{\cdot} \rightarrow H_2O + HO_2^{\cdot} \quad (1\text{-}4)$$

$$Fe^{3+} + HO_2^{\cdot} \rightarrow Fe^{2+} + H^+ + O_2 \quad (1\text{-}5)$$

Although there are many other possible process paths, Tomita, M. et al. provided strong experimental evidence supporting that the hydroxyl radical is the primary oxidizing species formed by Fe (II)-catalyzed decomposition of H_2O_2. [6] However, iron(II) could precipitate with pH values greater than 4.3 [7].

Many papers reported the degradation of a number of contaminants using Fenton reagents. Reactions were pH sensitive and acid conditions were normally applied. The optimum pH, according to Pignatello's paper, is about 2.8 for degradation of several species, and higher pH results in precipitation of iron(III) as hydrous oxyhydroxides, $Fe_2O_3 \cdot H_2O$[8]. Vella and Munder used Fe(II)/H_2O_2 for the degradation of phenolic compounds in water at pH equal to 4. Conditions close to neutral were only achieved with chelating reagents to prevent precipitation[9]. The iron chelates were found to be degraded at a lower rate. This indicates that the added organic species will not persist in the treated system, and close to neutral pH system could be applied.

Fenton reagents have also been used in degradations of perchloroethylene (PCE) and polychlorinated biphenyls (PCBs) adsorbed on sand[10]. These species were unable to be biodegraded due to their toxicity to microorganisms. The treatment required pH equal 3 and resulted in significant decomposition of PCE. PCB treatment resulted in formation of partially chlorinated degradation products.

Some studies involving soil/water systems have relied on naturally existing iron in soils to react with hydrogen peroxide added [11,12]**.** However, the pollutants and particles absorbed to the surface of soil could impede degradation. Due to the

difficulty in oxidizing at the liquid-solid boundary, higher than stoichiometric amounts of hydrogen peroxide were required to achieve complete degradation of the pollutants in the sites. The efficiency of the hydroxyl radical depends on a number of factors, including the activity of iron (II), the distance between the generation site and the target pollutant and the reactivity of the pollutant itself. Phosphorus-containing species were reported to inhibit hydroxyl radical production[13]. But later in 1995, Lemley A.T. and Dowling K.C. at Cornell University reported degradations of the phosphorus-containing pesticides malathion, parathion and methamidophos[14].

The hydroxyl radical formed could be consumed through reaction with matrix species. Common matrices include dissolved natural organic matter, such as humic acids and fulvic acids, in natural water system, as well as inorganic species in brackish waters. Due to the relatively high concentration of these species, only a small fraction of hydroxyl radical generated could reach the target pollutants. This process is a major limitation of Fenton chemistry for degradation of pollutants with matrix constituents and results in high peroxide demand and then higher costs.

The hydroxyl radical reacts with a wide range of species and most reactions show second order mechanism. The reaction rates with all the species vary in a huge range. The second order reaction rate constant with chloride at pH=2 is about 4.3×10^9 $M^{-1}s^{-1}$, while the rate constant for cadmium (II) is less than 10^5 $M^{-1}s^{-1}$. Within a single category of reactants, the reaction rate constant also varies considerable due to the target species' inherent reactivity. The second order rate constants for metal cations are in the range of 10^5 - 10^{10} $M^{-1}s^{-1}$ and for anions 10^6-10^9 $M^{-1}s^{-1}$, depending on the species valence. The rate constants with alkenes are within the range 10^9-10^{10} $M^{-1}s^{-1}$

and are higher than for alkanes, 10^7-10^9 $M^{-1}s^{-1}$ [15]. Steady state hydroxyl radical conditions in all systems facilitates the quantitation for the amount of the hydroxyl radical.

Normally the major direct products of reaction with organic species are the targeted species with an added hydroxyl group, e.g. hydroxyl naphthalene from naphthalene. For aromatic compounds, this causes hydroxylation. Further on, multi-hydroxylation is a possibility and the aromatic ring could even be broken. When hydroxyl radical reacts with un-substituted aromatics, hydrogen abstraction results in the formation of a free radical. A dimer can be formed by combination of two of these radicals. When hydroxyl radical reacts with substituted aromatics, it also causes hydroxylation of the aromatic compound. The *m*-position is the most favored due to stereo-preference [15]. An aromatic radical cation could be formed by transfer of an electron to the hydroxyl radical from the aromatic hydrocarbon. Side-chain cleavage is also a possible pathway [16]. When excessive hydrogen peroxide is available and the oxidation goes further to completion, the final products are carbon dioxide and water for species containing carbon, oxygen and hydrogen only.

Fenton oxidation has been applied in sites for remediation of contaminated soils. Stabilization of hydrogen peroxide was found necessary since it otherwise decomposes rapidly through reaction with minerals[17]. Monobasic potassium phosphate was found to be an effective stabilizer in soil system. In laboratory studies, the presence of KH_2PO_4 at optimal conditions triples the penetration depth of peroxide. Fenton reagents have been applied in industrial wastewater systems and paper mills. For example, the treatment of residual Kraft black liquor from the pulp-and-paper

industry has been shown to be effective. 95-100% lignin was degraded and decolorization was achieved under optimized conditions. Basic oxygen furnace slag was evaluated as a source of iron for degradation of 2-chlorophenol in industrial wastewater[18,19]. Industrial applications are less abundant than *in situ* applications since many of these applications are developed in commercial applications and are not disclosed in the literature.

In situ treatment of contaminated soil or groundwater requires specific site-dependent parameters. Since the Fenton reaction liberates both gas and heat, safety precaution are necessary, especially when high concentrations of peroxide are used. Treatment *in situ* involves several steps, including site assessment (contaminant identification and distribution as well as *in situ* geology and hydrology), bench scale or pilot field site testing, design of remediation strategy, implementation of remediation, and before-&-after site monitoring. Pressurized injection of concentrated peroxide and ferrous ion was mostly used and carried out with designed devices. In many cases, an array of injectors was installed at various depths in order to maximize the effectiveness of the degradation. Hydrogen peroxide and ferrous ion catalyst solution were mixed at the head of the injector just prior to injection into subsurface. Air was injected to facilitate reagent distribution. Groundwater pH, alkalinity, total iron, hydrogen peroxide concentration, chloride concentration, headspace VOCs (volatile organic compounds), oxidation-reduction potential, and conductivity were routinely monitored. pH values of less than 6 due to iron precipitation at high pH and total iron levels of greater than 5mg/l were needed. Off-gas production was monitored in order to follow the progress of the degradation. Carbon dioxide was indicative of organic pollutant degradation.

Oxygen production indicates Fenton reaction in the absence of organic compounds. In the case of VOCs (mainly trichloroethene, cis-1,2-dichloroethene and vinyl chloride contamination on marine terrace sand), *in situ* Fenton remediation carried out at the Naval Air Station, Pensacola, FL, VOC concentrations were found to have decreased dramatically[20]. In addition, Chromium(III) present in the site was not oxidized to Cr(VI) to any detectable level during the treatment. The formation of Cr(VI) in oxidizing treatment technologies is always a concern in any site that has substantial levels of Cr(III). However, contaminants in porous soil were found to be difficult to degrade.

Dissolved Organic Matter (DOM)

Dissolved organic matter (DOM) is ubiquitous. It comes from the degradation of animal and plant tissues. They are quite stable in the environment and play important roles in transportation and degradation of the pollutants [21-23]. One important consequence of DOM in natural water is the fact that DOM can significantly enhance the apparent water solubility of hydrophobic organics and therefore change their aqueous character, such as transportability and bioactivity [24]. In general, in the presence of dissolved or colloidal DOM, the more hydrophobic the compound, the higher the effects on total aqueous solubility since more could be entrapped within DOM. Bioavailability of compounds in the presence of dissolved or colloidal DOM is often decreased, although reports of increased [25] and unchanged [26] bioavailability are also available.

Two typical classes of DOM are fulvic acid (FA) and humic acid (HA) both of which are mixtures. Though hypothetical structural models of HA and FA are offered

[27], the exact structures of both are still unknown. The generally accepted values of molecular weight of humic acids are 2,000-20,000 and the ones for fulvic acids are 1,000-5,000. Comparatively, humic acid generally contains more aromatic character, while fulvic acid contains more carbonyl and aliphatic regions. In addition, the contents of humic acids and fulvic acids are region-dependent. Humic/fulvic acids from different geographic regions show different proportions of the elements. **Table 1-1** illustrates elemental analysis of humic acids and fulvic acids [28].

Significant solubility enhancements of relatively water-insoluble solutes by HA and FA were observed. The enhancements were attributed to partition-like inter-molecular interactions between HA/FA and the compounds [29]. and depends on the size and polarity of the HA/FA. The magnitude of this effect for an organic solute with respect to a specific DOM can be expressed as

$$S_w^* = S_w + X\,C_0 \qquad (1\text{-}6)$$

Where S_w^* is the apparent solute solubility in water containing DOM, as a cosolute, at concentration X, in grams per milliliter of water, S_w is the solubility in pure water and C_0 expresses the mass of solute partitioned into a unit mass of DOM. With $K_{dom} = C_0 / S_w$, the equation could also be expressed as

$$S_w^* = S_w\,(1 + X\,K_{doc}) \qquad (1\text{-}7)$$

Table 1.1 Elemental analysis data for IHSS standard and reference Humics and Fulvics[27]

Sample	C	H	O	N	S	P	Total	H2O	Ash	&13C	&15N
	Standard Humic Acids										
Stream	52.55	4.40	42.53	1.19	0.58	<0.01	101.2	10.0	3.10	-27.7	-1.41
Soil	58.13	3.68	34.08	4.14	0.44	0.24	100.7	8.2	0.88	-22.6	5.34
Peat	56.37	3.82	37.34	3.69	0.71	0.03	102.0	11.1	1.12	26.0	1.29
Leomardite	63.81	3.70	31.27	1.23	0.76	<0.01	100.8	7.2	2.58	-23.8	2.13
	Standard Fulvic Acids										
Stream	52.44	4.31	42.20	0.72	0.44	<0.01	100.1	8.8	0.46	-27.6	-1.85
Soil	50.57	3.77	43.70	2.72	0.56	0.03	101.4	8.8	0.86	-25.4	3.89
Peat	50.12	4.28	42.61	3.75	0.89	0.12	101.8	11.2	1.00	-25.6	5.40
Leomardite	50.45	3.52	45.47	2.56	0.73	0.02	102.8	11.7	4.61	-25.8	1.42
	Reference Humic Acids										
Stream	52.89	4.14	43.40	1.17	0.58	<0.01	102.2	9.8	3.46	-28.2	2.42
Soil	58.33	3.61	34.35	4.19	0.42	0.25	101.2	8.3	0.86	-23.0	5.45
Peat	56.84	3.60	36.62	3.74	0.70	0.03	101.5	10.4	1.72	-26.3	1.43
Leomardite	63.97	3.60	31.62	1.25	0.77	<0.01	101.2	8.9	2.25	-24.4	0.89
Nordic	53.33	3.97	43.09	1.16	0.58	0.01	102.1	9.1	0.31	-27.8	-1.55
Summit Hill	54.00	4.84	37.90	5.13	0.64	0.40	102.9	8.1	1.41	-26.3	2.99
	Reference Fulvic Acids										
Stream	53.04	4.36	43.91	0.75	0.46	<0.01	102.5	8.9	0.98	-27.9	-2.76
Peat	52.12	3.23	43.93	2.43	0.53	0.01	102.2	11.8	1.58	-26.1	0.98
Nordic	52.31	3.98	45.12	0.68	0.46	<0.01	102.6	9.2	0.45	-27.8	-3.19

Where K_{dom} is the defined solute partition coefficient between DOM and pure water and K_{doc} is the corresponding organic-carbon-based partition coefficient. The magnitude of the partition coefficient, K_{dom} or K_{doc}, depends on the type of solute and a

given DOM. When X K_{doc} is significant, the apparent solute solubility would be greater than the one in water. A linear increase in solubility was observed with an increase in DOM concentration. But with DOC ≤ 100 mg/L, the effect of DOM on solubility is minimal for relatively water-soluble solutes such as lindane [29].

Generally, hydrophobic pollutants exhibit greater binding to HA than to FA, especially with aromatic compounds. Consequently HA has a greater effect on the solubility, since HA has higher aromatic character and larger molecules. For the similar reasons, the solubility of FA is higher than for HA. FA is categorized as soluble at pH as low as 2, while HA will aggregate at such low pH conditions.

Cyclodextrins

Cyclodextrins (CDs) are cyclic oligosaccharides. α, ß, γ-cyclodextrins contain 6, 7, or 8 glucose rings respectively. The shape and dimensions of the α-, ß-, γ-cyclodextrin molecules are presented in table 1-2[30,31]. There are two kinds of hydrophilic hydroxyl groups, primary and secondary, while the interior of the cyclodextrin consists only of a ring of C-H groups. Therefore the interior of cyclodextrin is relatively non-polar compared to water.

The inclusion of hydrophobic species by cyclodextrins has been widely studied. The hydrophilic exterior of these oligosaccharides renders them water-soluble while their interior cavity is less polar than water, thereby allowing the CDs to accommodate guest molecules and therefore increasing their solubility. The guest compounds range from polar reagents, such as acids, amines, small ions such as ClO_4^-, and halogen

anions [32] to highly non-polar aliphatic and aromatic hydrocarbons and even rare gases [33]. Inclusion complexes can be formed either in solution or in the crystalline state. Water is usually used as solvent, although inclusion complex formation also takes place in dimethyl sulfoxide and in dimethyl formamide.

Inclusion complex formation can be directly measured by a variety of spectroscopic methods, e.g. NMR, absorption, fluorescence and optical rotation. The most direct evidence for the formation of guest-host complex was obtained by proton nuclear magnetic resonance spectroscopy. On complex formation with species whose benzene ring is entrapped into the cavity, the protons located in the cavity are subjected to anisotropic shielding, and thus appear at higher magnetic field, while individual protons have varied shift due to individual magnetic field changes [34-36].

Polycyclic Aromatic Hydrocarbons (PAHs)

Polycyclic aromatic hydrocarbons (PAHs) are made of fused benzene rings in linear, angular or cluster arrangements and contain only carbon and hydrogen. **Figure 1-2** illustrates the structure of some PAHs. PAHs are formed whenever organic substances are exposed to high temperature and may also be synthesized by some plants and bacteria [37]. However, the greatest amounts of PAHs released to the environment are formed during fossil fuel combustion and during anthropogenic forest and agricultural fires.

PAHs are fairly widely spread contaminants of aqueous environments[38]. Over the past two decades, scientists have increased their concern about PAHs since the harmful

Figure 1.1 Structure of some PAHs

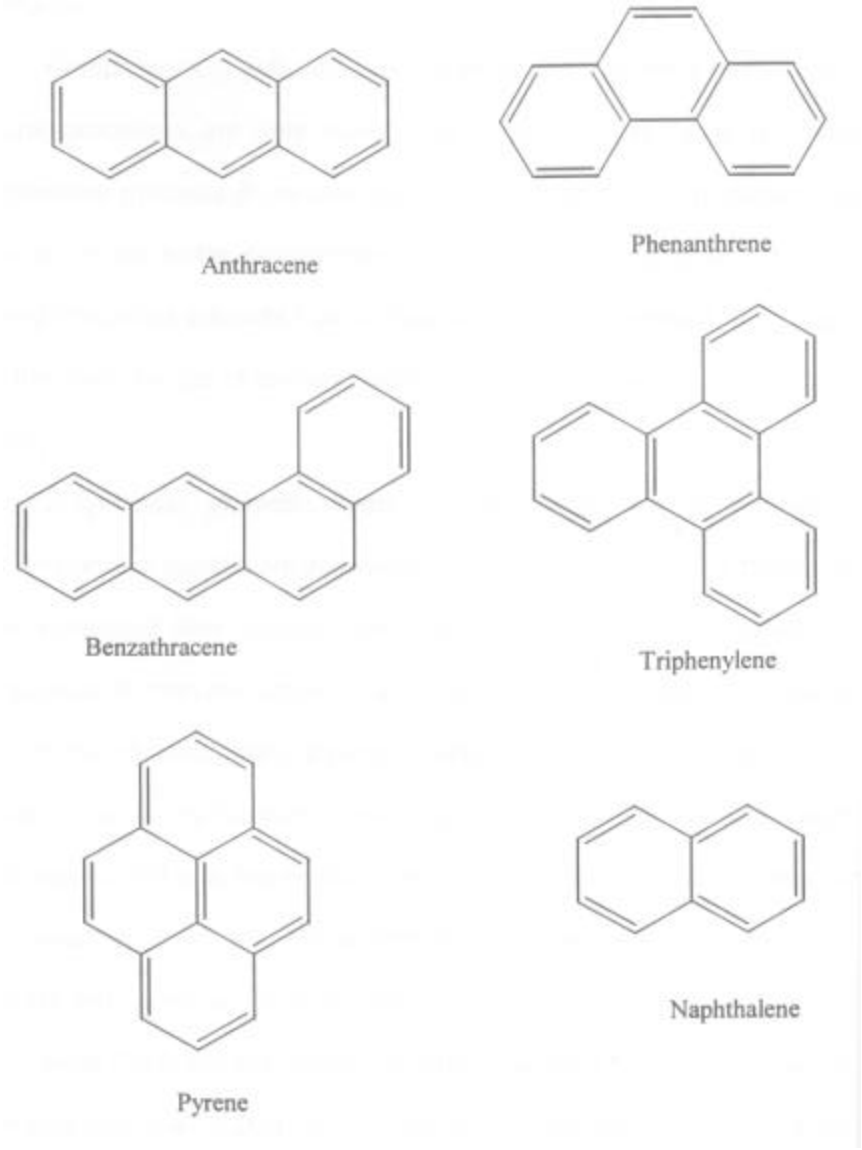

effects of these compounds to humans and other living organisms are more and more known, such as the toxicity and carcinogenicity. These effects are are of special concern because there is a strong potential for PAH accumulation in the terrestrial food chain. The need for more research on the carcinogenicity of PAHs in the environment becomes more and more important as the world energy consumption increases with population and geographic expansion.

Although PAHs are most frequently found in industrial areas, remote sites contaminated through long-range atmospheric transport have been reported [39]. Most PAHs are practically water insoluble, for example 0.009 μM for picene and 0.64 μM for pyrene. After entering water systems, PAHs quickly become adsorbed to particles and usually are deposited in the bottom sediments. Though re-suspension of sediment and uptake by benthic organisms, a small fraction of the PAHs associated with sediment may be returned to the water column. PAHs are readily accumulated by aqueous biota to levels higher than those in the ambient medium, and they can be transformed by biota. Relative concentrations of PAHs in aqueous systems are generally highest in the sediments, intermediate in biota and lowest in the water column.

PAHs in aqueous environments are subject to degradation through a number of processes, including chemical oxidation and biological transformation by aqueous bacteria, and fungi. The mechanism and products of these degradation processes depend on the chemical and physical properties of the particular compounds as well as on ecosystem-specific properties such as temperature, turbidity, concentration of the dissolved and particle material and the nature and concentrations of microbial populations. Many bacteria, fungi and algae can metabolize PAHs. Generally, compounds with linear structure and lower molecular weight (e.g. anthracene and naphthalene) are metabolized faster than those with more condensed rings (e.g. pyrene, or coronene) [40].

The chemical oxidation of PAHs depends on the concentration of oxidants, such as singlet oxygen, organic peroxides, hydrogen peroxide, and hydroxyl radicals. It is believed that these oxidants arise from photochemical processes[41]. The

concentration of oxidizing agents in natural waters will depend upon many factors, e.g. solar irradiation, temperature and concentration of humic substances, and exhibit wide variations. Some inorganic species, especially salts of iron and magnesium, are involved in the production of oxidants in natural water systems and then influence the chemical oxidation processes.

Chlorination and ozonation of PAHs have been studied. But chlorinated products such as polychlorinated naphthalenes and polychlorinated pyrene are highly toxic to aqueous organisms and persist in the environment, while ozonation is far less efficient though the products are less toxic [42]. Photoreactions of many PAHs are rapid in clear river water and the upper layer of ocean. In turbid rivers, however, photolysis is inhibited by light attenuation and the partitioning of PAHs to bottom sediments where light does not penetrate.

Phenoxyacetic Acids (PAs)

Phenoxyacetic Acids are a series of compounds, of which 4-CPA (4-chlorophenoxyacetic acid), 2,4-D (2,4-dichlorophenoxyacetic acid) and 2,4,5-T (2,4,5-trichlorophenoxyacetic acid) were used as herbicides commonly to control broadleaf weeds in grass and various crops [43].

The toxicology of the phenoxyacetic acid herbicides has been well determined and documented. **Table 1-3** contains toxicity of three phenoxyacetic acid herbicides[44]. Though 2,4,5-T is only moderately toxic to warm-blooded animals, industrial production had been halted in the late 1970s because its production generated about 0.1 ppm TCDD (tetrachlorodibenzo-p-dioxin), the most potent small-molecule toxin ever-known

[45]. A wide range of contamination of TCDD resulted from usage of 2,4,5-T. TCDD was found to be environmentally persistent and bio-accumulated. In addition to cancer, dioxins adversely affect the immune and endocrine systems and to cause birth defects [46]. However, no TCDD was generated in production of 2,4-D, which is still in use.

Table 1.2 Toxicity of Phenoxy Herbicides[43]

Chemical	Acute Oral LD50 for Rats(mg/kg)
2,4,5-T	300-500
2,4-D	300-1000
MCPA	700-800

Polychlorinated Biphenyls (PCBs)

Polychlorinated biphenyls (PCBs) are a class of chlorinated hydrocarbons with a biphenyl nucleus on which from one to ten hydrogen atom(s) has/have been replaced by chlorine. $C_{12}H_{10-n}Cl_n$ (n= 1-10) represents total 209 compounds, from monochlorobiphenyl through decachlorobiphenyl [47]. The term PCB, is used to refer to any one or any subset of compounds and PCBs routinely denotes the entire class. The entire set of 209 PCBs forms a set of congeners. Commercial PCBs were manufactured and sold as complex mixtures containing multiple isomers at different degrees of chlorination. PCBs are very stable compounds and do not degrade easily.

Commercial PCB mixtures were used in a wide variety of applications, including dielectric fluids in capacitors and transformers; heat transfer fluids; hydraulic fluids;

lubricating and cutting oils; and as additives in pesticides, paints, copying paper, carbonless copy paper, adhesives, sealants, and plastics. Their commercial utility was based on their stability, including low flammability, and desirable physical properties, including electrical insulating properties [48].

PCBs are one of several truly global environmental pollutants, in addition to PAHs, mercury and lead. PCBs are highly environmentally persistent and bio-accumulated. Though its industrial usage had been prohibited in the later 1970s, they can be prevalently found in nearly all marine plant and animals specimens, fish, mammals, birds (especially fish-eating birds), bird eggs, and, of course, humans [49].

PCBs have low volatility and high lipophilicity, with the consequence that more than 99% of PCB mass in the environment is found in soil. The environmental transport of PCBs is complex [50]. Volatilization of PCBs from spills, landfills, road oils, and other sources results in measurable atmospheric emissions. Atmospheric transport is the primary mode of global distribution of PCBs. Environment levels of PCBs increase near the source of the PCBs. Thus, urban areas have generally higher concentrations than suburban or remote environments. Similarly, indoor levels are roughly one order of magnitude higher than outdoor levels, a trend in-line with many other air pollutants. Human exposure to PCBs occurs primarily via low-level food contamination and exposure to in-door PCBs in paints or other utilities. The toxicology of PCBs has been well studied via in vitro and in vivo animal studies, as well as studies of humans exposed through occupation or residency. PCBs have been proven to be related to a variety of diseases including cancer, tumor and fetus deformation. PCBs pollution resulted from past industrial

usage is still a top environmental issue and agenda of Environmental Protection Agency (EPA)[51].

Calixarenes and Derivatives

The calixarenes are a class of cyclooligomers formed via a phenol-formaldehyde condensation. They exist in a 'cup' like shape with a defined upper and lower rim and a central annulus, **Figure 1.2**[52]. Their rigid conformation enables calixarenes to act as host molecules as a result of their preformed cavities. By functionally modifying either the upper and/or lower rims it is possible to prepare various derivatives with differing selectivities to accommodate various guest ions and small molecules. Calixarenes lend themselves well to many applications because of the multiplicity of options for such structural elaboration.

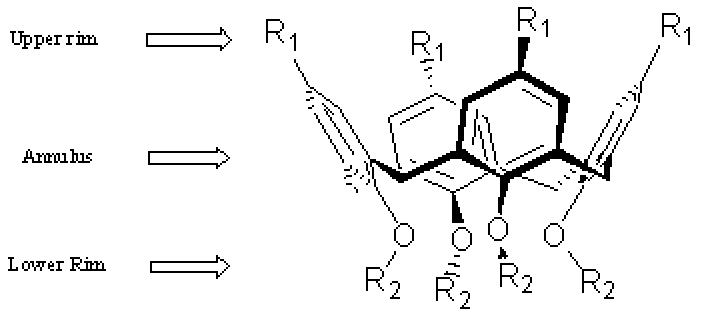

Figure 1.2: Cone conformation of a typical calix[4]arene.

Calixarenes, along with other macromolecules formed with cyclic repeated units such as calixpyrrole, offer potential elegant size control through changing the number of units and modifying either upper and/or lower rims. These kinds of compounds have shown binding ability with various species and can be applied in the field of ion-selective electrodes[53], chiral recognition[54], solid phase extraction[55], stationary phases[56] etc..

Calix[4]arenes have four conformations, which have been well investigated by X-ray crystallography, dynamic 1D and 2D NMR spectroscopy, as well as with a series of force field (PIMM) and semiempirical (PM3, MNDO) calculations. **Figure 1.3** illustrates the four conformations[57]. The stereo-electronic effects of the upper rim substituents of tetramethoxycalix[4]arenes characteristically influence the preferred arrangement of the phenyl rings in the partial-cone conformation. The in/out summarization taking place in 4 (Y = Bu, R = Me) is strongly hindered in 1 (Y = Br, R = Me) due to the smaller diameter of the upper rim. The ease of rotation of the methoxy group attached to the inverted ring in partial-cone-4 can be altered by using a solvent which is able to form a host-guest complex with the calixarene cavity. Cone/partial-cone and partial-cone/partial-cone equilibriums have been observed by 2D EXSY spectroscopy [58].

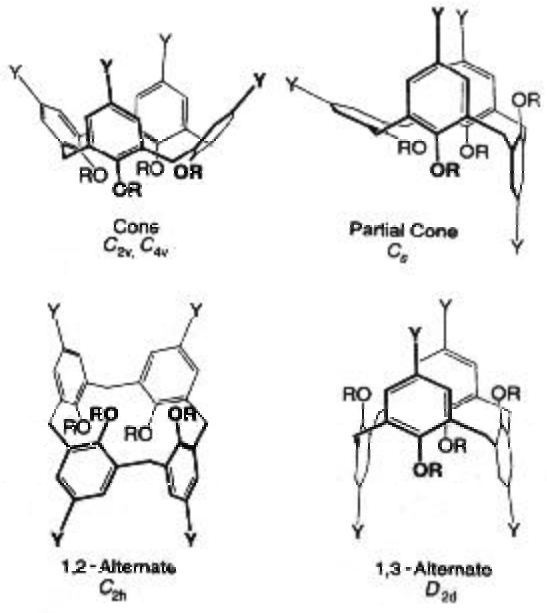

Figure 1.3, four possible conformations by calix[4]arenes.

However calix[6]arenes are relatively solid and shows cone conformation, though 1,2-alternate and 1,3-alternate can be synthesized with presence with cesium hydroxide.

Chapter II Experimental

Materials

Hydrogen peroxide (~30%) was purchased from EM Science. Purified water was obtained by further purification of distilled water with a NanopureUV (Barnstead) water treatment system. Suwannee River fulvic acid (SRFA) and Suwannee River humic acid standard materials were purchased from the International Humic Substances Society (http://www.ihss.gatech.edu). The SRFA and SRHA were used as DOM (dissolved organic matter) in these studies. SRFA and SRHA concentrations were reported as mg FA/L and mg HA/L. The carbon contents of these materials are 52.44% and 52.55% by weight respectively. Iron(II) perchlorate (99+%) was purchased from Alfa. Ferrous Sulfate ($FeSO_4 \cdot 7H_2O$; 99.6%) was purchased from J.T. Baker. 1-propanol (PrOH, 99+%) was purchased from Mallinkrodt. Benzoic acid (99.5+%) and p-hydroxybenzoic acid (p-HBA, 99+%) were purchased from Aldrich. All reagents were used as received.

Chlorinated phenoxyacetic acids, 2,4,5-trichlorophenoxyacetic acid (97%), 2,4-dichlorophenoxyacetic acid (98%), 3,4-dichlorophenoxyacetic acid (96%) and phenoxyacetic acid (99%), were purchased from Aldrich. 4-chlorophenoxyacetic acid (98%) was purchased from Sigma. All reagents were used as received. Phenol (99%), catechol, resorcinol (99%) and hydroquinone (99%) were purchased from Aldrich. Pyrene (99+%), phenanthrene (99.5+%), and anthracene (99+%) were all purchased

from Aldrich. Naphthalene (99+%) was purchased from J.T. Baker, while 2-naphtol (99%) and 2,3-dihydroxylnaphthalene (98%) were purchased from Across. α-cyclodextrin (α-CD, 99%, M.W. 972.9) was purchased from Sigma, while β-cyclodextrin (β-CD) and carboxymethyl-β-cyclodextrin (CM-β-CD, avg. M.W. 1375) were both received from Cerester.

1-Octanol (99+%), methanol (99.93%, HPLC grade), and trifluroacetic acid (99+%) were purchased from Aldrich. Chloroform (99.8%), acetone (99.8%), and acetic acid (99.7%) were purchase from EM Science. Methylene chloride (HPLC-GC/MS grade) and hexanes (pesticide grade) were obtained from Fisher.

Hydrogen Peroxide Determination. The concentration of hydrogen peroxide was determined by iodometric titration [59]. In this method, excess I^- was added to the hydrogen peroxide solution to form I_3^- which was then titrated with thiosulfate. Thiosulfate solution was standardized on the day of experiment against the primary standard potassium iodate. A starch indicator was used.

Hydroxyl Radical Generation and Quantification. Hydroxyl radical was produced using Fenton Chemistry. The major sink for hydroxyl radical was chloride (from hydrochloric acid used to adjust pH value or within sodium chloride) or methanol. These species were added to the system to minimize changes in hydroxyl radical scavenging upon addition of DOM or β-CD. In each set of experiments, the concentration of Fe(II) was kept constant.

Benzoic acid (BA) was used as a probe to measure hydroxyl radical concentration [60]. The initial concentration of BA was 0.1 mM, the pH was 2.5, the

concentration of $Fe(ClO_4)_2$ was 0.5 mM, hydrogen peroxide (5.0 mM) was added at a rate of 3.0 mL/h. Benzoic acid was quantitated by HPLC using a Shimadzu (LC-10AT) liquid chromatograph with UV-Vis detector. A spherisorb ODS-2 column (5 μm particle size, 25 cm length × 4.6 mm id) was used for all separations. The initial concentration of BA was 100 μM. Benzoic acid was chosen as hydroxyl radical trap because it has a known rate constant, exhibits a characteristic product (p-HBA) upon reaction, and has a low partition coefficient for binding to FA or HA[61]. Consequently, this probe was expected to yield hydroxyl radical concentrations that were representative of the bulk aqueous phase.

All the species, except an aliquot of daily prepared $Fe(ClO_4)_2$ solution, were added and shaken moderately to rule out the possible interference from different equilibrium stages. The iron(II) was added last since it is prone to be oxidized with exposure to air and it's binding to other species is fast. In each set of experiments the equilibration time was kept constant.

After Fe(II) was added and a five-minute equilibrium period was allowed, hydrogen peroxide was then added continuously with a syringe pump (KD Scientific). The flow rate varied from 0.5 mL/h to 3.0 mL/h, and the volume change due to the addition was negligible since the monitoring time was normally within 20 minutes. Continuous addition of H_2O_2 was used to establish a steady state hydroxyl radical concentration in each degradation reaction. The hydroxyl radical concentration increased while H_2O_2 was added. The steady state of hydroxyl radical was reached when the generation rate was balanced with the consumption rate. All reactions were preformed at room temperature with constant stirring.

Phenoxyacetic Acids

Humic acid and fulvic acid were selected to study the impact of DOM. When HA/FA was added to a phenoxyacetic acid solution, a 15-minute equilibration period was allowed. A stir bar was used to keep the solution homogeneous. The adsorption of phenoxyacetic acids to the stir bar was found to be negligible. The pre-equilibrium period was half an hour if carboxymethyl-beta-cyclodextrin was present.

Phenoxyacetic acids were monitored by HPLC with a mobile phase of methanol and water with trifluoroacetic acid (TFA).

Degradation of 2,4,5-T, 2,4-D, 3,4-D and 4-MPA. Solutions were prepared with five steps: 1) each compound was dissolved in methanol; 2) an aliquot of the methanol solution was deposited in a clean, dry flask; 3) the methanol was evaporated under a gentle nitrogen stream; 4) pH=2.5 water, adjusted with HCl, was added and 5) the sample was sonicated for twenty minutes to dissolve the solute. Solutions were stored in the dark until further use. A fresh $Fe(ClO_4)_2$ solution was prepared daily with water (pH=2.5, adjusted with HCl). Each degradation, except the ones for chlorine balance, was carried out at pH=2.5. The initial concentration of all the phenoxyacetic acids was 0.1 mM, the concentration of Fe(II) was 0.5 mM, and 5 mM hydrogen peroxide was added at a rate of 3 mL/h to generate a steady state concentration of hydroxyl radical. The total volume of the reaction was kept at 10 mL. At desired analysis times, an aliquot of the reaction solution was sampled and mixed with an equal volume of 1 % PrOH (aq.), which was used to terminate the reaction of hydroxyl radical with the target compound. Basically, 5 to 6 samples were collected within 20 minutes. Within this short time, we assumed that the reaction volume change due to addition of hydrogen

peroxide was negligible and decrease of the compound concentration was only due to degradation by hydroxyl radical. Solutions of SRFA and SRHA were made daily. An aliquot of one of these solution was added to generate 2.5 mg/L, 5 mg/L and 10 mg/L SRHA or SRFA to study the effects of DOM on the degradations.

Degradation with CM-β-CD. Degradation with CM-β-CD present was used to study the effect of CM-β-CD with and without the presence of DOM. 5 mg/L SRHA was added for some degradations; the concentration of Fe(II) was kept the same as previous experiments (0.5 mM). CM-β-CD concentrations of 0.1 mM, 0.2 mM and 0.5 mM were added. CM-β-CD was prepared daily with pH=2.5 HCl solution. In addition, with 0.5 mM CM-β-CD and 5 mg/L SRHA, the concentration of Fe(II) was changed to study the role of Fe(II); 0.1 mM, 0.2 mM and 0.5 mM Fe(II) were used.

Measurement of K_{ow} Values. Each compound's K_{ow} value was measured by the following steps: a weighed sample of one compound was dissolved in methanol first; 50 μl of the methanol solution was deposited to a vessel and, after evaporation of the methanol, 2.0 mL octanol was added; then 2.0 mL pH=2.5 water was added and shaken overnight; the aqueous phase was monitored with HPLC. The concentration in the octanol phase was calculated, based on the measured concentration in the aqueous phase. The K_{ow} was calculated by dividing the concentration in octanol phase by the one in aqueous phase [62].

Products of Degradation. To maximize the amount of product formed, a higher volume (50 mL) was used and hydrogen peroxide was added continuously for about 30 minutes. The resulting solution was extracted with 20 mL methylene chloride three times. The combined methylene chloride fractions were evaporated with nitrogen to 0.1

mL. The solution was injected and products were monitored with GC-MS (GC8000-AutoSpec). The temperature gradient was 80 to 240 °C at 15°C/min and remained at 240°C for 5 minutes.

2,4,5-T Degradation Chloride Balance. Since use of $Fe(ClO_4)_2$ could result in generation of chloride, ferrous sulfate was used as the source of Fe(II). The degradations were carried out without pH adjustment with HCl. The sample collection processes were similar to the previous degradations. The 2,4,5-T concentration was monitored with HPLC and the chloride was quantitated with a Dionex Ion Chromatograph (GP40) with AS-14 column and electrical conductivity detector. 4.8 mM sodium bicarbonate and 0.6 mM sodium carbonate were used at 1:1 ratio for the mobile phase at a flow rate of 1.0 mL/min.

Polycyclic Aromatic Hydrocarbons (PAHs)

Degradation of Pyrene, Phenanthrene and Anthracene. Individual solutions of each of these species were prepared with similar steps for phenoxyacetic acids. However, since their solubilities are much lower than those for phenoxyacectic acids, the solutions were sonicated for one hour to ensure complete dissolution. The pH was not adjusted in these studies. Daily $Fe(ClO_4)_2$ solutions were made and added as described for the degradations of phenoxyacetic acids. The initial concentration of individual PAHs was 0.1 μM. The samples were kept on an orbital shaker at 200 RPM for four hours for equilibration. In each degradation, 3.0 mL of solution was transported to a fluorescence cuvette with stir bar. Significant adsorption of PAH to the telfon stirring bar was observed (no adsorption without telfon stirring bar). To minimize this

unfavorable effect, 0.1 ml pure methanol was added in each degradation, meanwhile methanol served as the major radical scavenger. The degradation was monitored by fluorescence (PTI Quantamaster) with excitation/emission wavelengths of 336/372 nm for pyrene, 356/399 nm for anthracene and 252/364 nm for phenanthrene. After pre-equilibrium, hydrogen peroxide was continuously added thoug h a digital syringe pump at a constant flow rate [63].

Degradations with SRHA. To study the effect from DOM, 2.5 mg/L, 5.0 mg/L and 10 mg/L of SRHA were added in series. All the other conditions were the same as for degradation in the pure water system, including the amount of methanol added.

Degradation with CM-β-CD. To improve the degradation, CM-β-CD was further added to all the series with presence of 2.5 mg/L SRHA. 0.25 mM, 0.50 mM and 1.0 mM CM-β-CD were added within one set of experiments. All the other conditions were the same as for degradation in pure water system, including the amount of methanol added.

Ternary Complex of CD:Host:Fe(II). In previous sets of experiments, the existence of CM-β-CD was believed to increase the degradation rates even in the presence of SRHA. CM-β-CD is capable of binding ions with its hydroxyl groups and carbomehtyl groups. CM-β-CD is also capable of entrapping hydrophobic guest into its interior cavity. To prove the existence of this kind of ternary complex, various solutions were made and studied with electrospray-mass spectrometry (Quatro II). The concentration of CM-β-CD was 1.0 mM and the concentration of the guest was saturated. The mixtures of the two were shaken overnight. An aliquot of iron(II) solution was added just before introduction to the electrospray source of the mass spectrometer.

Phenol Degradation and Its Product Profile. Phenol, catechol, resorcinol and hydroquinone solutions were made daily since all of them are easily oxidized with exposure to air. With 3.2 mM chloride from sodium chloride and 1.0 mM Fe(II) from $Fe(ClO_4)_2$, the initial concentration of phenol was 1.0 mM and the total volume was 10 mL. All the degradations were made without pH adjustment. 10 mM hydrogen peroxide was added at 3.0 mL/h. Five samples were collected at 3, 6, 9, 12, 15 minutes after starting addition of hydrogen peroxide and were quenched with an equal volume of 1% PrOH (aq.). The samples were monitored with HPLC-UV. To study the potential improvement for phenol degradation; 0.25 mM, 0.50 mM and 1.0 mM CM-β-CD were added with all other conditions constant.

Naphthalene, 2-naphthol and 1,2-dihydroxynaphthalene. Individual solutions of naphthalene, 2-naphthol and 1,2-dihydroxynaphthalene were prepared as described for the other PAHs. Degradations were monitored by fluorescence at 281/333 nm, 303/345 nm and 317/386 nm excitation/emission wavelengths, respectively. To study the degradation enhancement with CM-β-CD, 0.25 mM, 0.50 mM, and 1.0 mM CM-β-CD were added with all other conditions constant. To study the effect of acidity on degradation, acetic acid, HCl solution and a buffer of 0.1 mM AcOH/AcONa (pH=4.7) were used.

Two-phase Degradation of PAHs and PCBs

To study the degradation enhancement with cyclodextrin derivatives in two phase systems, two kinds of highly hydrophobic species, PAH and PCB were selected. The reason is that persistence of water resource contamination relates to steady release of

hydrophobic pollutants from contaminated sediment to water systems. PAHs and PCBs are two routine persistent pollutants found in the environment.

Sample Deposition and Treatment. Solutions of naphthalene, phenanthrene and anthracene (1000 μM in methylene chloride), were prepared. In one set of experiments, 50 ml of the solution was deposited into 100 grams quartz sand, which was previously washed with acetone and dried. The sand was transferred into a round-bottom flask and then was further evaporated to remove the methylene chloride with a rotary evaporator (Yamato, RE500) for 30 minutes. The dried sand was transported to a beaker and stirred to make homogeneous. 20 mg sand was weighed and transferred to a glass vial. 10 mL water (pure or with CM-β-CD) was added to each sample and the samples were left in an orbital shaker overnight. An aliquot of iron(II) solution (iron concentration was varied) was added and the samples were equilibrated for 10 minutes before a single dose of hydrogen peroxide was added. The overall sample volume was kept constant at 25 mL. After addition of hydrogen peroxide, the mixture was allowed to react for 15 minutes. After reaction, 12.5 mL of the solution was pipetted out and transferred to a glass vial and then extracted with 5.0 mL methylene chloride. The remaining solution was decanted, and the semi-dry sand was weighed. Half of the sand was transferred to a glass vial and extracted with 5.0 mL methylene chloride. The concentration of each of the extracts was determined by GC-FID (flame ionization detector) and the total amount in each sample was calculated accordingly.

PCBs (3,3',5,5'-tetrachlorobiphenyl and 2,2',6,6'-tetrachlorobiphenyl) were determined using GC-ECD (electron capture detector). The initial concentration of PCB in a stock methylene chloride solution was 30 mg/L. 10 ml of this solution was diluted to

100 mL and then deposited into 200 gram sand using a similar deposition procedure and rotary evaporation method as previously described. 2.5 grams of the PCB loaded sand was weighed and transferred to a glass vial, then 2.5 mL water was added (including CM-β-CD in some experiments) and left on an orbital shaker to equilibrate for 3 days at 250 RPM. Iron (II) was added, and the sample was shaken for a further 10 minutes before a single dose addition of hydrogen peroxide was made. After adding the hydrogen peroxide, the solution turned dark due to formation of Fe(III) from oxidization of Fe(II). The sample was allowed to react for 15 minutes before 2.5 mL methylene chloride was added to extract the organic compounds. To ensure extraction efficiency, the sample with methylene chloride was sonicated for half an hour, then the methylene chloride was transferred to GC vial and monitored in duplicate by GC-ECD. In most sets of experiments, the extraction efficiency was found to be about 95% (standard deviation around ±3%). In each set of experiments, two identical samples were prepared and analyzed. In addition, in each set of experiments, two blank samples (no peroxide addition) were also prepared for extraction efficiency test.

Water-Soluble Calixarene Derivatives

Since the Carbomethyl-beta-cyclodextrin used is a mixture, of which we do not know the exact number of carbomethyl groups nor the exact location of them, to better study the impact of ternary complex formation and impact on degradation enhancement, calixarene derivatives were synthesized. Tert-butyl-calix[6]arene was used as the starting material. In each step, reaction conditions were controlled and the product was purified [57]. All six repeating units of the parent calixarene were substituted with the

same functional group by using excessive reagent under gentle conditions. Hexa-(carboxymethyl)-calix[6]arene was synthesized in three steps. Step one involved de-

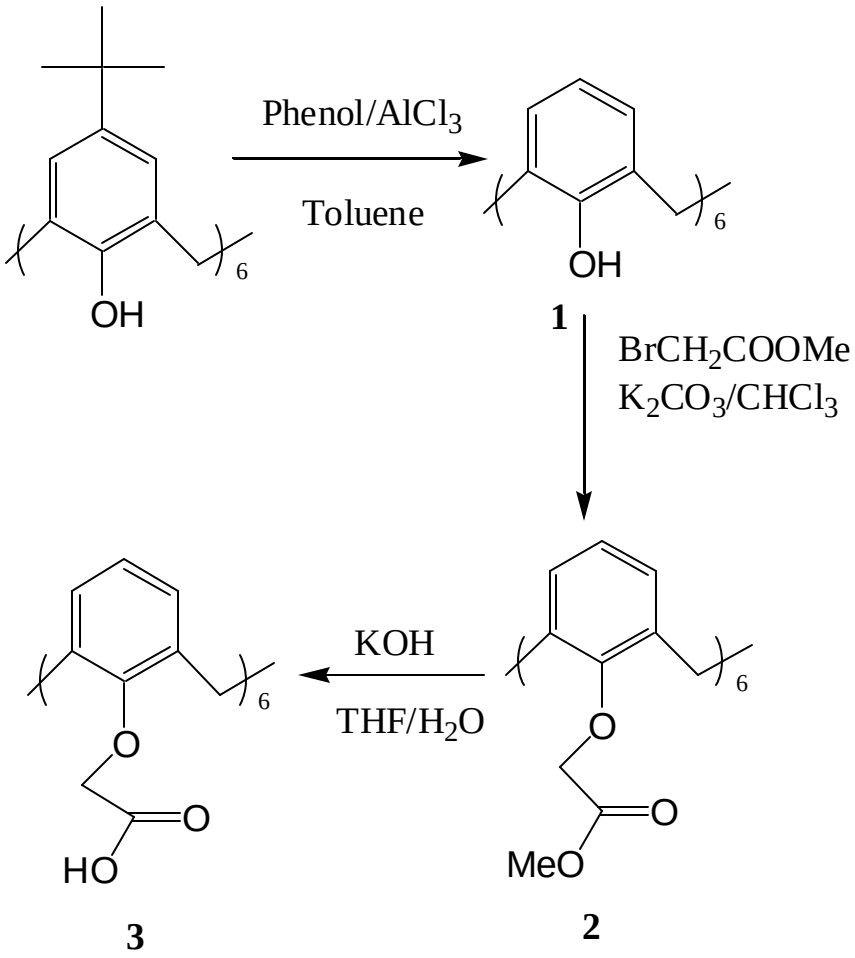

butylization of the initial tert-butyl-calix[6]arene with 1.5 eq. phenol and $AlCl_3$ in toluene at room temperature for two hours. This reaction mixture was quenched with ice water, and the organic layer was separated and extracted with two portions of toluene. After evaporating the toluene, the residue was washed with methanol three times to remove phenol and trace $AlCl_3$. Since calix[6]arene has very low solubility in methanol the product remained after methanol wash. A yield of 65% was obtained. In step two, the calixarene was linked with methyl bromoacetate. The debutylated callix[6]arene was

dissolved in $CHCl_3$, and 1.5 eq. methyl bromoacetate and 2.0 eq. K_2CO_3 were added with stirring at room temperature overnight. After evaporation of the solvent and column chromatography with 3:1 hexane:acetone, product **2** was recovered with a yield of 88%. Step three involved hydrolysis with KOH in THF/H_2O to form carboxymethyl calix[6]arene with a yield of 65%. The reaction was carried at room temperature and stirred for three days, after evaporating THF with a rotary evaporator, the solution was extracted with $CHCl_3$ three times. Following column chromatography, the analytically pure product **3** was obtained.

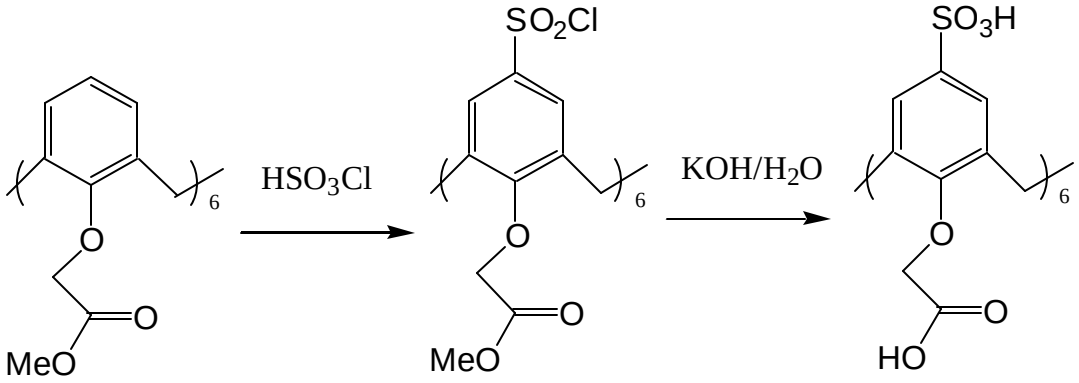

2 **4** **5**

Though product 3 contains six acid groups, it was still found to have extremely low water solubility (less than 20 μM). Further synthesis of sulfonated calix[6]arene derivatives was conducted. Dry calixarene derivative **2** in a test tube was mixed with 5 eq. pure chlorosulfonic acid. As soon as the chlorosulfonic acid was added, the reagent was dissolved and left for 30 minutes with sonication. The reaction was then quenched with ice water to yield a yellowish solid on the surface of the ice. Filtration was used to collect the product and the remaining mixture was extracted with $CHCl_3$ twice. The extract was evaporated with a rotary evaporator and the residue was added along with

aqueous KOH. The solid residue was immediately dissolved. Evaporation of the water and purification with column chromatography gave product **5** with a yield of 23%. Each product was identified with ^{1}H NMR [57].

Binding Constant Between Naphthalene and Synthesized Calix[6]arene Derivatives and Performance upon Addition of Iron(II) and Mg(II). Solutions of 25 µM naphthalene and varied concentration of sulfated calix[6]arene derivative **5**, were made and left on an orbital shaker for overnight. Fluorescence was measured and a plot of 1/[Flu] vs 1/[Conc.], where Flu denotes fluorescence intensity and Conc. denotes concentration of calixarene derivative has good linearity, indicating a 1:1 binding ratio.

An aliquot of freshly made solution of iron(II) perchlorate was added and, after 10 seconds for binding equilibrium, the fluorescence was stable and was measured. The fluorescence was strongly quenched down to one twentieth upon addition of 1 mM Fe(II), the routine iron concentration used in degradation. The fluorescence quenching could be due to the proximity of iron to naphthalene in a ternary complex. Since magnesium ion is reported to have less quenching effect, Mg ion was added in an effort to displace iron an recover fluorescence. However, addition of Mg caused further quenching rather than a recovery of fluorescence intensity. Another possibility is that addition of iron(II) and Mg(II) cause precipitation. However no precipitation was visually observed even after the solution was left undisturbed for one week.

Chapter III Phenoxyacetic Acids

Generation of Steady state concentration of hydroxyl radical

Hydrogen peroxide was continuously added with a digital syringe pump in all degradations within the phenoxyacetic acid series. Fe(II) worked as a catalyst to generate hydroxyl radical by reaction with hydrogen peroxide. With stirring, the concentration of hydrogen peroxide was constant, which means the consumption rate was equal to the addition rate. The consumption of hydrogen peroxide followed a pseudo-first-order mechanism with stable concentration of Fe^{2+}; consequently, as peroxide was added and its concentration increased, its rate or consumption through reaction with Fe^{2+} also increased until its consumption exactly balanced that of its addition rate. Under specific conditions, a constant concentration of hydroxyl radical will thus result for all experiments carried out with these conditions. This result was verified by the appearance of pseudo first-order reaction of chlorinated phenoxyacetic acids in this study.

In this study, all reaction systems, except those used for chlorine balance, were adjusted to pH=2.5 with hydrochloric acid (HCl). In these systems chloride, 3.2 mM, was the major sink for hydroxyl radical since its reaction with hydroxyl radical dominated over all other reactions of the radical. Hydroxyl radical concentration did not

significantly change over the reaction time. Chloride's second-order rate constant for reaction with HO· at pH~2 is 4.3×10^9 M^{-1} s^{-1} [49].

The reported average second-order rate constant for humic acids is $(1.7 \pm 0.7) \times 10^4$ (mg of C $L^{-1})^{-1}$ s^{-1} [64]. Though there are differences among humic acids based on different sources, Suwannee River humic acid will have a rate constant close to this magnitude, which is far below that for chloride. Although no value for fulvic acids was reported, based on the similarities between fulvic acids and humic acids, we assume that fulvic acids rate constants are close to those for humic acids. Fulvic acid rate constants are therefore much less than the one for chloride. Fulvic acid was added at a maximum concentration of 10 mg L^{-1} (~ 5.3 mg C L^{-1}). At the maximum concentration of fulvic acids, the reaction with chloride was 150 times more rapid than reaction with fulvic acid. Therefore chloride was the main sink for hydroxyl radical, and we can assume that the FA did not significantly alter the concentration of hydroxyl radical through scavenging. Although previous measurements have indicated that both FA and HA can alter the HO· formation rate, these effects are negligible at pH 2.5 [15, 29, 65]. It was reported that the measured hydroxyl radical concentrations with various FA concentrations showed no significant change upon addition of FA [61. 67]. The maximum concentration of humic acids added was 10 mg L^{-1} (~ 5.3 mg C L^{-1}). According to calculation, HA showed similar results [15,61]. Therefore, HA did not significantly change the generation of hydroxyl radical. In fact, pseudo first order kinetics were observed in the HO· quantitation measurements. These observations indicate that steady state hydroxyl radical concentration was reached and maintained throughout the degradations and that measured hydroxyl radical concentrations were reliable.

Furthermore, this conclusion was supported by degradations with PAHs monitored by fluorescence (in chapter IV).

Benzoic acid was used as a probe to measure hydroxyl radical concentration. Benzoic acid was chosen as a hydroxyl radical trap because it has a known rate constant, exhibits a characteristic product (p-hydroxybenzoic acid) upon reaction, and has a low partition coefficient for binding to FA or HA [27, 60]. Therefore, this probe was expected to yield hydroxyl radical concentrations representative of the bulk aqueous phase.

The concentration of HO· was measured by the following processes: an aliquot of BA solution was mixed with 0.5 mM $Fe(ClO_4)_2$ (the same concentration as applied in phenoxyacetic acids degradations) with a total volume 10ml. The pH was adjusted with HCl to pH=2.5. The amount of BA was determined with HPLC in order to prepare a plot of ln [BA] vs. time, in which the negative of the slope is the apparent first order rate, as illustrated by **figure 3.1**.

The decrease in concentration of a reagent with a second-order kinetics can be expressed by Eq 3.1

$$- d[A]/dt = k'' [A] [HO\cdot] \qquad \text{Eq 3.1}$$

With a constant concentration of hydroxyl radical, the equation can be converted to Eq. 3.2,

$$- d[A]/dt = k' [A] \qquad \text{Eq 3.2}$$

where k" and k' assigned to the second-order and pseudo-first-order reaction rates respectively and k' is equal to k" $\times$ [HO·]. Using a plot of ln[A] vs time, the

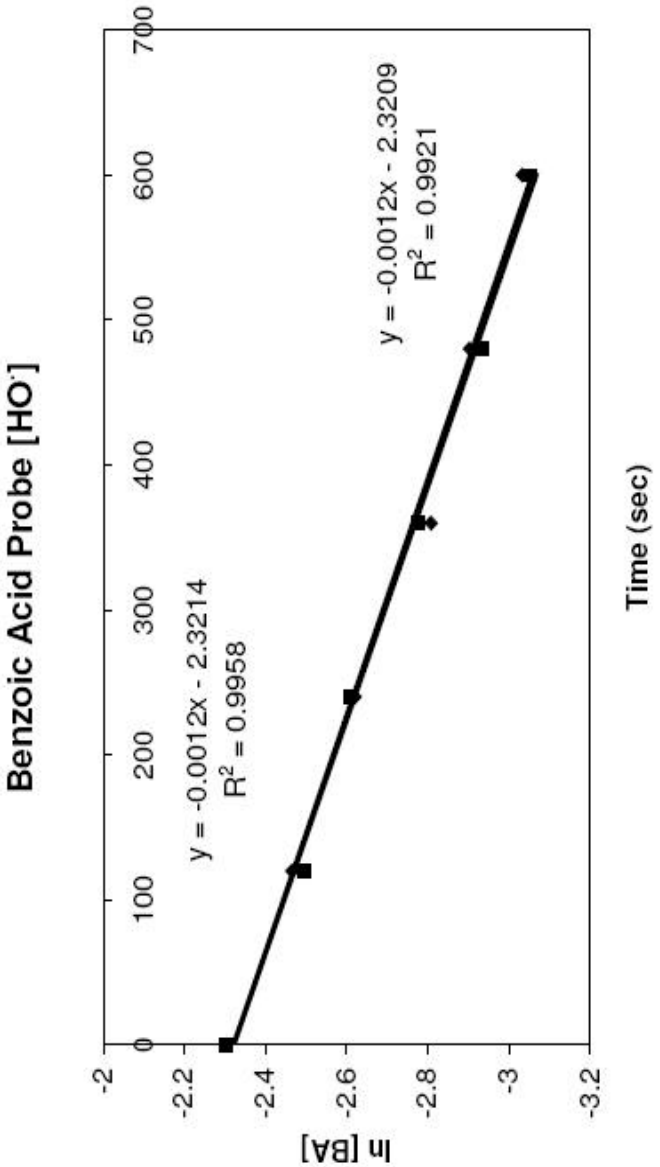

Figure 3.1. Plots of ln[BA] vs Time. BA-Benzoic Acid. Conditions: pH=2.5, initial [BA]=0.1mM; 0.5mM $Fe(ClO_4)_2$; Hydrogen Peroxide 5.0mM × 3.0ml/h.

value of k' can be obtained from the negative value of the slope. Since the second-order reaction rate constant of benzoic acid with hydroxyl radical is known, the observed value of k' can be used to determine the hydroxyl radical concentration from [HO·]=k'/k". The measured concentration of hydroxyl radical with 3.2 mM chloride, 0.5 mM $Fe(ClO_4)_2$ and 5.0 mM hydrogen peroxide added at 3.0 mL/h at pH=2.5 and 25 °C was $(2.87 \pm 0.02) \times 10^{-13}$ M.

Degradation of Phenoxyacetic acids

In Fenton chemistry, the degradation kinetics are often second order. With generation of a steady state concentration of hydroxyl radical, the reaction appears first-order in which the apparent reaction rate constant is equal to the second order rate constant times the concentration of the hydroxyl radical. Therefore, a plot of the log of the target species concentration vs. time is linear. For a compound with an unknown rate constant for reaction with hydroxyl radical, utilization of the measured hydroxyl radical concentration under specific conditions, the second order rate constant can be calculated. **Table 3.1** lists the absolute second order rate constants in water system for the four species of phenoxyacetic acids.

The degree of binding of a hydrophobic compound to dissolved DOM can be predicted by the following equation (**Eq 3.3**), according to Chin et al. [67, 68, 69]

$$f = \frac{[OC]K_{DOC}}{1 + [OC]K_{DOC}} \qquad \text{Eq. 3.3}$$

where f is the fraction of the compound bound to DOM (dissolved organic matter), K_{DOC} is the partition coefficient for binding to the DOM (normalized to dissolved organic

Table 3.1 Second-Order Rate Constants for four Phenoxyacetic Acids

Species	Second-Order Reaction Rate ($M^{-1}S^{-1}$)
2,4,5-T	3.88E+09 ± 1.25E+08
3,4-D	3.62E+09 ± 1.01E+08
2,4-D	3.60E+09 ± 7.67E+07
4-CPA	2.54E+09 ± 1.02E+08

carbon, DOC), and [OC] is the concentration of organic carbon in the DOM solution (equal to concentration of DOM multiplied with carbon percentage). If the measured values for K_{DOC} were not available, values could be calculated from K_{ow} with Equation 3.4 as proposed by Chin et al [70]:

$$\log K_{DOC} = 0.82 \times \log K_{ow} + 0.1923 \qquad \text{Eq. 3.4}$$

where K_{ow} is the octanol water-partition coefficient, the ratio of concentration in octanol and water phases. **Table 3.2** lists measured partition coefficients for several compounds.

Table 3.2 K_{ow} Values of 2,4,5-T, 3,4-D and 2,4-D

Species	K_{ow}
2,4,5-T	$(2.9\pm0.2)\times10^2$
3,4-D	$(3.0\pm0.2)\times10^2$
2,4-D	$(2.4\pm0.2)\times10^2$

Since hydrophobic species tend to bind with DOM in environmental systems, their bioactivity and transport is changed by DOM. From the measured K_{ow} values and with Eq. 3.3 and Eq. 3.4, the fraction bound can be calculated. If it is assumed that the bound material did not react with hydroxyl radical (rate constant = 0), then the resulting apparent rate constant can be calculated by multiplying the rate constant in pure water by the fraction of compound freely dissolved [$(1 - f)$ for pseudo first order, $(1 - f)^2$ for pseudo second order], This approach assumes that no other factors change upon addition of HA/FA. The resulting calculated rates would be the maximum expected effect from HA/FA on the oxidation activity of pollutant. This effect is presumably caused by restricted access of the hydroxyl radical to the bound phenoxyacetic acids.

In order to compare the calculated maximum inhibition with experimental observations, rate constants were measured under steady state hydroxyl radical concentration as a function of added FA or HA concentration. The negative of the slope of curves of ln[A] vs time yielded pseudo first order rate constants for all compounds. The second order rate constants were then calculated by dividing by the steady state [HO·] measured with BA probe. **Figure 3.2** illustrates 2,4,5-T degradation rates at different concentrations of FA and HA, in which the top solid line represents the maximum quenching due to binding to HA (The divergence between experimental observation and modeling for other phenoxyacetic acids is similarly obvious). **Figure 3.3** is the combination of apparent first order rates of four species in the presence of HA. **Figure 3.4** is combination of apparent first order rates of four species to allow easy comparison of the effect of FA on different compounds.

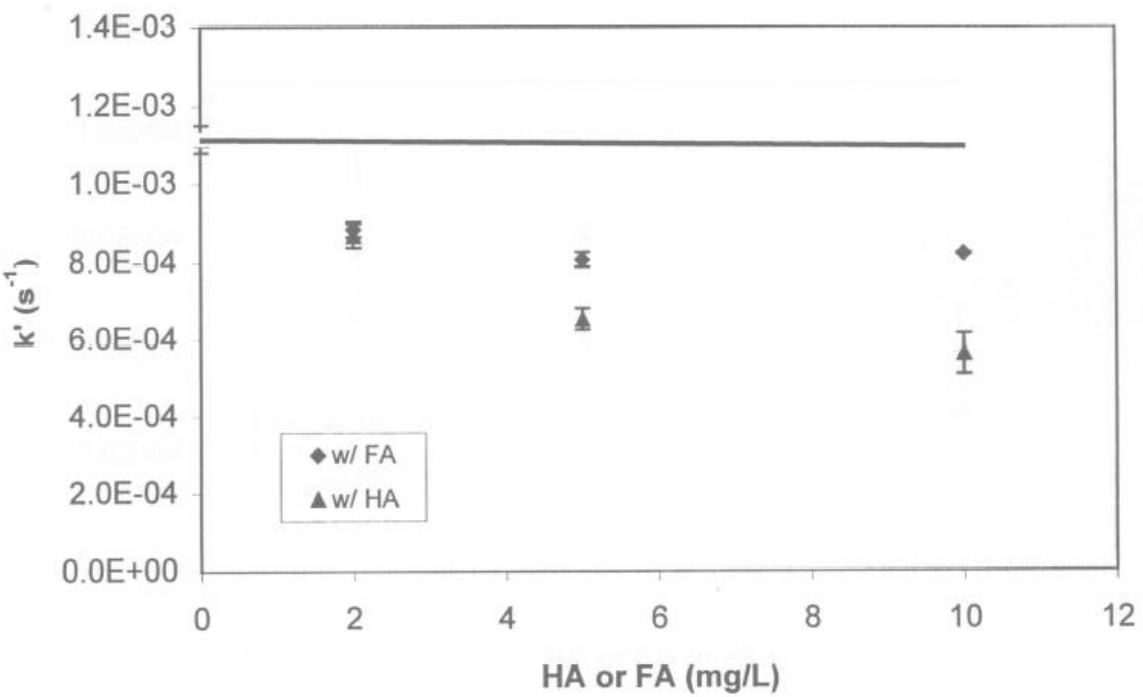

Figure 3.2 illustrates degradations of 2,4,5-T with different concentrations of HA or FA. Conditions: pH=2.5; 0.1mM 2,4,5-T, 0.5mM $Fe(ClO_4)_2$; hydrogen peroxide: 5mM × 3.0ml/h. Solid line represents the expectation value based on Eq. 3.3

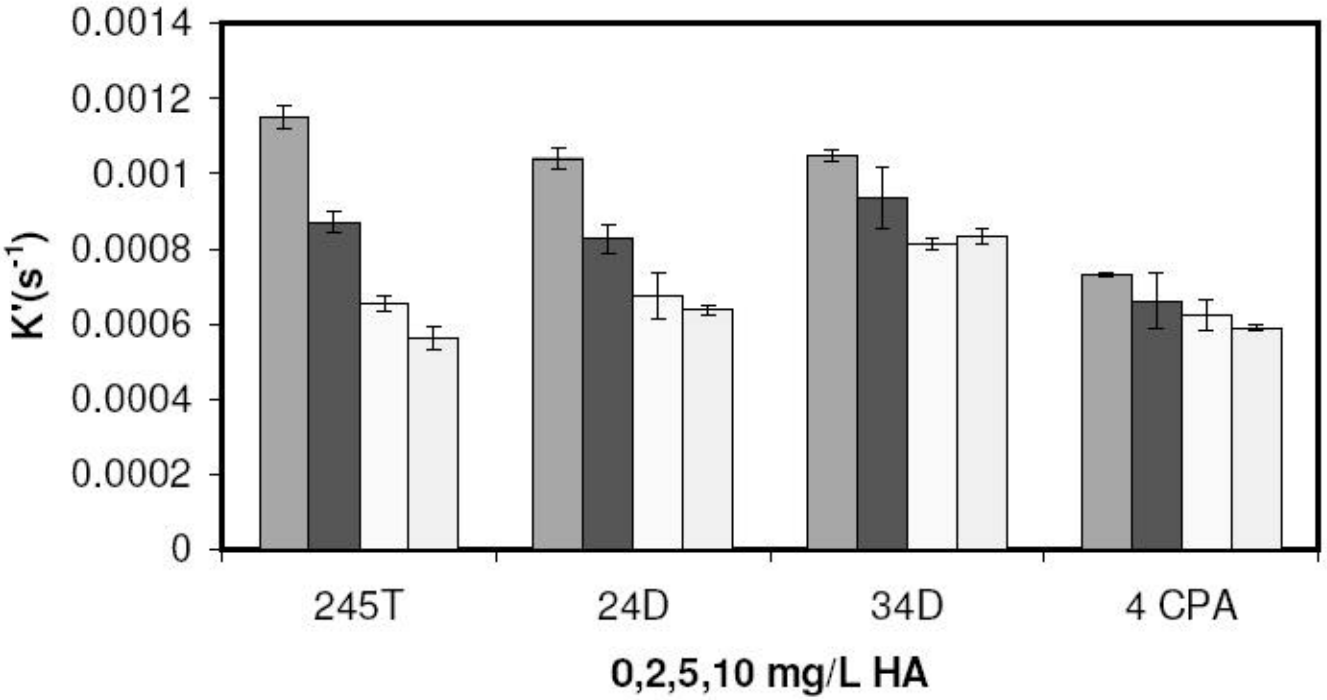

Figure 3.3 Combination of degradations of 2,4,5-T, 2,4-D, 3,4-D and 4-CPA with 0, 2.5, 5.0, 10.0mg/l HA. Y-axis: apparent 1st order rate.

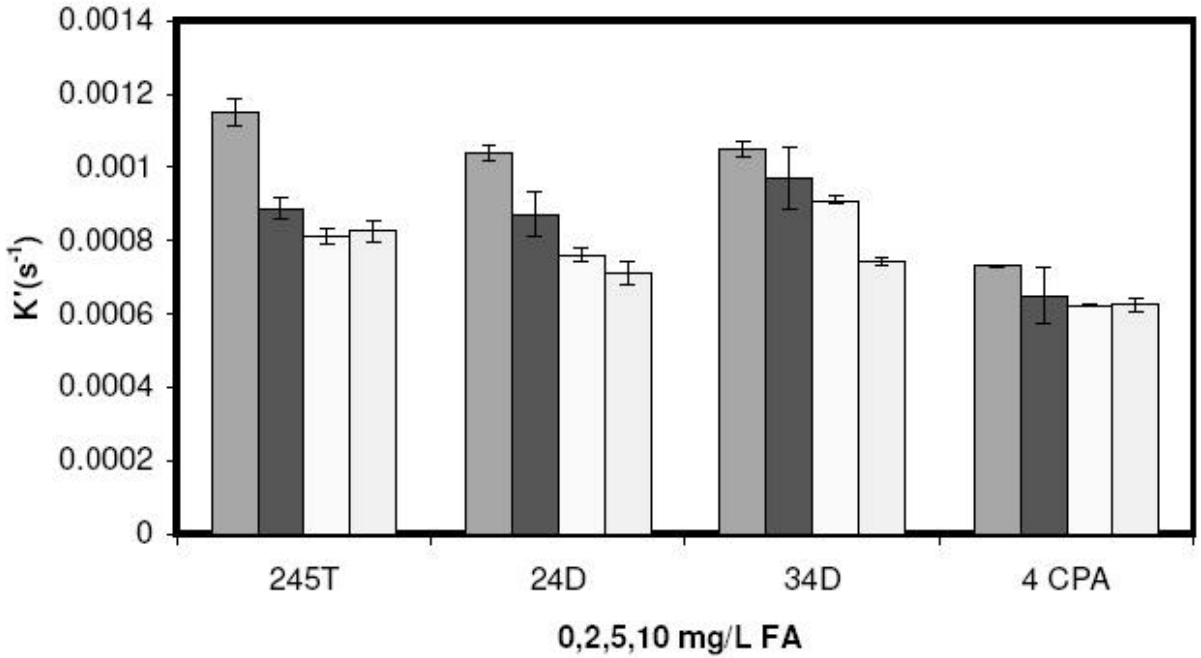

Figure 3.4 Combination of degradations of 2,4,5-T, 2,4-D, 3,4-D and 4-CPA with 0, 2.5, 5.0, 10.0mg/l FA. Y-axis: apparent 1st order rate.

As all the figures show, addition of both HA and FA caused reduction in the oxidation rate, and the effect of HA is generally bigger than the one for FA. The impact of HA/FA on different species varies, as illustrated with figure 3.3 and 3.4. The extent of FA or HA effect is correlated to the hydrophobicity of the phenoxyacetic acid with the biggest reduction for 2,4,5-T and the smallest for 4-CPA. 2,4-D and 3-4-D showed similar effects.

On comparison with calculated values, as can be seen from the figures, there are significant differences between the predicted values using the model and the experimental values. At 10 mg/L FA, 2,4,5-T is expected to have only less than 1% binding to HA. The corresponding observed reduction in apparent rate constant is almost 50%. Similar phenomena were observed for the other three phenoxyacetic acids. Binding of the phenoxyacetic acids to HA/FA is not enough to trigger such big differences.

Another possibility is whether a change in bulk hydroxyl radical concentration was responsible for the different apparent decreases in k. If the bulk concentration of hydroxyl radical changes and this is a dominant contribution to the observed reduction of the observed pseudo-first-order reaction rate constants, then all the compounds would have shown the same fractional change in the observed reaction rate constants at each level of added HA or FA. In contrast, the experimental data showed significantly different fractional changes for each compound studied. For example, 2,4,5-T changed from $(1.12 \pm 0.04) \times 10^{-3}$ in a pure water system to $(5.63 \pm 0.02) \times 10^{-4}$ with 10 mg/L HA (roughly 50% reduction) meanwhile the change for 4-CPA was only from $(7.3 \pm 0.3) \times 10^{-4}$ to $(5.90 \pm 0.07) \times 10^{-4}$ (roughly 20% reduction). These changes are correlated with

the solubility of the compounds. Lower solubility compounds showed a more dramatic decrease in observed k', indicating that partitioning plays an important role in the apparent decreases in rate constants.

As discussed previously, the current partitioning model cannot explain the magnitude of change. The effective radical concentration is related to the generation rate of HO· and the arrival of the HO· upon the target. With DOM, the arrival rate of the HO· could be changed and then the apparent rate constants changed. FA and HA molecules have physically separate hydrophobic and hydrophilic regions, and metal binding sites are spatially isolated from hydrophobic sites [32,33,71]. The physically separated hydrophobic and hydrophilic sites would bind corresponding groups. For example, hydrophobic benzene rings and saturated aryl chains tend to bind with hydrophobic sites, while carboxylic and hydroxyl groups tend to chelate with iron (II). Hydrophobic compounds, even those with considerable water solubility, would tend to avoid such strongly polar carboxylic and hydroxyl sites. So binding of iron (II) to the hydrophilic sites would localize hydroxyl radical formation to these sites, from which hydrophobic species are separated. Furthermore, this tendency would be proportional to the hydrophobicity of species. This two-fold mechanism, in which hydroxyl radical is concentrated into polar regions and non-polar compounds partition into hydrophobic regions, could explain why organic compound partition coefficients are not sufficient to explain the observed rate constant effects and why higher hydrophobic compounds have more dramatic decrease in degradation rates with the same levels of HA and FA.

As discussed formerly, if the pesticides can be brought into proximity with iron, it would likely increase the degradation rate. Carboxymethyl-beta-cyclodextrin (CM-ß-CD)

can behave in this manner. Its non-polar cavity complexes hydrophobic compounds and the carboxymethyl groups can chelate the iron. Meanwhile cyclodextrin increases the solubility of the hydrophobic pesticides. So expectedly it would bring the compounds closer to the hydroxyl radical formation site, and then contribute to an increase in the degradation rate. **Figure 3.5** shows the effect of CM-ß-CD on the degradation of 2,4,5-T with 5 mg/L HA. The degradation rate constant is increased with CM-ß-CD added. The increase of the degradation could be contributed from two possibilities: 1) increase of the concentration of the hydroxyl radical and 2) the effect of CM-ß--CD. In Fenton chemistry, the concentration of the hydroxyl radical depends on two elements, the added peroxide rate, equal to concentration multiplied with flow rate of the peroxide added, and the activity of the catalyst. Since the peroxide concentration and its addition rate were kept constant, any increase in the hydroxyl radical concentration can only result from the effective concentration change of iron(II). **Figure 3.6** shows the 2,4,5-T degradation rates with 0.5 mM CM-ß-CD but different concentrations of iron (0.5, 1 and 5 mM respectively). This data shows that any change in the rate constants was within the error range. So the effect of an increase in degradation is caused by CM-ß-CD, which brings the pesticides closer to the iron or the hydroxyl radical formation site. Evidence for the existence of a ternary complex of iron, cyclodextrin, and a hydrophobic pollutant has been provided using electrospray mass spectrometry as discussed in Chapter V.

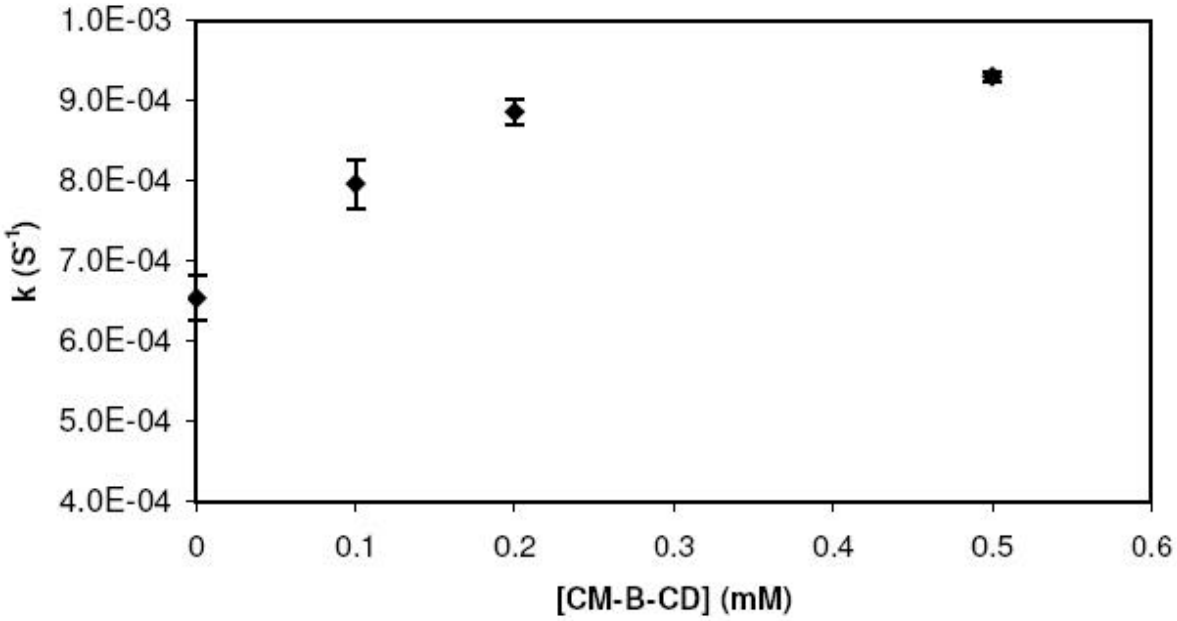

Figure 3.5 illustrates degradations of 2,4,5-T with CM-β-CD. Conditions: pH=2.5 (with HCl); 0.1mM 2,4,5-T; 0.5mM Fe(ClO4)2; 0.5mg/l HA with 0.1, 0.2, 0.5mM CM-β-CD.

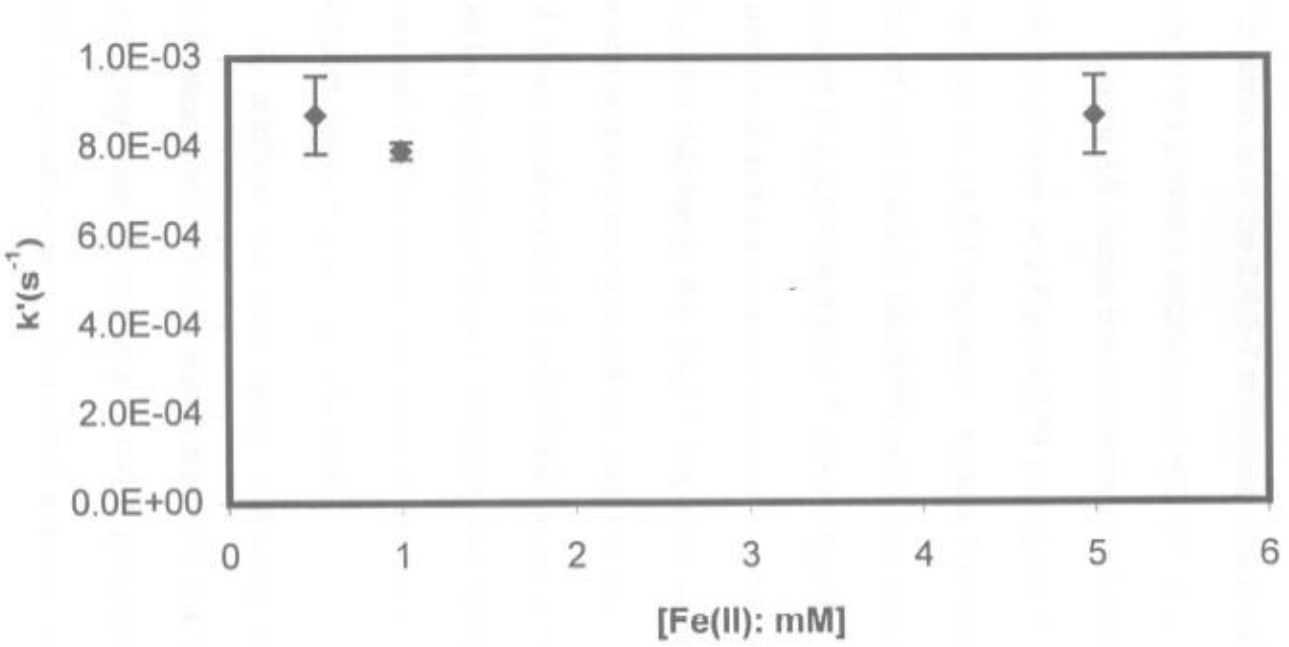

Figure 3.6 illustrates degradations of 2,4,5-T with different concentrations of Fe(II). Conditions, pH=2.5 (with HCl); 0.1mM 2,4,5-T; 5mg/L HA; 0.5 mM CM-β-CD with 0.5, 1.0, 5.0 mM Fe(II).

Products and chlorine balance.

Dechlorination was observed and reported[72] in 2,4,5-T degradation. In chlorine mass balance experiments, since ferrous sulfate was used in place of ferrous perchlorate, and the solution was not adjusted with HCl, the only source of chloride was dechlorination in the degradation. Chloride ion was monitored by ion chromatography (Dionex DX 500) eluting with 4.8 mM Na_2CO_3/0.6 mM $NaHCO_3$ at 1.5 mL/min. As in previous experiments, 2,4,5-T was monitored with HPLC with conditions similar to the previous degradations with pH adjusted to 2.5.

Figure 3.7 shows the chloride generated vs. the amount of 2,4,5-T degraded. **Figure 3.8** shows the total amount of 2,4,5-T remaining and 2,4,5-T degraded with two assumed conversions: 3:1 and 1:1 chloride generated to 2,4,5-T degraded. Dechlorination occurred and as reaction time increased more and more chloride was generated. However the ratio of the chloride produced to the 2,4,5-T degraded, in figure 3.7, did not go up much over one and at 8 minutes the ratio of chloride to 2,4,5-T degraded went down to about 0.8. If dechlorination were the only reaction, then the ratio should be over 1.0 at least. This indicates that some other reactions, for example hydroxylation, breakage of benzene ring and oxidation of the acetic-acid chain, happened at the same time.

2,4-D was reported as a product of 2,4,5-T degradation [73]. As seen in figure 3.7, at the beginning of the degradation of 2,4,5-T, the ratio of chloride generated to the amount of 2,4,5-T consumed is about 1.2. The combination of dechlorination must contain mono-dechlorination, which may suggest 2,4-D was generated. With GC-MS,

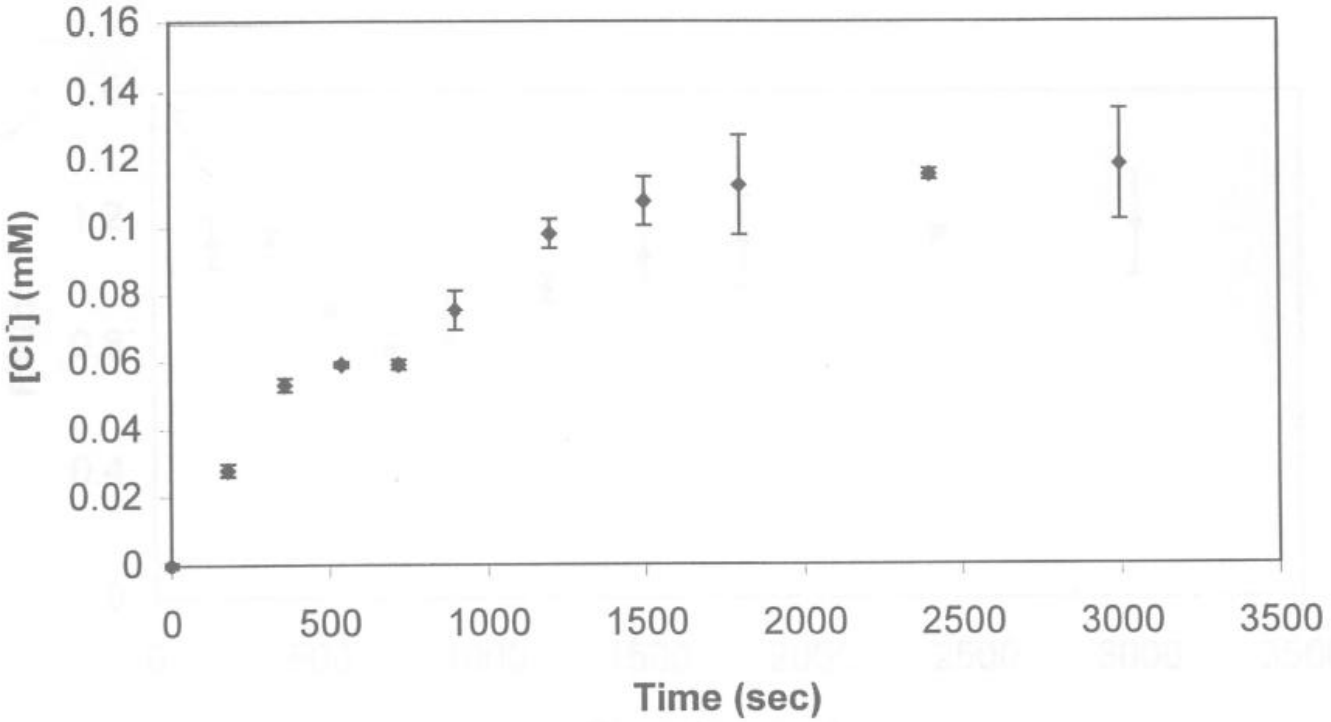

Figure 3.7. Concentrations of chloride as function of time. Conditions: pH unadjusted; initial [2,4,5-T]=0.1mM; 0.5mM $Fe(ClO4)_2$ and hydrogen peroxide: 5mM × 3.0ml/h.

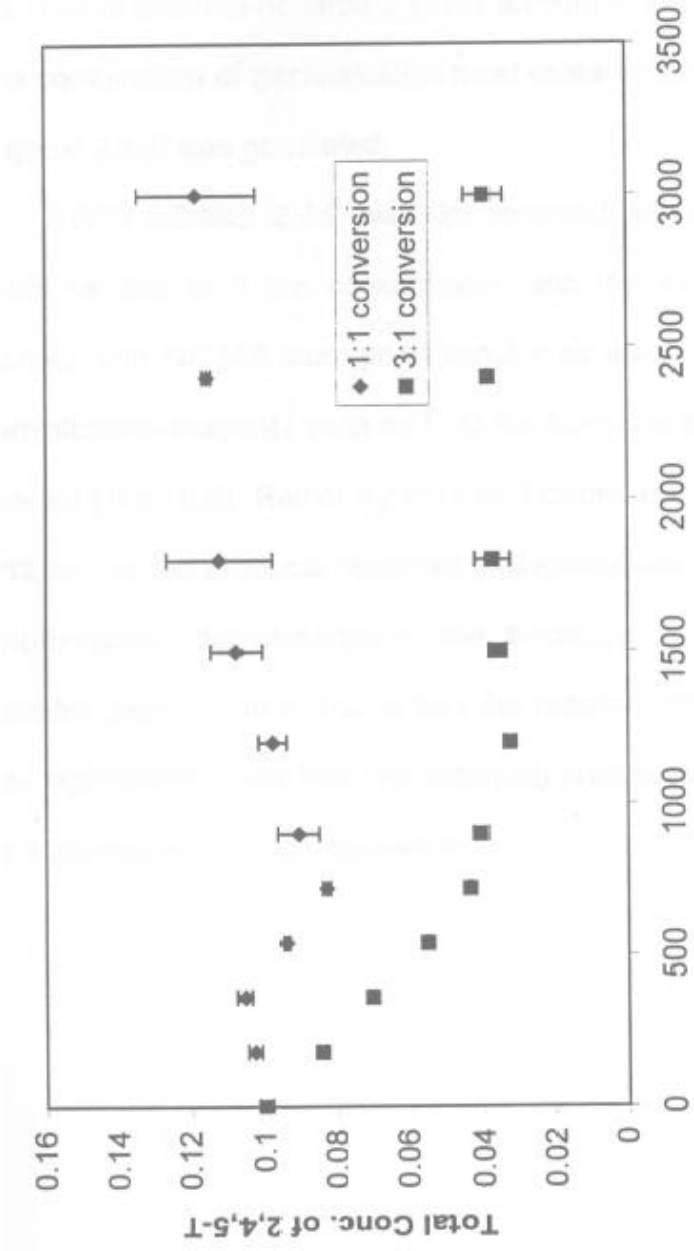

Figure 3.8. The total 2,4,5-T (remained + degraded) with two conversions: 3:1 and 1:1 chloride generated to 2,4,5-T Degraded. Conditions, same as in figure 3.7.

2,4-D was not observed with degradation of 2,4,5-T. This could be due to high polarity of phenoxyacetic acids and their low extraction efficiency. Normally to observe highly polar species, such as acids and aldehydes/ketones, derivatization reagents such as O-(2,3,4,5,6-pentafluorobenzyl)hydroxy amine are needed[74,75]. Monohydroxy-dichlorobenzene and dihydroxy-monochlorobenzene were detected, indicating hydroxylation, decarboxylation and breakage of the side chain.

Chapter IV PAHs

Generation of Steady State Concentration of Hydroxyl Radical

Similar to the experiments with phenoxyacetic acids, PAH studies utilized a steady state concentration of hydroxyl radical that was generated by a continuous addition of hydrogen peroxide with a syringe pump. Time-base fluorescence spectroscopy was used with individually optimized excitation/emission wavelengths for each PAH. In each set of experiments, a scavenger (e.g. chloride or methanol) was used to balance the generation of the hydroxyl radical. The steady state concentration was generally reached within roughly 15~20 seconds. As discussed in Chapter III, if the concentration of hydroxyl radical remains constant, then the reaction follows pseudo-first-order kinetics, in which the apparent pseudo-first-order reaction rate constant is equal to the second order rate constant multiplied by the concentration of the hydroxyl radical. The linearity of the plot of ln[conc.] vs. time was obvious and straight. The R^2 value, close to 1, indicates that steady state hydroxyl radical concentration was maintained and that the scavenger was present in high enough amounts so that its concentration change during the degradation was negligible.

Degradation of PAHs in the Presence of Humic Acids

PAHs are strongly hydrophobic species. In natural aqueous systems, they tend to sorb to hydrophobic species including porous surfaces and sediments. With natural

dissolved organic matter, hydrophobic species tend to partition into hydrophobic sites of humic acids[76] and the solubility will be increased. Dissolved soil humic acids were assumed to provide a sufficiently large intramolecular non-polar organic environment for promoting a partition-like interaction with relatively non-polar organic solutes.

Figure 4.1 is the combination of degradation of pryene, phenanthrene and anthracene with humic acids. As illustrated in figure 4.1, humic acids prohibit the degradations of pryene, phenanthrene and anthracene and the effect varies significantly. With 10 mg/L humic acids, the rate constant for phenanthrene was decreased about 60% while pryene and anthracene exhibited only a 20% decrease. Generally with more humic acid added, the degradation became slower. Since the initial concentration of each species was the same, this indicates that more PAHs partitioned into the humic acids.

The partition constant can be expressed with (**Eq. 4.1**)

$$K = [PAH:HA] / ([PAH] * [HA]) \qquad (4.1)$$

Higher concentration of HA results in higher amounts of PAH bound to HA, which means more percentage of PAH partitioned into HA. Though the hydrophobicity of one species is one contribution to how much the species would partition into humic acids, the size and geometry of the structure could affect the partitioning also. It was reported that time course batch experiments revealed that the association of PAHs to humic acid included a slow stage with equilibrium time of 5-7 days[77]. In the experiment, humic acids was added and left for equilibrium for about 4 hours. Therefore, any long-term equilibration was not achieved in these experiments. Long time for equilibrium leaves problems of PAH loss by absorption by the vessel[78].

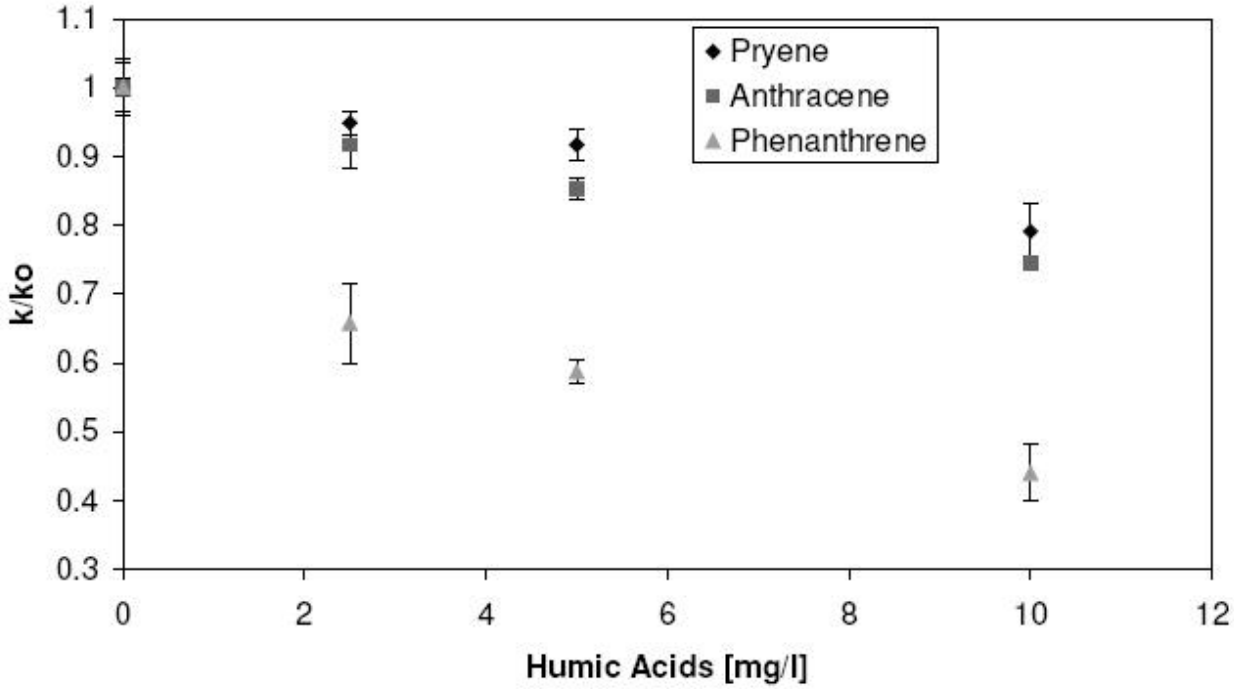

Figure 4.1 illustrates degradations of pryene, anthracene and phenanthrene with HA. Conditions: 3.0ml 0.1µM PAH, 0.1ml methanol, hydrogen peroxide: 5mM *1.0 ml/h with 0, 2, 5, 10 mg/l HA. Fluorescence wavelength: 336/372nm, 356/339.4nm and 252.1/364.4nm respectively.

Fortunately, with the same equilibrium time for each species, comparison of results between species can reveal the general effects of humic acids on the degradations.

As was discussed in Chapter III, assuming that partitioning into humic acids inhibits degradation completely, the maximum inhibition in reaction rate due to binding alone could be calculated from multiplying the rate constant by the fraction of the compound freely dissolved [$(1 - f)$ for pseudo first order, $(1 - f)^2$ for pseudo second order], where the fraction bound could be calculated from Eq 3.2. Li *et al* reported the log values of partition coefficients for phenanthrene, pyrene and anthracene as 4.12, 4.62 and 4.00 respectively [79]. When calculated rate constant values were compared with the experimental data, there was a significant difference between the experimental values and the calculated values for phenanthrene as illustrated by **figure 4.2.** Based on the same comparison, similar phenomena were observed with pyrene and anthracene, although the magnitude of the deviation between predicted and observed values is different for these two compounds. As was discussed in chapter III, the reasonable explanation for these observations is isolation of the hydroxyl radical generation site from the target species binding site within humic acids.

The measured pseudo-first-order reaction rate constants for phenanthrene, anthracene and pyrene were $(5.4 \pm 0.2) \times 10^{-3}$, $(3.3 \pm 0.4) \times 10^{-3}$ and $(2.8 \pm 0.1) \times 10^{-3}$ s^{-1}, respectively. Based on calculations using eq 3.3 and eq 3.4, these three PAHs have similar partition coefficients. Therefore, the three compounds should have similar extents of binding to the humic acids. The fact that the observed rate constants for

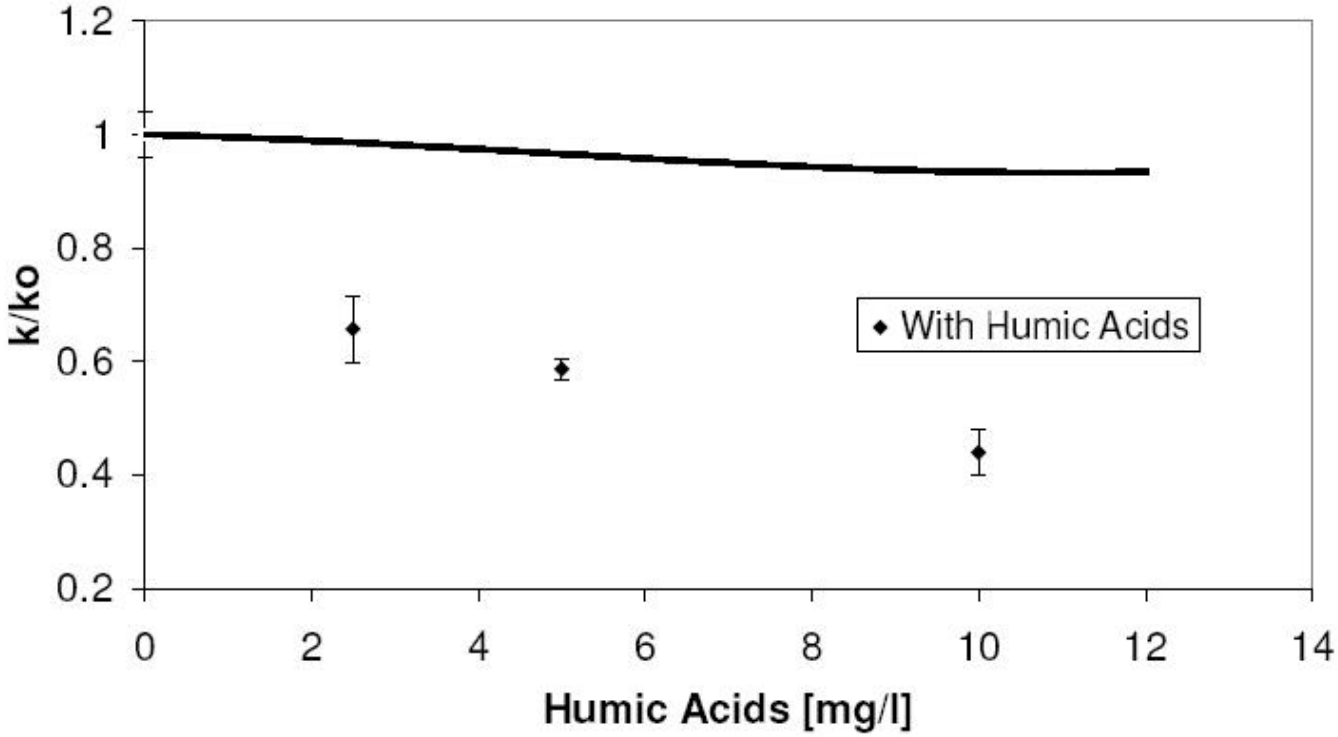

Figure 4.2 illustrates degradations of phenanthrene with HA with comparison of calculated values. Conditions: 3.0ml 0.1µM PAH, 0.1ml methanol, hydrogen peroxide: 5mM *1.0 ml/h with 0, 2, 5, 10 mg/l HA. Wavelength: 252.1/364.4nm. The solid line represents the calculated value according to Eq. 3.3 and 3.4.

these compounds showed different responses upon addition of humic acid indicates that the reactivity is not simply related to how much PAH is bound to the humic acid.

Degradation Remediation with Carboxymethyl-β-Cyclodextrin

Based on the previous discussion and explanation of the degradation kinetics with humic acids and fulvic acids, it is apparent that the distance between iron(II) and the PAH is crucial. If there is species which could bring the radical generation site into proximity with the target pollutants, the degradation would be improved. Carboxymethyl-β-cyclodextrin (CM-ß-CD) fits in this way. It entraps PAHs, which are highly hydrophobic, into its internal hydrophobic cavity. Meanwhile, its carboxymethyl groups can chelate iron. So it might be expected that it would bring the pollutant compounds close to the hydroxyl radical formation site, and then contribute to increasing the degradation rate. Another advantage could be that CM-ß-CD increases the solubility of the hydrophobic pollutants and aids in removing them from sorption sites. **Figure 4.3** illustrates the degradation rates of pyrene, phenanthrene and anthracene with application of CM-ß-CD up to 1.0 mM. The observed enhancement in degradation persists even in the presence of 2.5 mg/L HA with only a slightly lower enhancement than without HA. **Figure 4.4** illustrates the degradation of naphthalene with application of CM-ß-CD up to 1.0 mM. As we assumed that CM-ß-CD can entrap hydrophobic pollutants and chelate with iron(II) at the same time, the percentage of the pollutants entrapped will definitely affect the apparent reaction rate. If appearance of the ternary complex increases the reaction rate by bringing the target pollutants closer to the iron

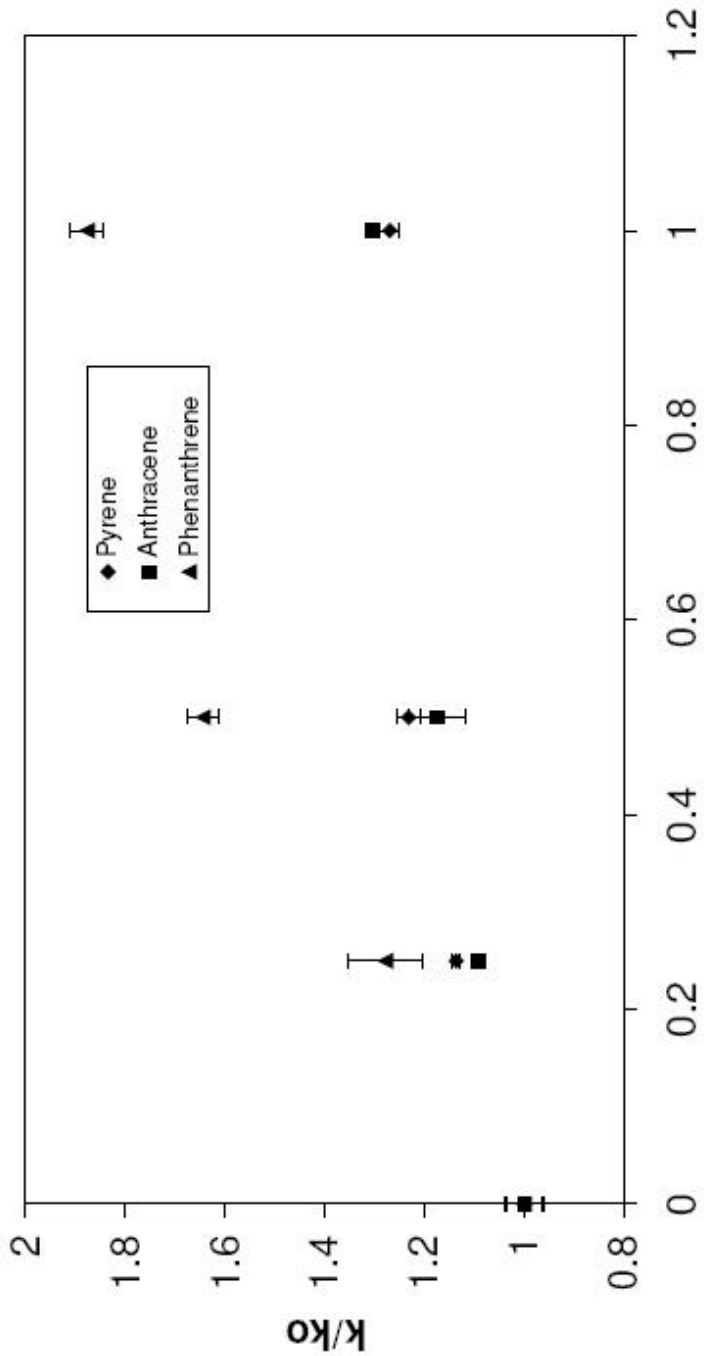

Figure 4.3. Impact of CM-β-CD on degradations of pyrene, anthracene and phenanthrene.

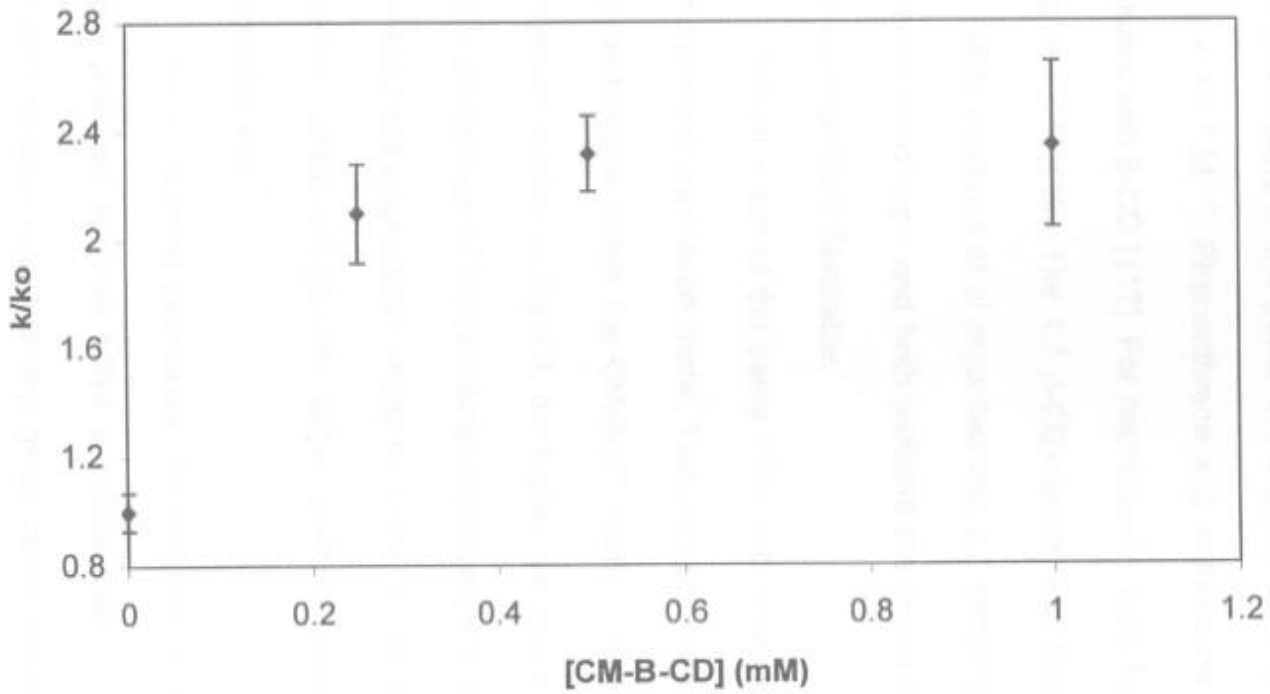

Figure 4.4 illustrates degradations of naphthalene with CM-β-CD. Conditions: 25μM naphthalene, 3.2mM [NaCl]; Hydrogen peroxide, 10.0mM × 0.7ml/h with 0, 0.25, 0.50 and 1.00 mM CM-β-CD. Fluorescence: 281/333nm.

site than without CM-ß-CD, then the apparent rate would be bigger than the one in pure aqueous system without CM-ß-CD. As seen in the figures, application of CM-ß-CD dramatically increases the degradation of PAHs (including pryene, phenanthrene, and anthracene), even in the presence of humic acids. This indicates the potential applicability of CM-ß-CD to a real system which contains humic acids.

As we see in figure 4.3, the enhancement of CM-ß-CD is different for different pollutants. The biggest observed effect was with naphthalene. With 1.0 mM CM-ß-CD, the enhancement is about 2.4 times, while roughly 1.9, 1.3 and 1.2 times for phenanthrene, anthracene and pyrene respectively. This could be due to the percentage of entrapment and the geometry of the complex. In fact, pyrene was reported to form a 1:2 (ß-CD:pyrene) complex [80] though 1:1 was formerly reported [81]. According to the paper of Pena, the binding constant for 1:2 formation is 8.53×10^5 M^{-1}. Phenanthrene and anthracene were reported to form 1:1 complexes with ß-CD [82]. For naphthalene, both formation of 1:1 and 2:2 were reported [83]. The 1:1 ß-CD:naphthalene formation constant was 377 ± 35 M^{-1}, while Avakyan et al regarded that 2:2 formation, in which ß-CD exists as a "head-to-head" type and both partners are linked by a system of H-bonds, was more energetically favorable.

With a given PAH, the more CM-ß-CD was added, the greater the reaction enhancement was. This effect was attributed to a higher percentage of the PAH entrapped within the CM-ß-CD cavity, as indicated by the binding constant expression (Eq 3.3). The apparent degradation would be further improved by greater formation of the complex, which brings the target species closer to iron(II) or the radical generation site.

As discussed previously, the distance of the hydroxyl radical from the target pollutant species plays a critical role in the degradation rate. Some pollutant species with hydroxyl groups could complex directly with iron(II) to a certain degree. Such compounds would therefore have a close proximity to iron(II) in aqueous solution. With added CM-ß-CD, although these pollutant species bind to the cavity of CM-ß-CD, the accumulative effect would be different from that seen previously for the four PAHs studied.

Figure 4.5 illustrates CM-ß-CD effects on the degradation of 2-naphthol with the same conditions used for naphthalene as represented in figure 4.4. As illustrated in figure 4.5, with CM-ß-CD added, the degradation decreased rather than increased. This could be due to the negative effect of CM-ß-CD on bringing 2-naphthol closer to iron(II), since 2-naphthol initially binds with iron(II) closely. Another contribution is that lower binding of 2-naphthol to CM-ß-CD could result in a loss of the enhancing effect while scavenging effects are increased by the presence of the cyclodextrin.

If this is true, 2,3-dihydroxynaphthalene, which could chelate with iron(II) much more strongly than 2-naphthol does, would have more substantial decreases in degradation rate. In fact, chelation by the 2,3-dihydroxynaphthalene is so strong that the degradation is initially very fast, as illustrated as **figure 4.6**. For the same reason, if the species initially binds to Fe(II), then addition of CM-ß-CD in effect takes the pollutant away from Fe(II), resulting in decreased degradation rates.

Figure 4.7 illustrates degradation of 2-naphthol with CM-ß-CD with different percentages of acetic acid. As figure 4.7 illustrates, addition of acetic acid altered the

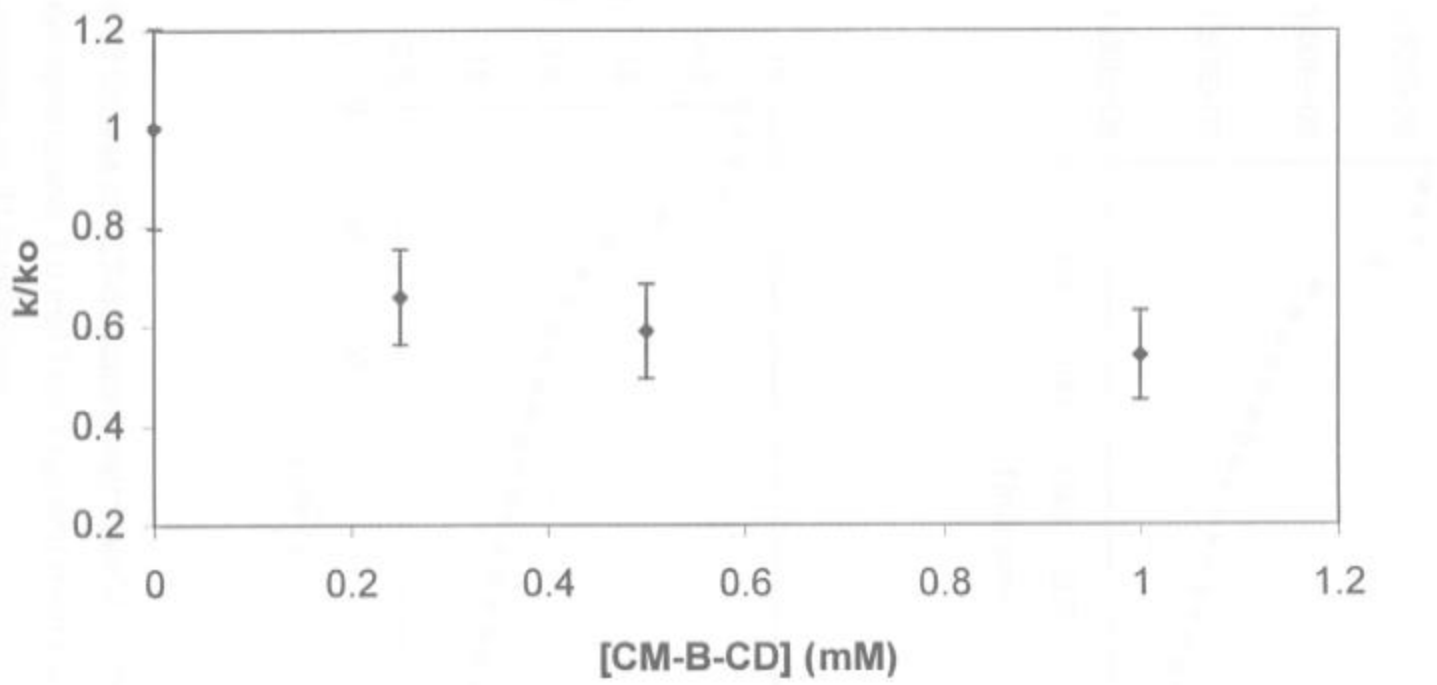

Figure 4.5 illustrates degradations of 2-naphthol with CM-β-CD. Conditions: 25μM naphthol, 3.2mM [NaCl]; Hydrogen peroxide, 10.0mM × 0.7ml/h with 0, 0.25, 0.50 and 1.00 mM CM-β-CD. Fluorescence: 303/455nm.

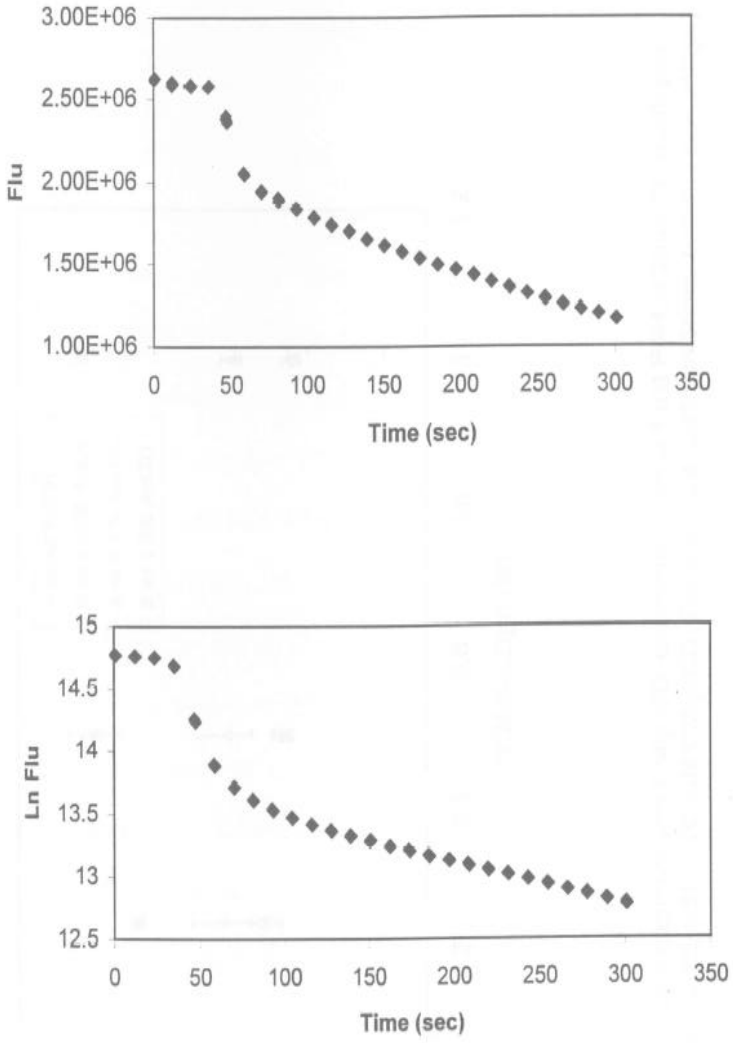

Figure 4.6. Curves for 2,3-dihydroxylnaphthalene. Conditions: 25μM 2,3-dihydroxylnaphthalene; 1.0 mM Fe(ClO4)2 and hydrogen peroxide: 10.0mM × 0.7ml/h. Fluorescence wavelength: 317/386nm.

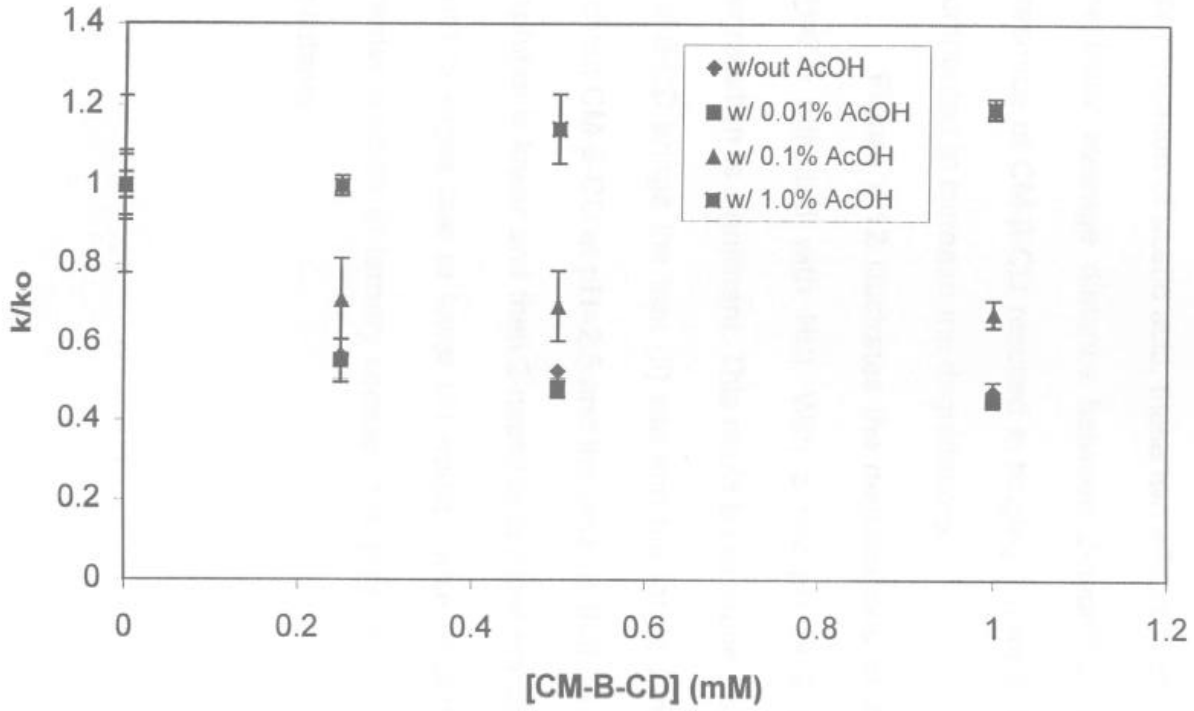

Figure 4.7 illustrates degradation of 2-naphthol with CM-β-CD with various amount of AcOH. Conditions: 25μM 2-naphthol, 3.2mM [NaCl], hydrogen peroxide: 10.0mM × 0.7ml/h with 0, 0.25, 0.50, 1.00mM CM-β-CD. Wavelength 303/455nm. Amount by volume percentage.

degradation rates. Since the added acid would keep 2-naphthol in its protonated form, the binding of 2-naphthol to iron(II) would be less, and the entrapment into the CM-ß-CD cavity would be stronger. Meanwhile acetic acid itself binds to iron(II) as a competition against the binding or 2-naphthol to iron (II). With increased concentration of acetic acid, these two effects both become stronger, resulting in a greater separation of 2-naphtnol from the iron. Under these conditions, the presence of CM-ß-CD resulted in bringing 2-naphthol closer to iron(II) and consequently contributed to increase the degradation rate.

Figure 4.8 illustrates the degradations of 2-naphthol with CM-ß-CD at pH=2.5 adjusted with HCl. With a low pH of 2.5, the enhancement of the degradation is significant. This could be explained by two points: one is that the CM-ß-CD brings the iron(II) site and the target 2-naphthol closer compared to without CM-ß-CD at pH=2.5 and the other is that, at lower pH, the solubility of 2-naphthol is lower and 2-naphthol is more entrapped in the CM-ß-CD cavity. Both changes due to lower pH would cause formation of a greater amount of ternary complex, bringing the iron(II) site closer to the target pollutants.

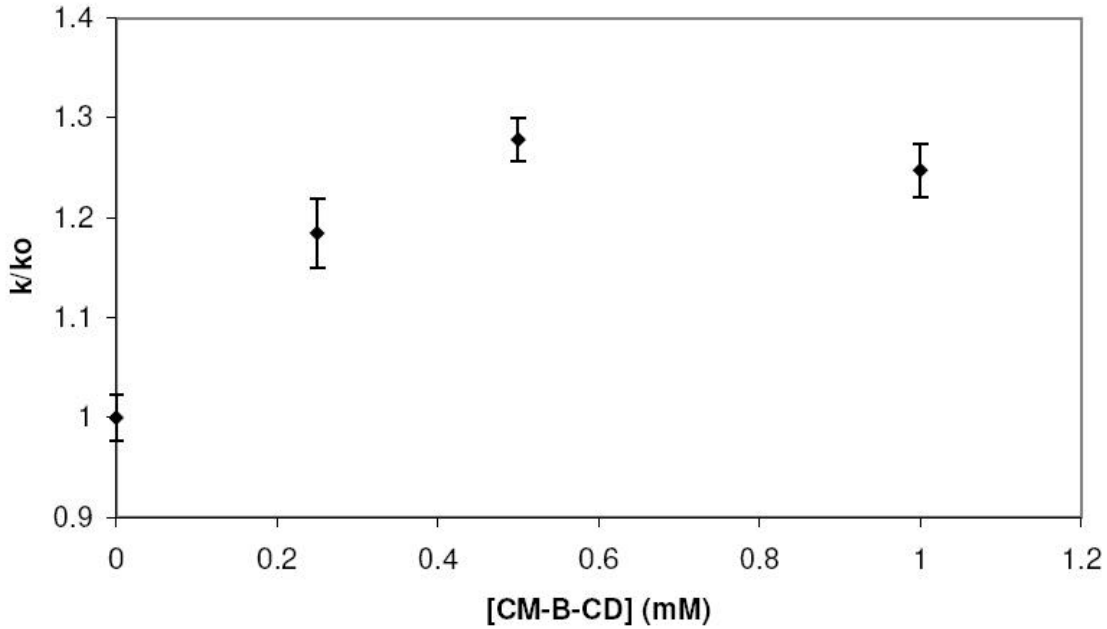

Figure 4.8 illustrates degradations of 2-naphthol with CM-β-CD. Conditions: pH=2.5(HCl), 25μM 2-naphthol, 3.2mM [NaCl], hydrogen peroxide: 10.0mM × 0.7ml/h with 0, 0.25, 0.50, 1.00mM CM-β-CD. Wavelength 303/455nm.

Chapter V Ternary Complex

Existence of the complexes

Both the inner surface of cyclodextrin and the exterior of guest molecules suitable for formation of inclusion complexes are hydrophobic. To form the binary complex, it is the hydrophobic surfaces which come into contact with each other, while contact of the hydrophobic guest and water is reduced. This is the main driving force for formation of guest-host complex. Generally, all suitably sized hydrophobic species can enter the cyclodextrin cavity. The existence of the binary complex was reported many years ago and was proven with various methods, including ^{1}H-shift in NMR, spectrum variance with appearance of cyclodextrin, etc [69].

One good way to detect the ternary complex is through electrospray mass spectrometry (ES-MS). Samples were made simply by mixing saturated guests with 1.0 mM cyclodextrin in aqueous media. Samples were injected under conditions with low sampling cone voltages, since higher accelerating voltages tend to break the non-covalent binding between the guest and host. The binding of PAH-cyclodextrin complex would be much weaker than complexes of guests such as phenylphenol or 2,4-5-T. Since PAHs would not have hydrogen bonding with hydroxyl groups of the cyclodextrin, the binding of a PAH in the non-polar cavity of cyclodextrin is a non-polar, non-covalent interaction, which is very weak and not prone to be stable.

ES-MS peaks of binary pollutant-cyclodextrin complexes were observed. MS-MS of these isolated complexes yields peaks for free cyclodextrin. Singly-charged and doubly-charged (with sodium) peaks were both observed. When iron(II) was added, ternary complexes with Fe(II) were observed. Similarly MS-MS spectra support the existence of the complexes. **Table 5.1** lists peaks observed on complexes of various guests. Figure **5.1** shows spectra of a ternary complex of ß-CD:2,4,5-T:Fe(II), m/z 722.1, and ß-CD:2,4,5-T(2):Fe(II), m/z 850.4. MS-MS of the peak at 722.1 yielded peaks for the binary complex ß-CD:Fe(II) as well as the parent peak of ß-CD:2,4,5-T:Fe(II).

2) The radical concentration and Fe(II) activity/concentration.

The radical concentration of the hydroxyl radical can be expressed by **Eq. 5.1** [60]:

$$k_1 [Fe(II)] [H_2O_2] = [HO^{\cdot}] \Sigma(k_i [S_i]) + k_2 [HO^{\cdot}] [H_2O_2] + k_3 [HO^{\cdot}]^2 \qquad (5.1)$$

in which k_1 is the rate constant for Fe(II) reaction with hydrogen peroxide, k_i is the rate constant for individual scavengers (except hydrogen peroxide), k_2 is the rate constant for hydroxyl radical reaction with peroxide and k_3 is the rate constant for hydroxyl radical reacting with itself. In the presence of a scavenger, whose concentration is in the millimolar range and whose second-order rate constant is over 10^9 $M^{-1}s^{-1}$, the term k_3 $[HO^{\bullet}]^2$ is negligible since the concentration of the hydroxyl radical is about 10^{-12} M. So Eq. 5.1 can be simplified to **Eq. 5.2**

$$k_1 [Fe(II)] [H_2O_2] = [HO^{\cdot}]\Sigma(k_i [S_i]) + k_2 [HO^{\cdot}] [H_2O_2] \qquad (5.2)$$

Table 5.1 Electrospray Data on Complexes

Guest	Peaks Observed (*: After MS-MS)	Corresponding Complex
3-phenylphenol	1327.38 1242.34	β -CD:3-phenylphenol:Na^+ (2) β -CD:3-phenylphenol:(2) Na^+
2,4,5-T	850.0 722.1 595.3*	β -CD:(2)2,4,5-T : Fe(II) β -CD: 2,4,5-T : Fe(II) β -CD: daughter of 722.1
2,4-D	704.7 816.1 595.3 */705.7*	β -CD:(2)2,4-D : Fe(II) β -CD: 2,4-D : Fe(II) β -CD/ β -CD:2,4-D : Fe(II)
Toluene	640.4 595.3*	β -CD:Tolulene : Fe(II) β -CD: daughter of 640.4
2,3-dihydroxynaphthalene	675.3 595.3*	β -CD:2,3-dihydroxynaphthalene: Fe(II) β -CD: daughter of 675.3

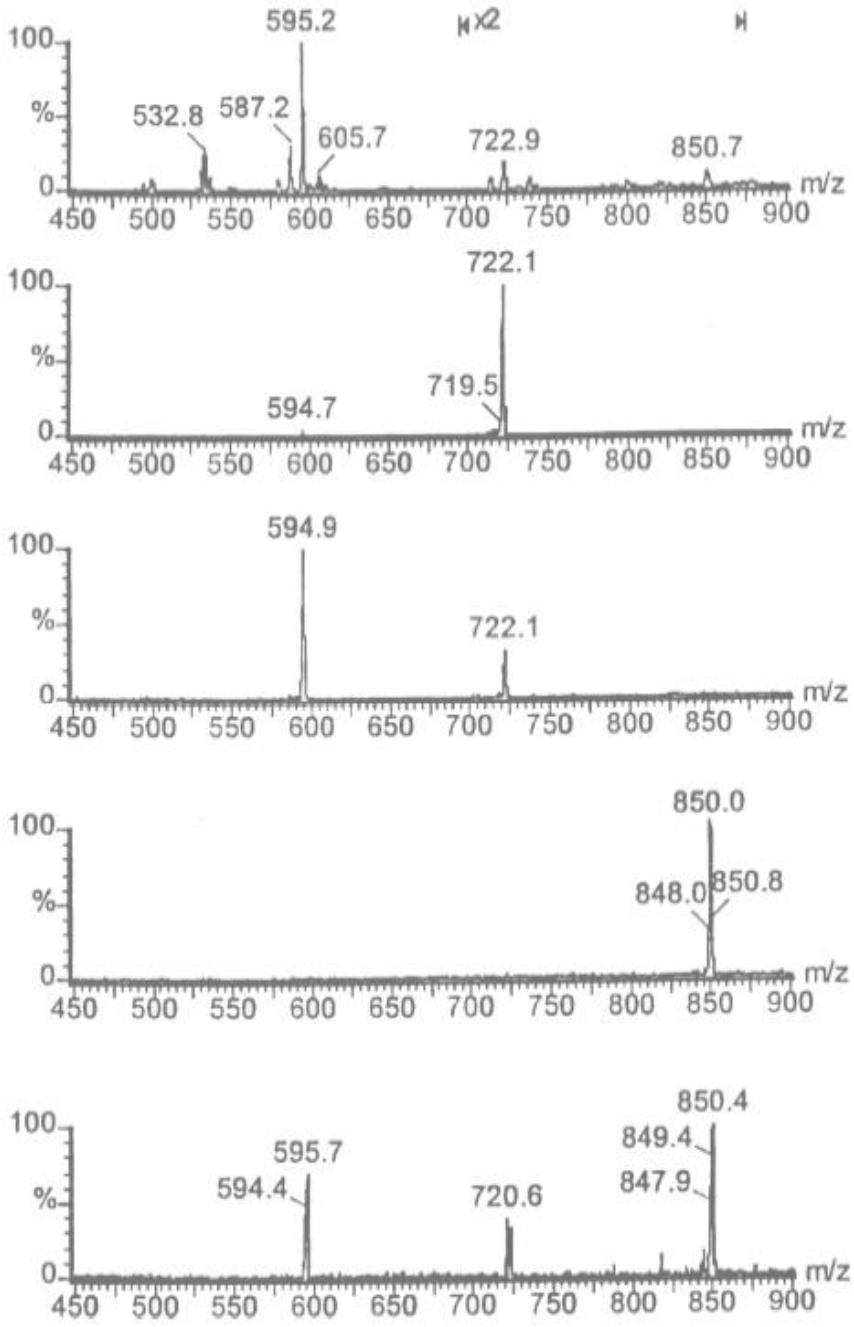

Figure 5.1 Electrospray-Mass spectra of solution of 1.0mM CM-β-CD, 1.0mM Fe(II) and saturated 2,4,5-T and MS-MS spectra on peaks of 722.1 and 850.0.

As we know, Fe(II) coordinates a broad range of species, from inorganic anions such as chloride, which was used as major sink in most sets of experiment, to organic species such as 2,3-dihydroxylnaphthalene. So the term on the left side should be changed to Σ (k" [Fe(II)"] [H_2O_2]). The apparent activity of iron(II) is the accumulated effectiveness of all the iron(II) species.

Within one set of experiments the only variable is [CM-ß-CD], the concentration of hydrogen peroxide is kept constant through continuous addition, and the total contribution of scavengers is relatively constant. Under steady state hydroxyl radical concentration, the two sides of the equation would be equal. If the radical concentration changes, it can only result from a change in the accumulative activity or concentration of Fe(II) and the scavenger change from CM-ß-CD added. Since the increasing scavenging with CM-ß-CD added can only decrease the steady concentration of the hydroxyl radical, the only possible reason of the radical concentration to increase is the increased activity or concentration of Fe(II). However, the measured rate constants reflect the local radical concentration rather than the bulk concentration. Therefore, an observed increase in rate constants can be the result of either increased hydroxyl radical concentration due to enhanced iron activity or an elevated radical concentration at the site of the pollutant caused by the proximity to the catalytic site.

CM-ß-CD, as ß-CD, has hydroxyl groups, either primary or secondary. Upon reaction with hydrogen peroxide, the iron(II) transforms to iron(III), while iron(III) can switch back to iron(II) through reaction with hydrogen peroxide and other species generated within Fenton chemistry. Since the only variable is the CM-ß-CD concentration, the change of activity of iron(II) could result from binding to CM-ß-CD. In

addition, reaction of alcohols with hydroxyl radical produces alkoxy radicals, which can reduce iron(III) to iron(II). In order to test the effect of the cyclodextrin alcohol groups, glucose was used as a comparable source of alcohol groups. Since glucose has similar alcohol functional groups but cannot bind hydrophobic compounds, its effect on the Fenton system will help elucidate the effect of alcohol vs the ternary complex theory. The data in **Figure 5.2** show that glucose decreases the apparent rate of pollutant degradation. Therefore, it is highly unlikely that cyclodextrin enhances degradation rates through increased radical production rates, but rather cyclodextrin enhances degradation through formation of the radical at the location of the pollutant.

As we see in both figures, with/without chloride, the glucose added decreases rather than increases the reaction rate. Since at the same time, glucose works as scavenger, one possibility is that glucose does increase the activity of iron(II) and then increases the degradation, but this increasing effect is less than the decreasing effect from scavenging. But the concentration of CM-ß-CD used is up to 1 mM. The second-order reaction rate is 4.2×10^9 M^{-1} S^{-1} for ß-CD and 1.5×10^9 M^{-1} S^{-1} for glucose (www.ncdc.nd.edu). So the scavenging effect of CM-ß-CD would be bigger than the one of glucose. The hydroxyl group number in ß-CD is 21 (14 primary and 7 secondary) and the hydroxyl group number in D-glucose is 5 (4 primary and 1 secondary). So the number of both the primary and secondary hydroxyl groups per unit in ß-CD (ß-CD contains 7 glucose units) is less than in glucose. Though there could be different effects for primary and secondary groups, the effect of D-glucose would show the general trend of ß-CD based on the similarity of structure. Though CM-ß-CD used is a mixture and contains two carboxymethyl groups on average, the effect could only be less. So even

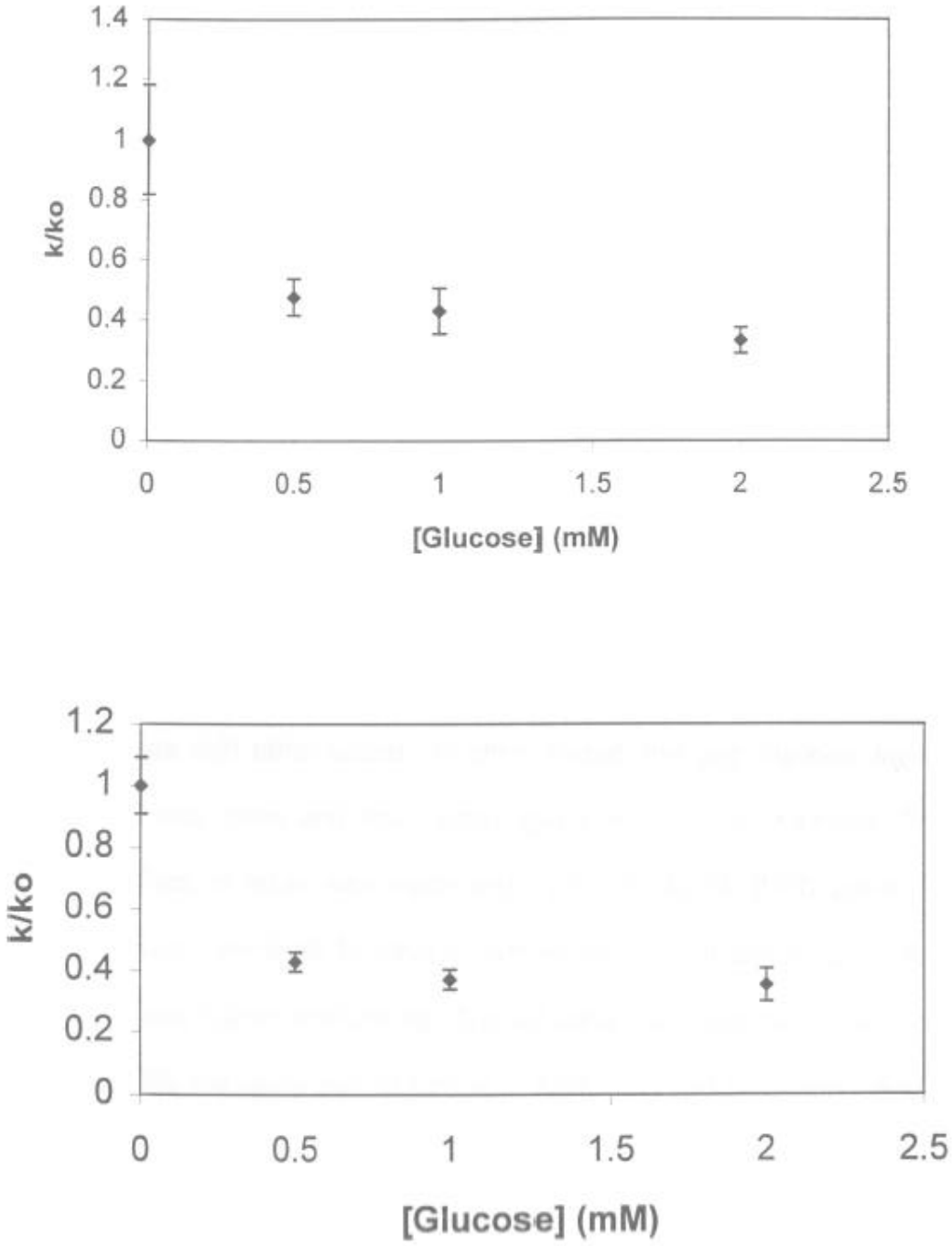

Figure 5.2 illustrates degradations of naphthalene with glucose. Conditions: 25μM naphthalene, 1.0mM Fe(II), hydrogen peroxide: 10mM × 1.5ml/h and with 3.2mM [NaCl](top)/without(bottom).

if there is an activity enhancement with glucose, it would be much bigger than the one with CM-ß-CD in general. This indicates that the iron(II) activity enhancement with CM-ß-CD, if any, would be much less than the contribution from scavenging. As we saw significant enhancement of degradation of PAHs and their derivatives, the reasonable possibility is that, as we assumed and discussed in the previous two chapters, the unique structure of CM-ß-CD brings the target species closer to iron site, or the hydroxyl radical generation site.

Calixarene Derivatives

Since the CM-ß-CD applied is a mixture of carboxymethyl derivatives in which both the number and location of carboxymethyl groups are not known, to better understand the impact of the ternary complex, calixarene derivatives were synthesized. t-Butyl-calix[6]arene was debutyilized first and carboxymethyl groups were added to the bottom rim after hydrolysis. The species were characterized by NMR and/or ES-MS. The carboxymethyl groups were expected to make it water-soluble and comparable to the CM-ß-CD used. However caroxymethyl calix[6]arene was found to have a negligible water solubility. The solubility was less than 20 µM and less than 100 µM even in 50:50 THF:H_2O. The debutylized calix[6]arene was further functionalized with sulfonic groups, which made it very water soluble. The binding experiment of naphthalene into the calix[6]arene sulfate was carried out with a fluorometer and the strong linearity of 1/[delta-flu] vs 1/[Conc.] plot, as shown in **figure 5.3**, indicates a 1:1 binding ratio, with a binding constant of 5,400 which is comparable to the one of naphthalene and CM-ß-CD.

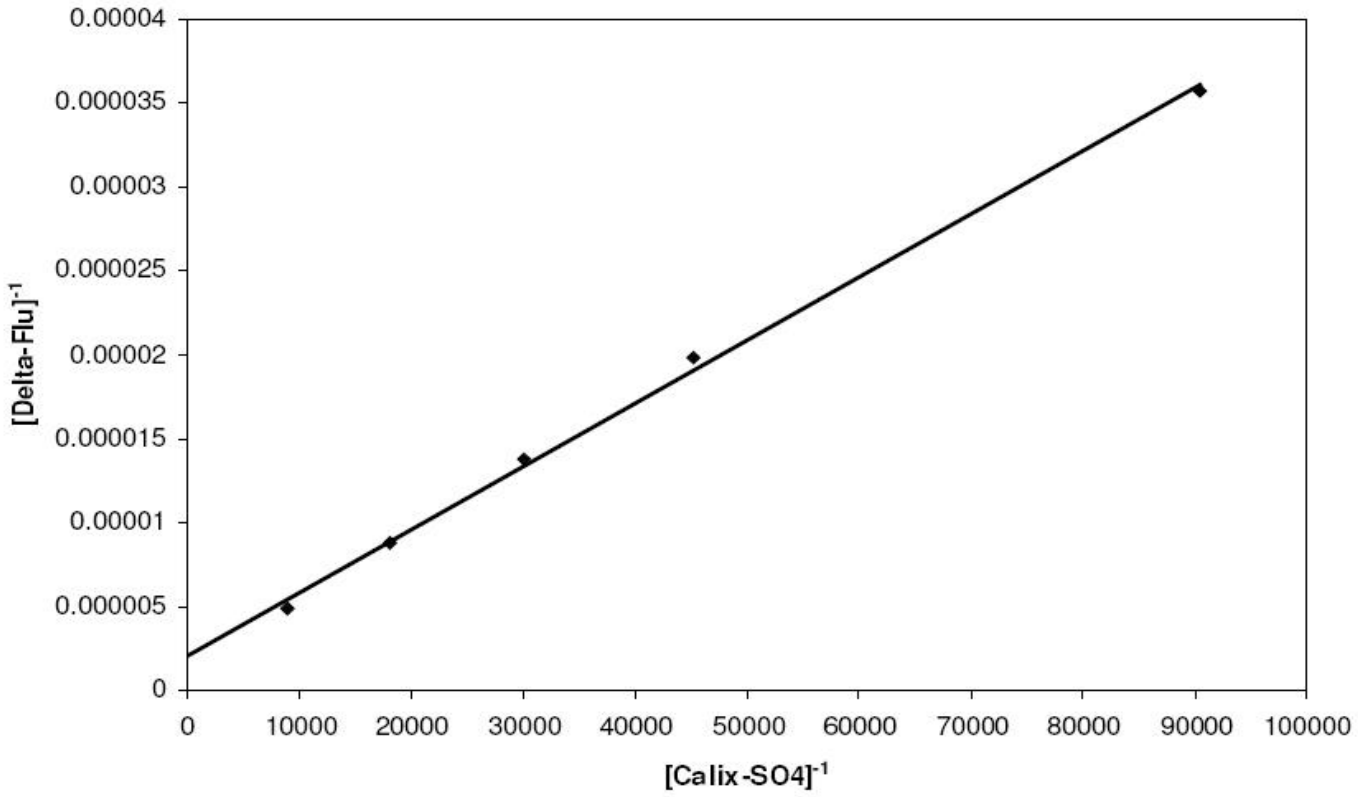

Figure 5.3 Plot of binding constant between naphthalene and calixarene sulfate derivative. Condition, [naphthalene]=25um. [calix-sulfate]=0.012, 0.024, 0.036, 0.060, 0.120 g/l.

However addition of Fe(II) makes the fluorescence intensity decrease dramatically. When 1.0 mM Fe(II) was added, the fluorescence decreased to less than 5% of the original value, as shown in **Figure 5.4**. This could be due to Fe(II) binding to the calix[6]arene sulfate and then quenching the naphthalene or precipitation of the ternary complex. $FeSO_4$ has a solubility over 1 mM under the conditions applied. In addition, no precipitate was visually observed when Fe(II) was added and even after the resulting solution was left to stand for days. However if the solution was left longer than one week, the solution turned greenish and precipitate was observed. This may indicate that Fe(II) was converted to Fe(III) which is much more prone to form a precipitate. Addition of Mg(II) resulted in further quenching of the fluorescence, as illustrated in Figure 5.4 (lines with triangle). If the iron-based decrease in fluorescence was due to quenching by Fe(II), Mg(II), which is a poorer quencher than Fe(II), could replace Fe(II) and cause the fluorescence intensity to increase.

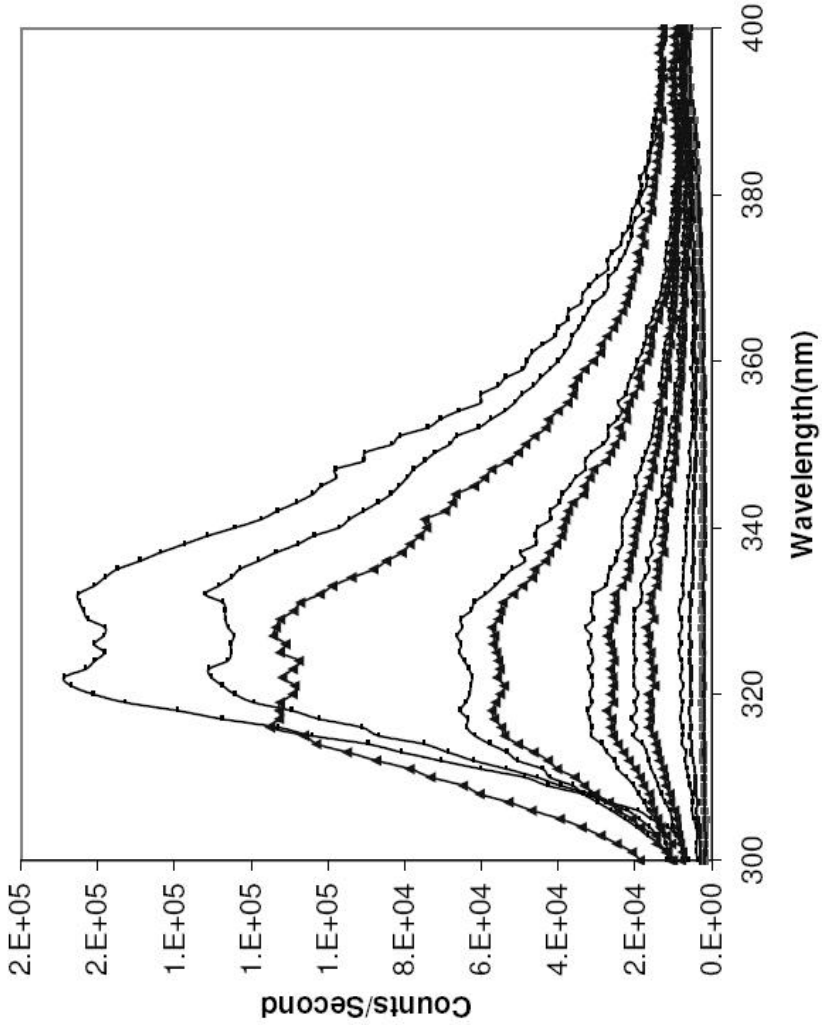

Figure 5.4, Fluorescence Spectra of 25um naphthalene with 0.12g/l calixarene sulfate derivative added with 0.1mM, 0.2mM, 0.3mM, 0.5mM, 1.0mM and 0.2mM $Fe(II)(ClO_4)_2$ only (lines with small dot) and additional equal amount of $MgCl_2$ (lines with triangle).

Chapter VI Two-Phase Degradation of PAHs and PCBs

PAHs and PCBs are responsible for many health concerns and have been proven linked to a variety of diseases, such as organ malfunctions, cancer and birth defects. They are highly hydrophobic, environmentally persistent, and bio-accumulate. Either PAHs or PCBs can be prevalently found in nearly all marine plant and animals specimens, fish, mammals, birds, bird eggs, and, of course, humans. For these reasons, PAHs and PCBs pollution resulted from industrial usage is still a top environmental issue and agenda of the U.S. Environmental Protection Agency (EPA) [51].

Most amounts of PAHs released to the environment are formed during fossil fuel combustion and during anthropogenic forest and agricultural fires, while PCBs resulted from pre-1970's industrial use. As they enter the environment such as water systems, PAHs and PCBs quickly become adsorbed to particles and usually are deposited in the bottom sediments. Their environmental persistence relates not only to their low reactivity but also to their low solubility. Once adsorbed, they are slowly released into water systems and cause prolonged pollution.

As shown previously, cyclodextrin derivatives can enhance degradation efficiency through entrapping hydrophobic species and chelating with Fe(II) at the same time. Meanwhile, it is widely regarded that cyclodextrins increase solubility of

hydrophobic species. To extend application of cyclodextrins enhancement on degradation, a simple two-phase system was applied. Quartz sand was deposited with either PAH or PCB, the sand sample was covered with water and cyclodextrins and Fenton reagents were added, and the PAH or PCB was extracted and then quantified with GC.

Two-phase degradation of PCBs

1) Binding of PCB to Cylcodextrins

Beta-cyclodextrin has an upper rim diameter of 6.2 Â (alpha and gamma cyclodextrins have upper rim diameters of 4.9 and 7.9 Â respectively) [84]. This is much greater than the width of the two PCBs applied. 3,3',5,5'-tetrachlorobiphenyl and 2,2',6,6'-tetrachlorobiphenyl (the maximum width of 2,2',6,6'-tetrachlorobiphenyl is 5.437 Â) . Due to the extremely low solubility of PCBs, measurement of binding constants between the two PCBs and cyclodextrin are challenging or not reliable. However, it is regarded that cyclodextrins have the capacity of entrapping hydrophobic species with suitable size, such as PCBs. In addition a mass transfer study of PCBs indicated that cyclodextrins can remove PCBs from a site [85].

2) Sample Preparation and Initial Data

Two PCBs, 3,3',5,5'-tetrachlorobiphenyl and 2,2',6,6'-tetrachlorobiphenyl, were used. Initial methylene dichloride solutions, 30 mg/L, were made and stored in the dark. 10ml of this solution was diluted to 100 mL and then deposited to 200 grams sand and the sample was left overnight to air dry. Before weighing 2.5 gram samples and transferring them into glass vials, the sand was further dried with a rotovaporator

(water bath-60°C; rotation-120RPM) for 20 minutes. Reagents (except Fe(II) and hydrogen peroxide) were added and the sample was left on an orbital shaker for several days. Extraction efficiency, around 95%, was easily achieved and relatively stable. After Fenton reaction under specified conditions, 2.5 mL methylene dichloride was used to extract PCBs left and the sample was monitored with GC-ECD without further concentration. In each set of experiments, extraction efficiency was guaranteed and the amount of PCB left was recorded as percentage vs the proposed concentration of PCB in methylene dichloride solution.

In each experiment, hydrogen peroxide was added in a single dose rather than by continuous addition with a digital pump applied in previous degradations in the pure aqueous phase. Since the Fenton reaction mechanism is complex, different reaction rate and pathways may have occurred in the single dose system. However, the ternary complex exists and comparisons between degradations with and without cyclodextrin derivatives still make sense.

With single dose addition of hydrogen peroxide, the concentration of hydrogen peroxide used was much higher than that applied with continuous addition. As mentioned in the Fenton mechanism discussion in the introduction, hydroxyl radicals can be scavenged by numerous species including iron ions and even itself. With the fact that PCB is very stable, a large amount of hydrogen peroxide was needed. Furthermore, high concentrations of Fe(II) were also required.

After stable and good extraction efficiency was achieved, effects from scavenger and CM-ß-CD were first studied. **Figure 6.1** illustrates the effect of propanol, a scavenger, on PCB80 (2,2',6,6'-tetrachlorobiphenyl) degradation with

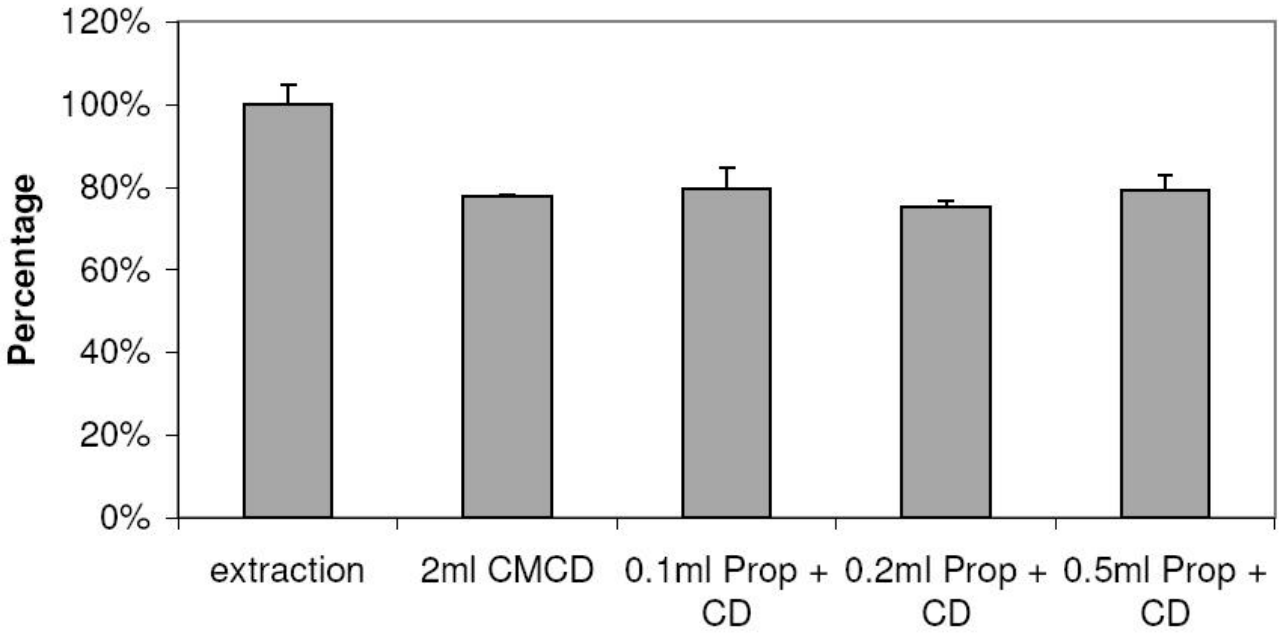

Figure 6.1. Effect of propanol on PCB80 degradation. Condition, [CMBCD]=20mM; $Fe(ClO_4)_2$: 0.1M * 0.5ml; H_2O_2 : 0.5M * 1.0ml. Samples with propanol have CMBCD also.

0.10 M $\times$0.50 ml $Fe(ClO_4)_2$, 0.50 M $\times$ 1.0 mL H_2O_2 and 20 mM $\times$ 2.0 mL CM-ß-CD. **Figure 6.2** illustrates the effect of CM-ß-CD with conditions of 0.10 M $\times$ 0.50 mL $Fe(ClO_4)_2$, 0.50 M $\times$ 1.0 mL H_2O_2. As shown in figure 6.2, there is a significant impact of CM-ß-CD. The PCB80 amount left is about 75%, 50% and 80% with 0.5 mL, 1.0 mL and 2.0 mL CM-ß-CD (20 mM) respectively. As indicated for degradation in the pure aqueous system, a scavenger lowers the degradation rate of a pollutant. However here the effect of propanol is negligible, at least, with the presence of CM-ß-CD. This is due to the extremely low solubility of PCB80 and, even with presence of CM-ß-CD, the amount of PCB80 in the aqueous phase is not significant. Then the PCB80 is either de-adsorbed or entrapped into the CM-ß-CD cavity. The Fenton reaction has the greatest impact on species in the aqueous phase, including the pollutant entrapped in CM-ß-CD cavity, rather than those compounds that are adsorbed/deposited on glassware or porous materials like sand. This contributes to degradation enhancement of CM-ß-CD. However, with 2.0 mL CM-ß-CD, the amount of un-degraded PCB80 is much greater than with 1.0 mL CM-ß-CD. Though it is natural to presume that higher amount of CM-ß-CD would entrap higher amount of PCB into its cavity, this is not a guarantee. The transfer of PCB from sand to CM-ß-CD must go through the aqueous phase. However this process is complicated. Even if there were a higher amount of PCB entrapped in the cavity, CM-ß-CD could be a scavenger especially with a low concentration of hydroxyl radical. Or the enhancement potential is shielded by its internal quenching effect.

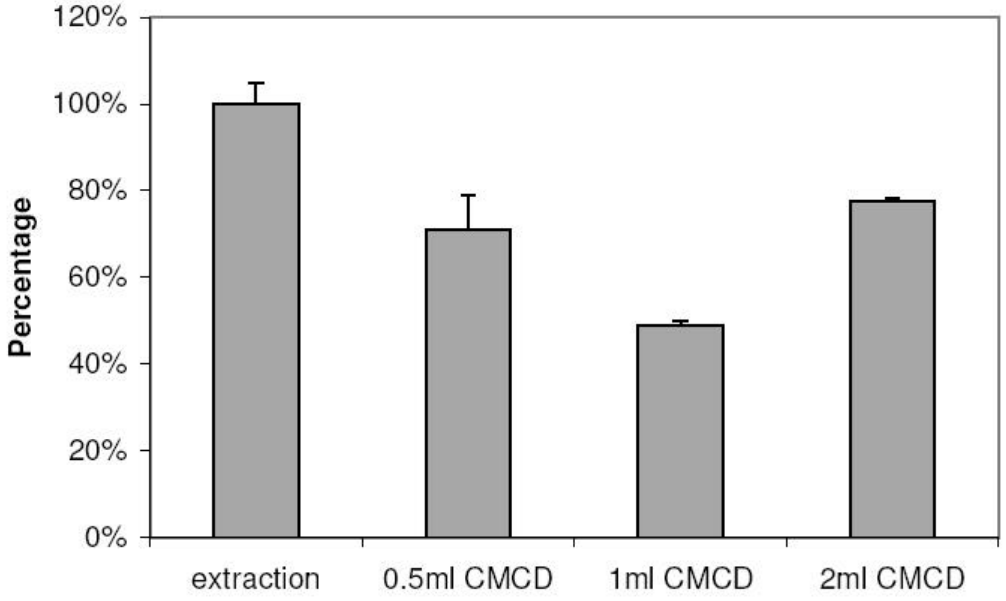

Figure 6.2. Effect of CMBCD on PCB0 degradation [CMBCD]=20mM; $Fe(ClO_4)_2$: 0.1M * 0.5ml; H_2O_2 : 0.5M * 1.0ml.

3) Condition Optimization

Due to single dose addition of hydrogen peroxide, the ratio between the amount of hydrogen peroxide and Fe(II) could be important. Excessive Fe(II) could quench the hydroxyl radical generated, while excessive amount of hydrogen peroxide can transform the active Fe(II) to the less active Fe(III). **Figure 6.3** illustrates impact of the amount of hydrogen peroxide with comparison between samples with and without CM-ß-CD ([CM-ß-CD]: 20 mM × 1.0 mL; Fe(II): 0.10 M × 0.5 mL; [H_2O_2]: 0.5 M; sample left on the orbital shaker with 250RPM for three days unless otherwise stated). As shown in figure 6.3, the presence of CM-ß-CD significantly boosts the degradation efficiency. With 1.5 mL × 0.5 M hydrogen peroxide, only about 57% PCB80 was left with CM-ß-CD present, while 84% was left without CM-ß-CD presence. As mentioned previously, PCB enters CM-ß-CD cavity and then enters the aqueous phase. Without CM-ß-CD present, PCB80 is mostly adsorbed to the sand, where it is not easily reachable by hydroxyl radical. In addition formation of ternary complex among CM-ß-CD, PCB and Fe(II) could enhance degradation on the PCB entrapped. The second obvious observation is that the amount of hydrogen peroxide indeed plays a role in degradation. As discussed before, the complexity of the Fenton reaction in this system makes condition optimization necessary to achieve further degradation.

In figure 6.3, the degradation efficiency roughly correlates to the amount of hydrogen peroxide added. The optimal amount was 1.5 mL × 0.5 M. **Figure 6.4** illustrates the impact of CM-ß-CD at the optimal amount of hydrogen peroxide (1.5 mL × 0.5 M). The impact of CM-ß-CD under these conditions is similar the one as shown in figure 6.2. The amount of PCB80 left correlated to the amount of CM-ß-CD added.

However the degradation efficiency of PCB80 does not continually increase as more and more CM-ß-CD was added. The percentage of PCB80 left with 2.5 mL CM-ß-CD (20 mM) was about 54%, much higher than the result with 2.0 mL CM-ß-CD (31%). **Figure 6.5** illustrates degradations with PCB54 under conditions of: Fe(II) 0.5 M × 1.0 mL; CM-ß-CD 20 mM × 2.0 mL; H_2O_2 1.0 M. At the conditions optimized with PCB80, degradation enhancement with CM-ß-CD is obvious. While the percentage of PCB54 left stays around 80% without presence of CM-ß-CD, the amount of PCB54 left gradually went down from 54% to 27% as hydrogen peroxide (1.0 M) was added from 0.5 mL to 2.0 mL.

Two-phase degradation of PAHs

In real systems, PAHs are mostly adsorbed to sediment and released slowly, causing persistent pollution. As mentioned in the introduction and chapter VI, PAHs are highly hydrophobic and readily bind to cyclodextrins. Following the platform that cyclodextrins can remove PAHs through desorption and enhance the Fenton degradation by forming ternary complexes, we expected to observe enhanced degradations similar to PCBs. However this result was not achieved after numerous trials. **Figure 6.6** illustrates results for phenanthrene with/without CM-ß-CD with the following conditions: [CM-ß-CD], 20 mM; [HA], 18 mg/L [H_2O_2], 40 mM × 5 mL. The PAHs were monitored with a flame ionization detector (FID), which has detection limit much poorer than the ECD used with PCBs. Consequently, the amount of PAHs used was much greater than for PCBs, and the sample treatment is somehow different. PAH solutions of 1000 μM in methylene chloride were prepared, and 100 mL of each

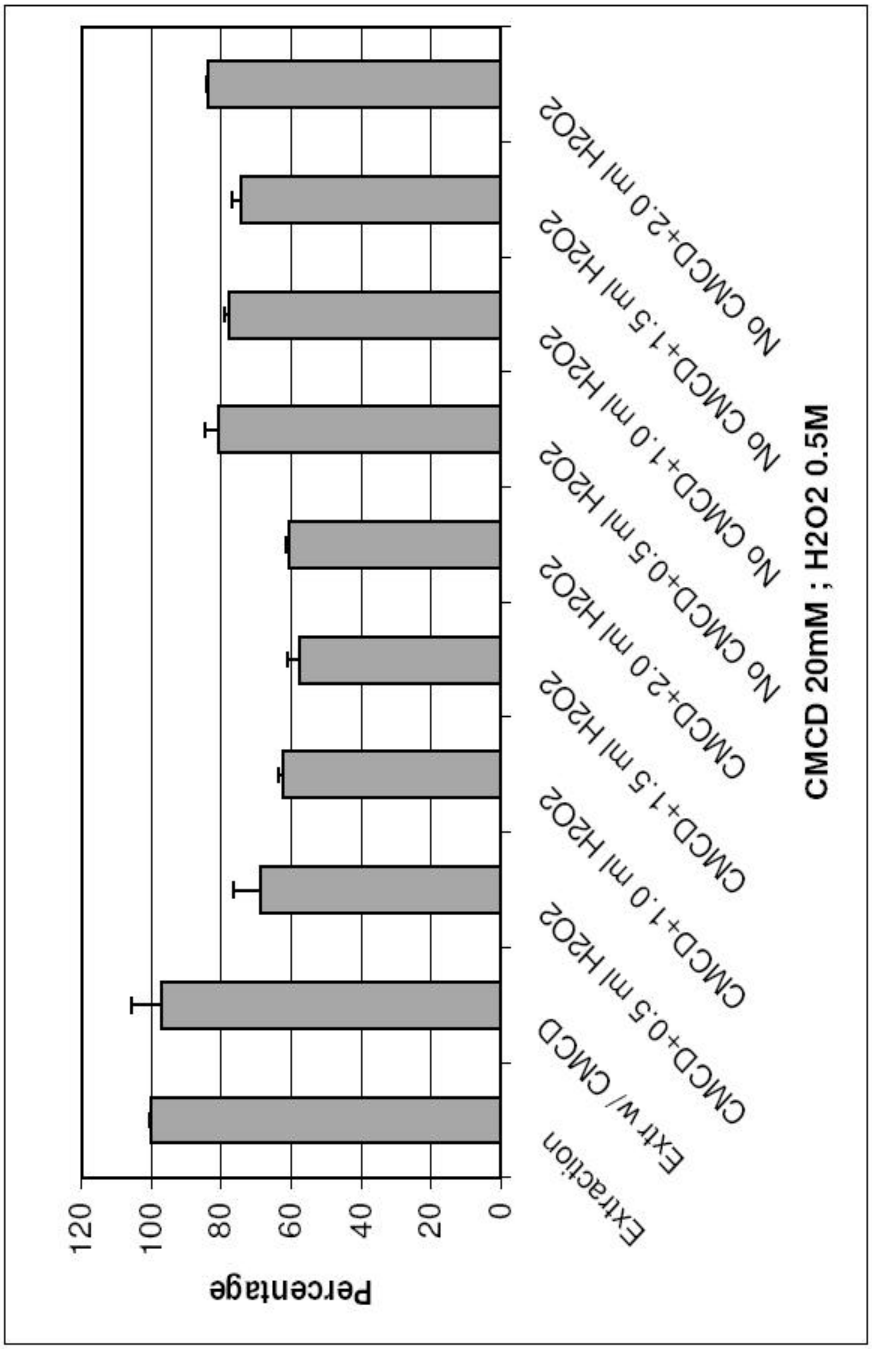

Figure 6.3, Impact of the amount of hydrogen peroxide and CM-β-CD. [CM-β-CD]: 20mM × 1.0ml; Fe(II): 0.10M × 0.5 ml; [H_2O_2]: 0.5M. Sample left on the orbital shaker at 250 RPM for three days.

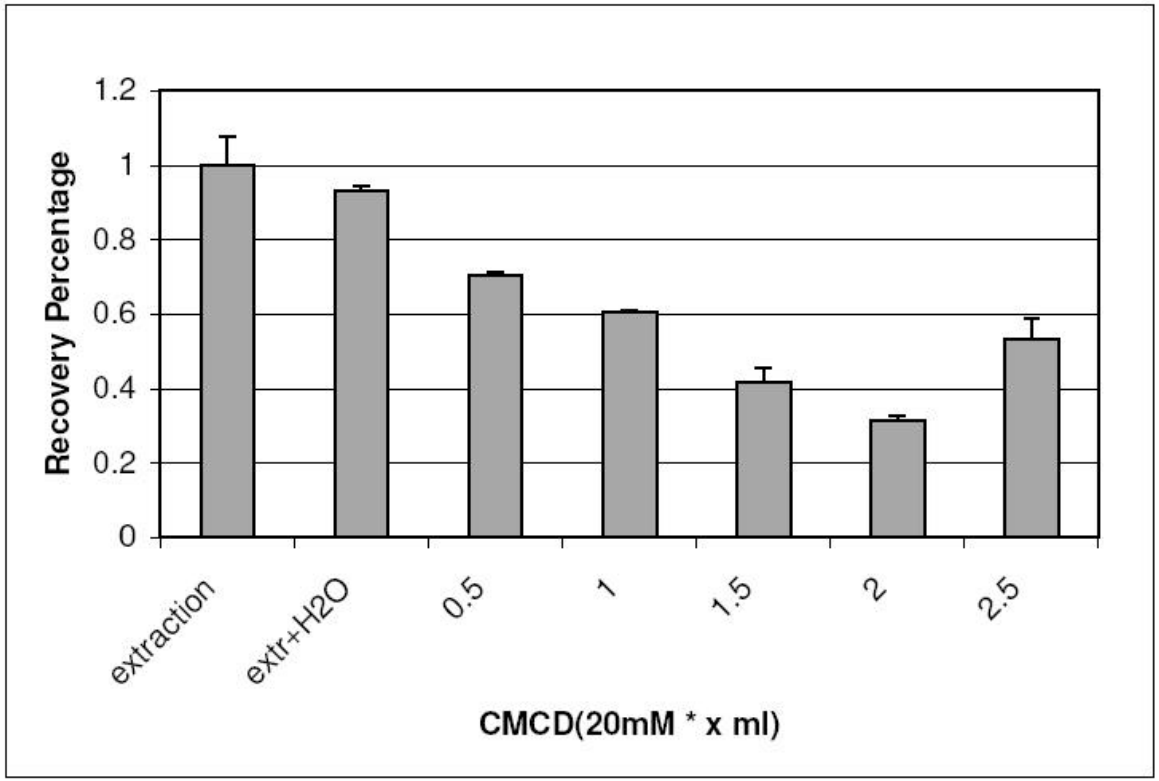

Figure 6.4, the impact of CM-β-CD on degradations of PCB80 at condition: [CM-β-CD]: 20mM; Fe(II): 0.10M × 0.5 ml; [H_2O_2]: 0.5M × 1.5 ml

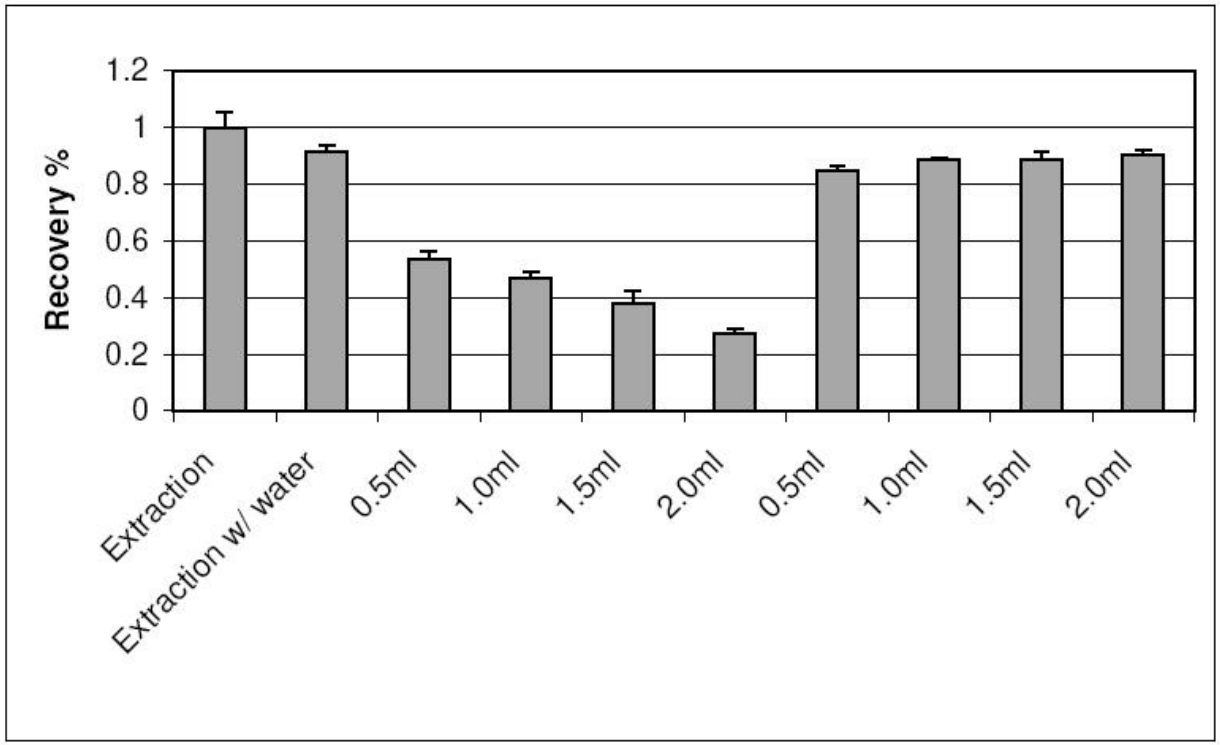

Figure 6.5. Degradations with PCB54 at conditions: Fe(II) 0.5M × 1.0ml; CMCD 20mM × 2.0ml; H2O2 1.0M. The last four bars represent degradation without CM-β-CD.

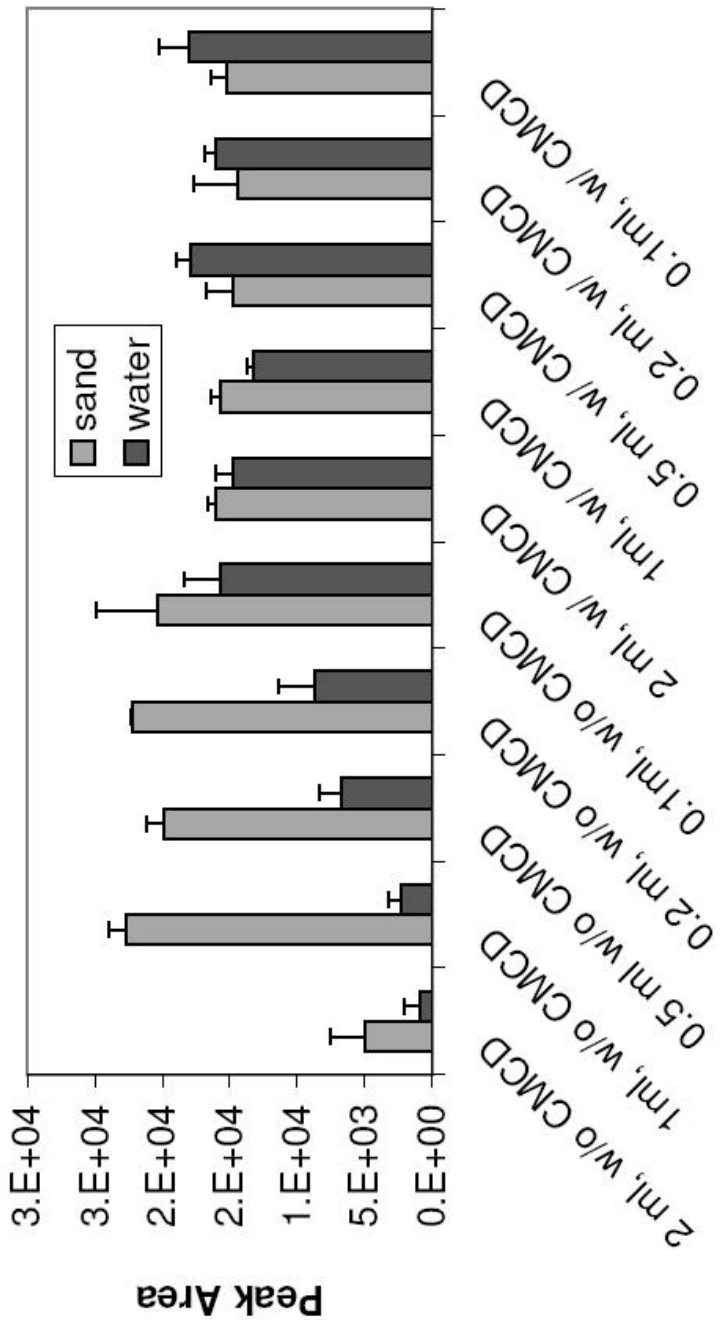

Figure 6.6. Two-phase degradation on phenanthrene with conditions: [CM-β-CD], 20mM; [HA], 18mg/L [H2O2], 40mM * 5ml; First five bars represent without CM-β-CD.

solution was deposited into 200 grams sand and left to air dry overnight. After further drying with a rotovaporator, a 20 gram sample was transferred to a glass vial. Reagents, except hydrogen peroxide and Fe(II), were added and the samples were left on a orbital shaker for three days. After Fenton reaction, half of the supernatant liquid was transferred and extracted with 2.5 mL methylene chloride. Half-by-weight of the sand, after decanting the supernatant, was extracted and monitored separately. As figure 6.6 shows, the presence of CM-ß-CD did not enhance the degradation efficiency, but rather lowered the degradation rate in both the aqueous phase and sand. In addition to phenanthrene, naphthalene and anthracene were tried with numerous conditions. The results with CM-ß-CD were all negative. This could be due to the fact that the amount of PAHs deposited was excessive. One choice would be to lower the amount of PAHs applied, however, due to the poor detection limit associated with the FID detector, it was not possible to work with lower PAH loadings. Another choice would be to apply higher amount of CM-ß-CD. **Figure 6.7** illustrates degradations of phenanthrene with the following conditions: [CM-ß-CD], 100 mM × 2 mL; [NaCl], 100 mM × 5 mL; [H_2O_2], 40 mM. However the result that CM-ß-CD does not enhance the degradations is still not changed. This does not necessarily mean that the PAHs are not excessive. The amount of PAHs is still 10^4 fold greater than the amount of PCB used, which makes comparable conditions for PAHs unachievable.

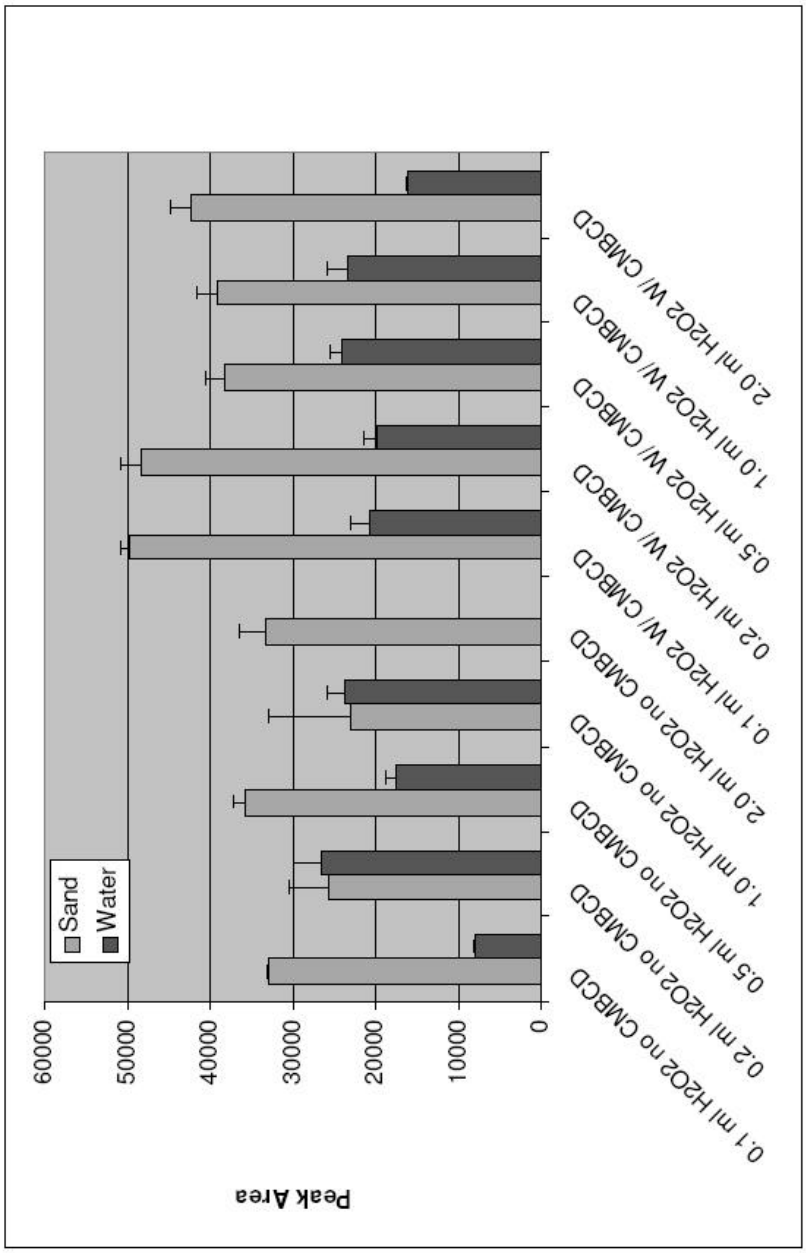

Figure 6.7. Degradation of phenanthrene with conditions: [CM-β-CD], 100mM × 2ml; [NaCl], 100mM × 5ml [H2O2], 40mM; First five bars represent without CM-β-CD.

Chapter VII A Novel Halide Fluorescence Sensor

Introduction

A sensor is defined as a device or chemical that can distinguish curtain species selectively by differential physical or chemical character, such as UV/Vis absorbance, color change, or electronic potential. While many very early sensors used UV/Vis, neither the detection limit nor the linear detection range of these sensors was suitable for application in many circumstances. Sensors with a color change in the presence of the target species are straightforward and attractive. However, such sensors cannot normally be used in quantitative analysis due to the very limited linear range. Electronic probes for many species have been well developed. However these sensors require routine maintenance and calibration, and are consequently costly. In addition, the detection limits restrict their applicability, and their large size precludes certain applications such as in vivo intracellular measurement and imaging [86].

Sensing of chemical and biochemical analytes is an active research area. Rapid and low cost testing methods are always in demand in clinical, bioprocess and environmental applications [87]. In the last decades, fluorescence sensing has surged as a promising sensing tool [88].

Fluorescence, along with phosphorescence, is one of two types of luminescence. In fluorescence, which occurs from excited singlet states, the electron in the excited orbital has an opposite spin compared to its corresponding electron in the ground-state orbital [89]. Consequently, return to the ground state is spin-allowed and occurs rapidly by emission of a photon. The emission rate of fluorescence is typically in the nanosecond range. The fluorescence process can be illustrated with a Jablonski diagram, **Figure 7.1**. The singlet ground, first, and second electronic states are depicted by S_0, S_1 and S_2, respectively. At each of these electronic energy levels the fluorophores can exist in a number of vibrational energy levels, denoted by 0, 1, 2, etc. Following light absorption, several processes usually occur. A fluorophore is usually excited to some higher vibrational level of either S_1 or S_2. With a few rare exceptions, molecules in condensed phases rapidly relax to the lowest vibrational level S_1. This process is called internal conversion and generally occurs in 10^{-12} s or less. Since fluorescence lifetimes are typically around 10^{-8} s, internal conversion is generally complete prior to emission. Hence, fluorescence emission generally results from a thermally equilibrated excited state, that is, the lowest-energy vibrational state of S_1.

Fluorescence typically occurs from aromatic molecules, such as naphthalene, quinine, anthracene, and coumarin [90, 91]. While there is no single rule to predict the fluorescence intensity, the intensity of fluorescence can be decreased by a wide variety of processes, such as collisional quenching, static quenching, a combination of collisional and static quenching, and energy transfer quenching [92]. Collisional quenching happens when the excited-state fluorophore is deactivated upon contact with some other molecule.

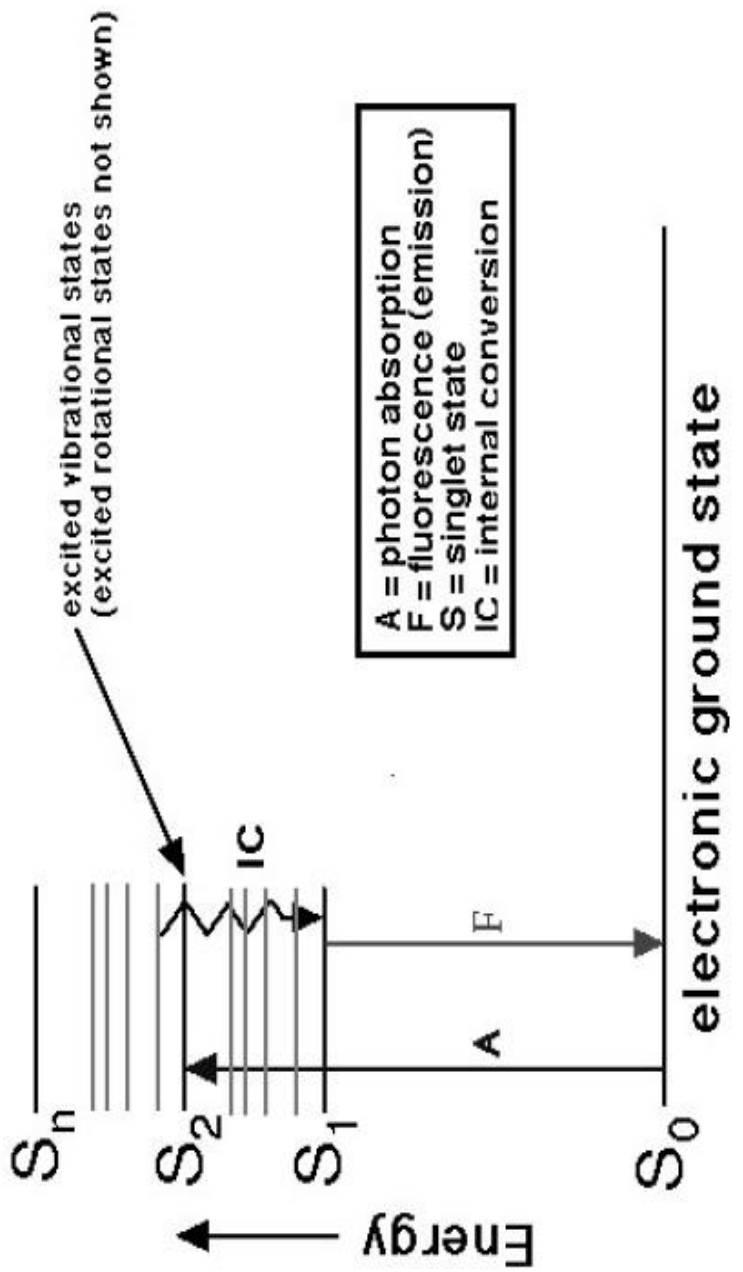

Figure 7.1 Jablonski diagram on fluorescence

in solution, which is called a quencher, such as oxygen, halogens, amines and some electron-deficient molecules like acrylamide [93]. Static quenching happens when the fluorophores form nonfluorescent complexes with quenchers. Static quenching is often observed if the fluorophore and quencher can have a stacking interaction, such as the one between purine and pyramide [94]. Resonance energy transfer happens when the donor fluorophore has an emission spectrum overlapping with the absorption spectrum of the acceptor, which can be fluorescent or non-fluorescent [95]. At certain conditions, different quenchers have different quenching effects, and many sensors apply this effect to distinguish certain species among quenchers and from non-quenchers. For example, oxygen sensors, $[Ru(Phphen)_3]^{2+}$ and $[Ru(phen)_3]^{2+}$, function through a collisional quenching mechanism. In addition, $[Ru(Phphen)_3]^{2+}$ has a unit response about four-fold that for $[Ru(phen)_3]^{2+}$, due to the longer unquenched lifetime of the diphenyl derivative [96]. Normally the selectivity can be controlled through derivatives with different functional groups. Examples for chloride sensors with collisional quenching are SPQ (6-methyoxy-N-(3-sulfoproxyl)quinolinium), SPA (N-sulfopropylacridinium), Lucigenin (N,N'-dimethyl-9,9'-bisacridinium nitrate), MACA (N-methylacridinium-9-carboamides) and MAMC (N-methylacridinium) [97], as shown in **figure 7.2**. These sensors all contain a quinolinium ring that can be quenched by chloride anion. It was found that all the quinolines are not equally sensitive to chloride, and the quenching constant depends on the chemical structure. These chloride sensors have been applied to measure chloride transport across cell membranes. However, they are subject to interference from quenching effects from other anions, such as bromide, iodide, thiocyanate, and even free amine for SPQ. The quenching constants in cells is only about one-tenth of the

Figure 7.2. Chemical structure of some chloride sensors.

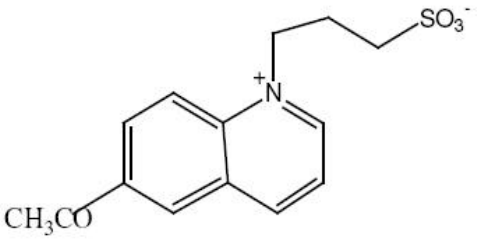

SPQ

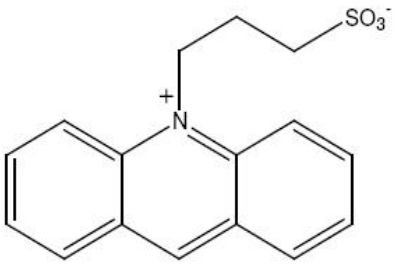

SPA

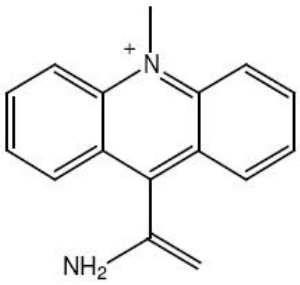

MACA

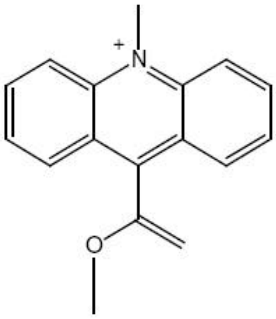

MAMC

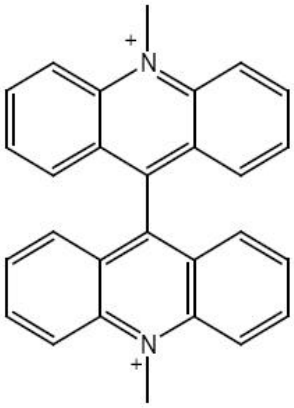

Lucigenin

quenching effect in pure aqueous solution. Meanwhile the fluorophores cannot be used ratiometrically and leak out of the cells, causing routine under-measurement. Tepel, et al. reported the chloride concentration in lymphocytes as 28 mmol/L (stdev = 4 mmol/L, n=15) while the concentration reported by other measurements was 47 mmol/L to 54 mmol/L [98].

By contrast, the measurement of cations, such as potassium, calcium and sodium, are more convenient and accurate. First, cations bind strongly to certain groups, such as crown ethers, amines and carbonates. There are various fluorescence sensors for each cation, such as sodium green and sodium-binding benzofuran isophthalate (SBFI) for Na^+, potassium-binding bezonfuran isophthalate (PBFI) and CD222 for K^+, and fura red, calcium green and calcium orange for Ca^{2+} [99]. Normally excitation wavelengths in the visible range are preferred since UV wavelengths cause cell auto-fluorescence which causes interference. Routinely all the cation probes function with increased fluorescence with addition of the specific cation. Changes in fluorescence intensity are typically due to different quantum yields of the free and the complexed forms, rather than difference in the absorption spectrum. The increased fluorescence with cation probes are believed to be due to the energy increase of TICT state (twisted intramolecule charge transfer) [100].

Typically anion sensors offer sites suitable for anion binding through amine/guandium groups or amide groups and function through fluorescence quenching. In halide sensing, most sensors respond to halides through PET (photoinduced electron transfer)

mechanisms, quenching the fluorescence signal or decreasing the signal with addition of halides. All the previously reported halide sensors function with fluorescence quenching. Following is one example [88-d], shown in **Figure 7.3**. The anions bind to the calixopyrrole rings and then quench the fluorescence of the fluorophoric dye. The fluorescence decreases with all measured anions, halides, phosphate, bicarbonate and carbonate. This sensor offers superior selectivity to fluoride due to the best accommodation of fluoride to the cavity in the calixo-pyrrole ring.

Previously reported halide fluorescence sensors are based on quenching of fluorescent signals and there are always collision quenching interference from other species. Therefore there would be an advantage if an anion sensor functioned through a different mechanism, thereby offering a brand-new choice to address the quenching interference existing with current anion sensors. For example, if one sensor offers different signal change direction with different anions or an increase with one anion and decrease with other anions, would be advantageous especially in qualitative sensing. In addition, if the sensor is initially non-fluorescent, then the difficulties with prevalent quenching could be highly suppressed.

Figure 7.3. A fluorescence-quenching example of halide sensor recently reported.

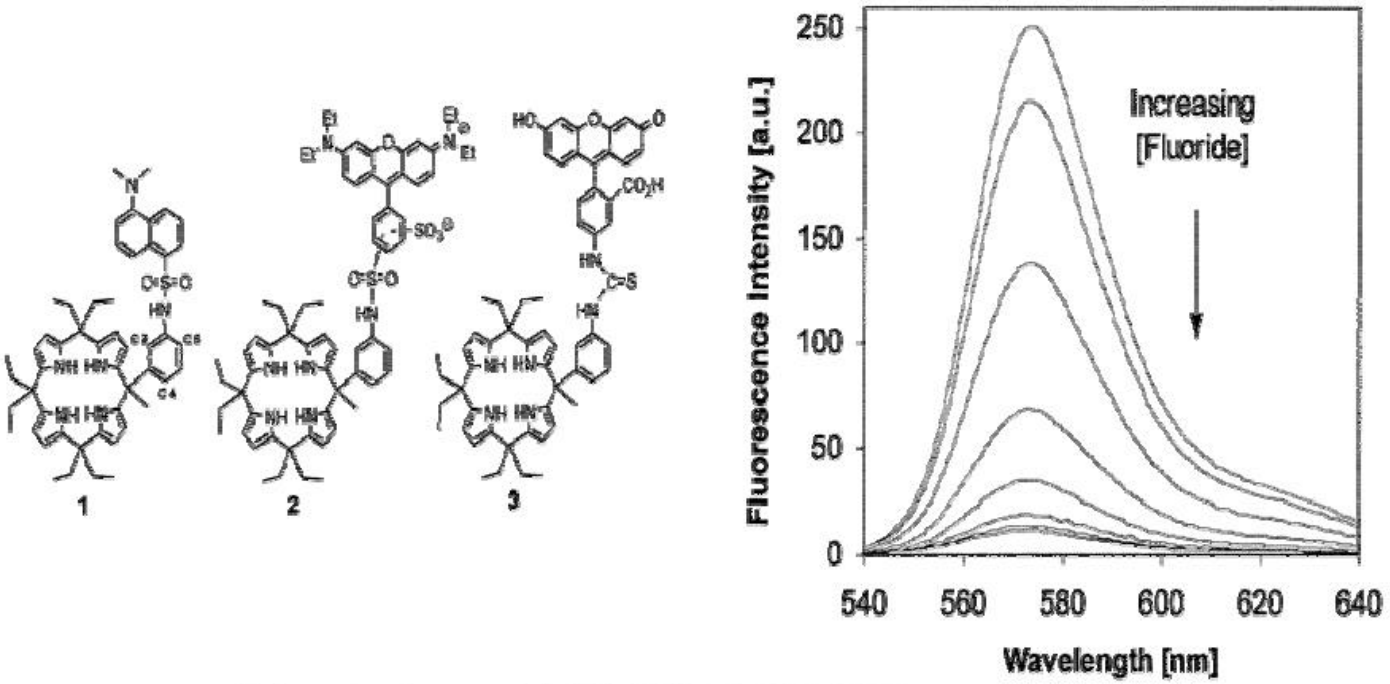

*P. Anzenbacher etc., J.A.C.S., **2000**, 12, 9350-9351*

Experiment

1) Synthesis

Sensor **1**, 1,8-di(phenyl)ureaylnaphthalene, and an analog **2**, 2,3-di(phenyl)-ureaylnaphthalene, were synthesized readily with diaminonaphthalene and phenylisocyanate.

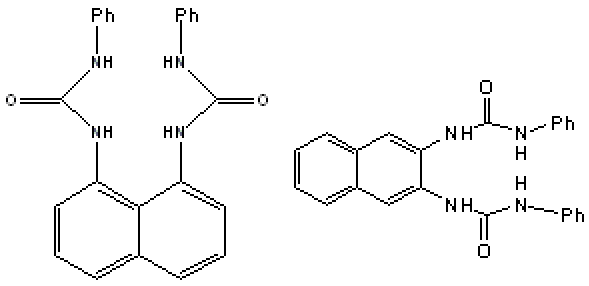

Figure 7.4 Sensor **1** and analog **2**

Synthesis of 1,8-di(phenyl)ureaylnaphthalene (sensor 1). 0.10 g (0.63 mM) 1,8-diaminonaphthalene was dissolved in 10 mL dry dichloromethane and 0.15 g (1.26 mM) phenylisocyanate was added in one dose. A white precipitate was formed as soon as phenylisocyanate was added. The mixture was stirred at room temperature for overnight. The precipitate was filtered out and washed with 5 mL dichloromethane and 5 mL acetone. Analytically pure molecule 1 was obtained in 82% (0.20g), m.p. 298^{o}C. ^{1}H NMR (DMSO-d_6): d 9.02 (s, 2H), 8.82 (s, 2H), 7.71 (d, 2H, *J* = 8.0), 7.69 (d, 2H, *J* = 8.0), 7.44(t, 2H, *J* = 8.0), 7.41(d, 4H, *J* = 8.0) 7.22(t, 4H, *J* = 8.0). ^{13}C NMR (DMSO-d_6): d 153.29, 139.90, 135.60, 133.90, 128.55, 125.35, 124.98, 122.26, 121.61, 118.28. Calculated elemental composition: 72.71% C, 5.08% H, 14.13% N; measured elemental composition: 72.42% C, 5.04% H, 14.12% N. Analog 2 was synthesized in similar way. 50 mg (0.32 mM) 2,3-diamino-naphthalene in 10 mL dry dichloromethane was added

with 75 mg phenylisocyanate and stirred at room temperature overnight. The precipitate was washed with 5 mL dichloromethane and 5 mL acetone. The yield was 70% (80 mg). m.p. 276^{o}C. ^{1}H NMR (DMSO-d_6): d 9.15 (s, 2H), 8.26(s, 2H), 8.16(s, 2H), 7.79 (dd, 4H, *J*=3.0), 7.51(d, 4H, *J*=8.0), 7.39 (dd, 4H, *J*=3.0), 7.30(t, 4H, *J*=*8.0*), 6.98(t, 2H, *J*=8.0). ^{13}C NMR (DMSO-d_6): d 153.77, 140.17, 130.88, 130.67, 129.37, 127.37, 125.55, 122.45, 120.61, 118.63. Calculated elemental composition: 72.71% C, 5.08% H, 14.13% N; measured elemental composition: 71.93% C, 5.04% H, 13.87% N. COSY experiments were also performed. **Figure 7.5** shows the COSY spectra of molecule sensor 1 and analog 2.

2) NMR and Fluorescence study with halides

Because of the low solubility of both in $CDCl_3$ or acetone-d_6, the NMR data were obtained in DMSO-d_6 and each peak was assigned based on the COSY spectrum. Figure **7.6** shows partial NMR spectrum of sensor 1 and spectra with addition of fluoride and chloride. Upon the addition of two eq. chloride, the NH protons shift (from 8.837ppm and 9.038ppm to 8.876ppm and 9.077ppm respectively), but no significant signal decrease was observed. In contrast, upon the addition of fluoride, the NH proton signal decreased quickly with 0.50 eq. fluoride the NH proton signal almost disappeared completely. Meanwhile, by comparison, the aromatic proton peaks became board and the ^{1}H splits were merged (spectra d with 0.5 eq. fluoride). These peaks could be resolved with a low temperature experiment. However due to the high melting point of DMSO, these experiments were not accessible.

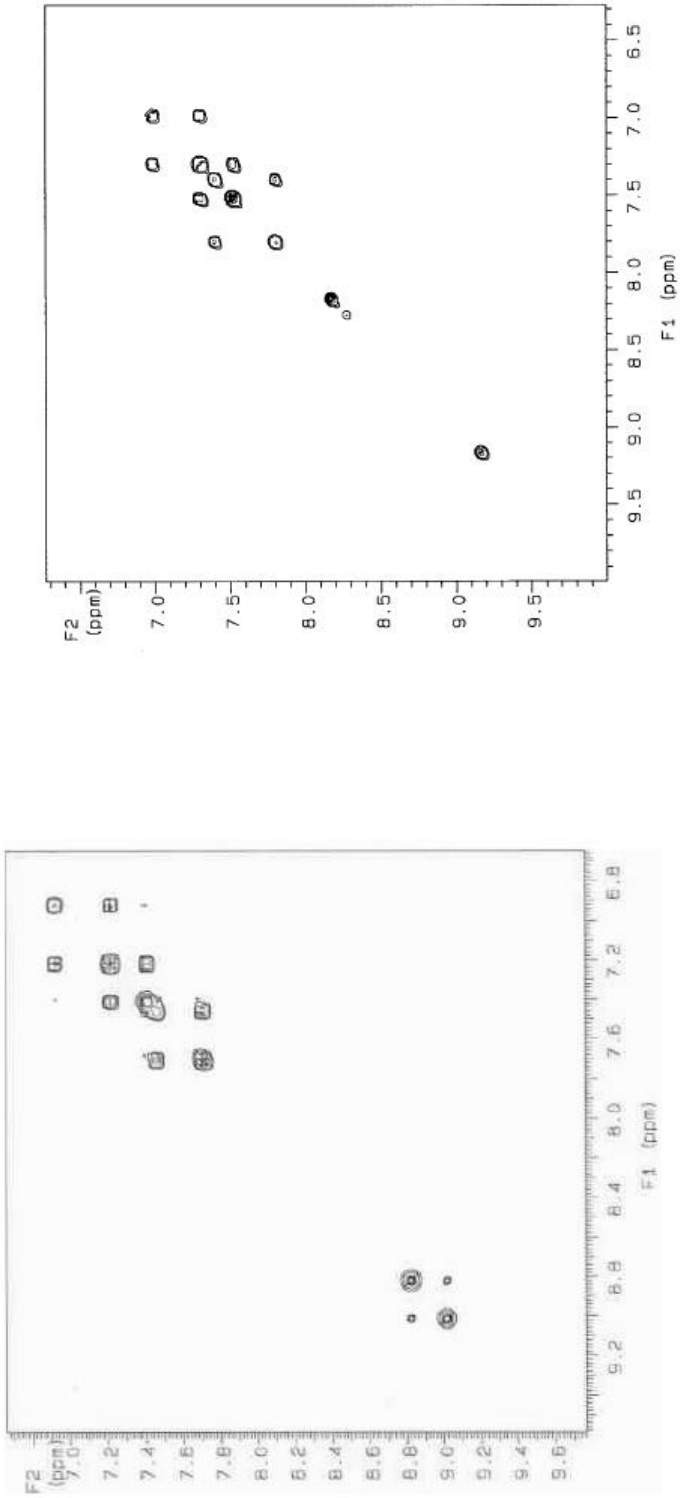

Figure 7.5 COSY spectra of molecules of sensor 1 (left) and analog 2 (right).

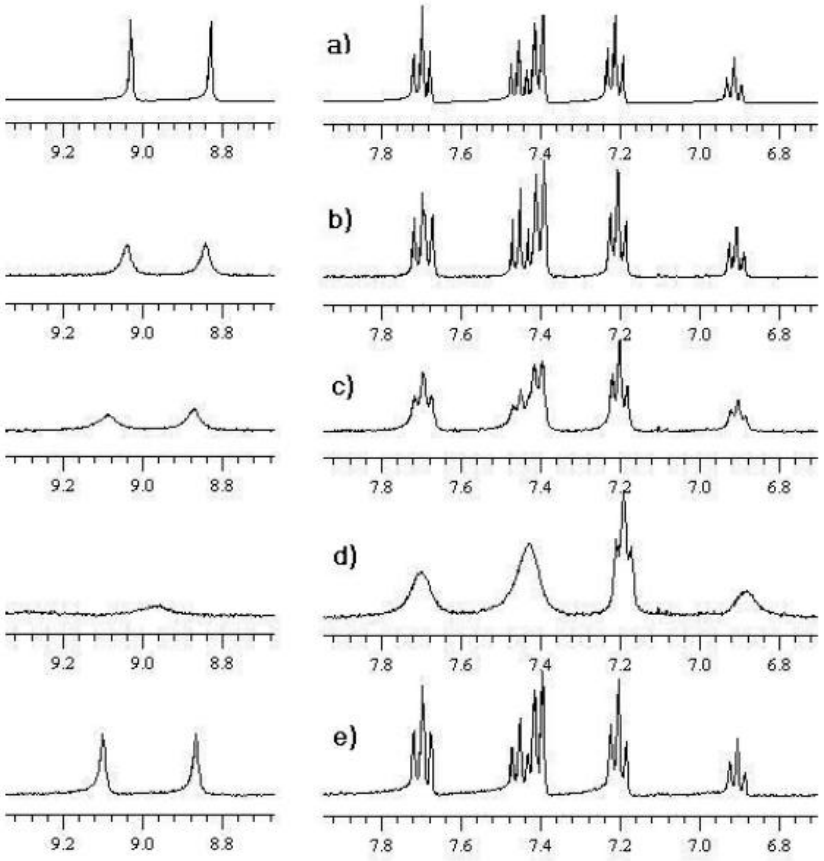

Figure 7.6. Partial ^{1}H NMR (400mHZ) spectra of sensor 1 (1 mM) in DMSO-d_6. (a) sensor 1 only; b) 1 + 0.10eq.; c) 1 + 0.25eq.; d) 1 + 0.50eq. tetrabutyl ammonium fluoride; e) 1 + 2.0eq. tetrabutylammonium chloride.

Fluorescence experiments were carried in the polar organic solvent of DMSO-AcCN (4:6,v/v). Fluorescence emission spectra were collected twice for each sample; duplicate spectra showed no noticeable differences. **Figure 7.7** shows fluorescence emission change with addition of Fluoride and three other halides (chloride, bromide and iodide).

As Figure 7.7 indicates, addition of fluoride increased the fluorescence intensity while all other three halides decreased fluorescence. The binding constant, as shown in **Figure 7.8**, between sensor 1 and fluoride is over 73,650 M^{-1}, while the ones measured for chloride, bromide and iodide are only 690, 345 and 76 M^{1} respectively. This indicates significant binding with fluoride compared to the other halides. This conclusion is in agreement with the NMR spectra upon addition of fluoride and chloride. While two equivalent chloride, from tetrabutylammomium chloride, did not decrease the NH proton intensity, addition of fluoride, from tetrabutylammonium fluoride trihydrate, significantly lowers the NH proton signals and caused substantial peak broadening. Although in fluorescence experiments the solvent used was DMSO-AcCN (4:6,v/v) and in NMR experiments the solvent used was *d*-DMSO, both data sets indicate strong binding with fluoride over other halides.

For comparison, a fluorescence experiment with analog 2 was carried out under identical conditions, DMSO-AcCN (4:6,v/v), 5μ M analog 2 and the same ratio of halides from tetrabutylammonium salts. The intensity of fluorescence decreased with addition of

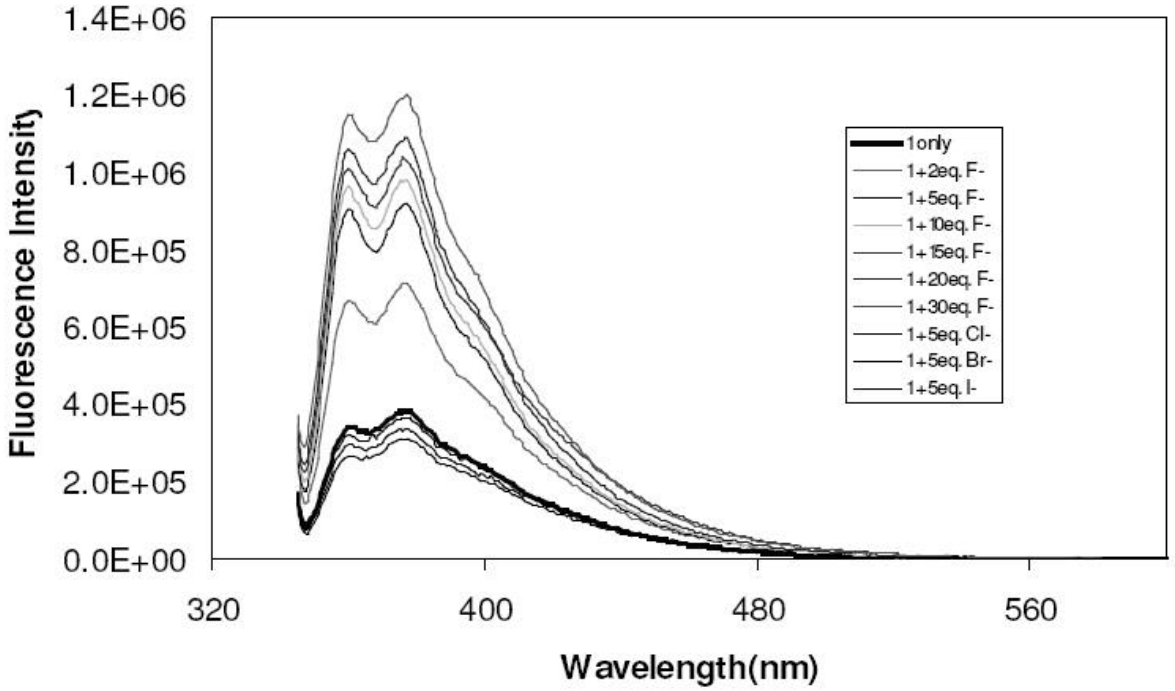

Figure 7.7. Fluorescent emission change of sensor 1 upon addition of halides. Solvent is DMSO-AcCN(4:6,v/v). The thick blue line is sensor 1 (5um) only. The lines above are with increment addition of fluoride and the three lines below are with 5eq. chloride, bromide and iodide, in order, respectively.

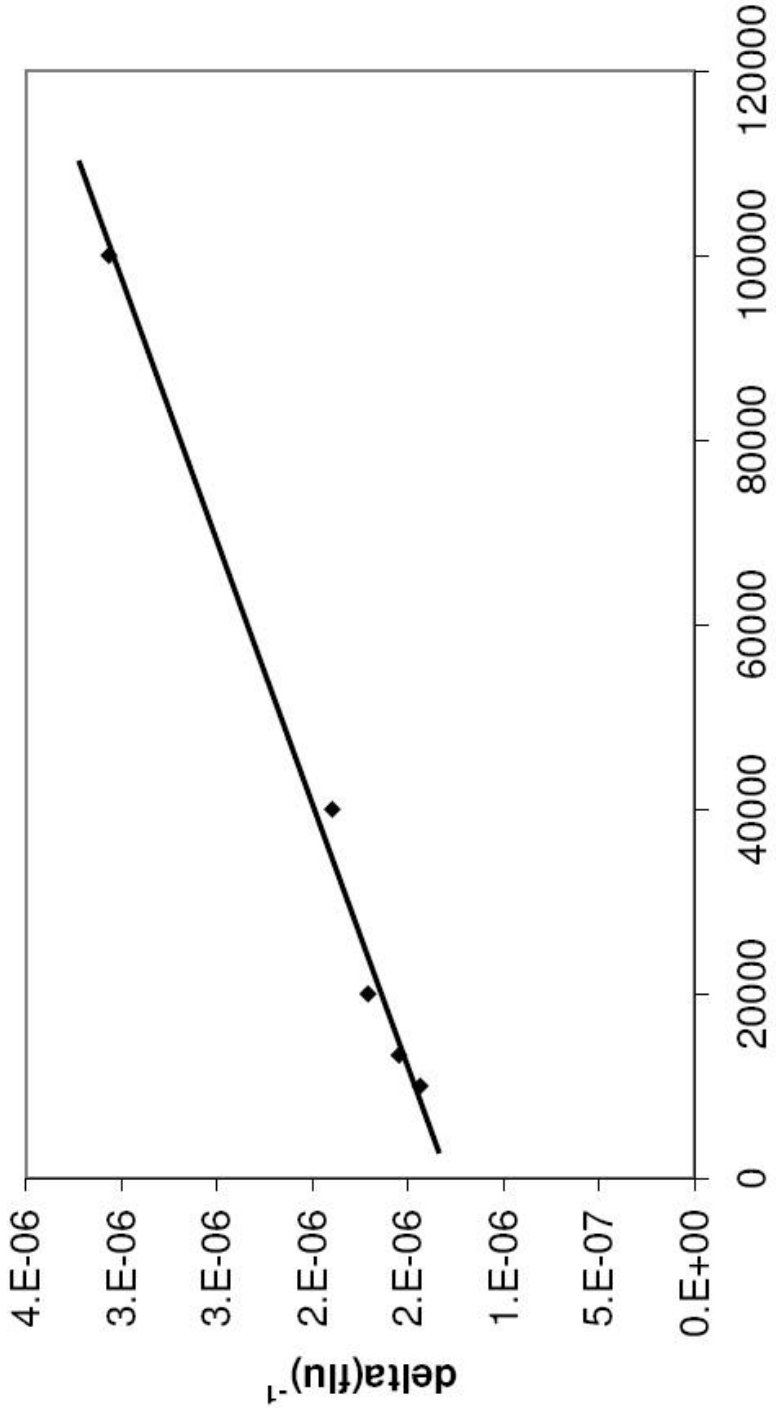

Figure 7.8, Binding constant (1:1 ratio) plot between sensor 1 and Fluoride.

all the halides, as shown in **Figure 7.9**. In addition, fluorescence experiments with 1,8-diaminonaphthalene were performed under identical conditions, shown in **Figure 7.10**.

Result and Discussion

As indicated by fluorescence experiments, sensor molecule **1**, 1,8-di(phenyl)ureaylnaphthalene, yields increased fluorescence intensity with addition of fluoride and decreased intensity with addition of other halides. Fluorescence experiments of 2,3-di(phenyl)ureaylnaphthalene (analog molecule **2**) and 1,8-diaminonaphthalene both indicate quenching effects with all the halides. These data indicate that two urea groups with the correct orientation are necessary for the selective interaction with fluoride.

With hydrogen bonding between fluoride and N-H in the urea groups, a three-ring structure, counting with the two aromatic rings from naphthalene, could be formed. Molecular modeling with Spartan (PC) [101], as illustrated in Fig. **7.11**, shows the space between two urea groups accommodates fluoride rather than the other three halides (chloride, bromide and iodide). While the fluoride ion formed a relatively planar complex with sensor molecule 1, the other halides did not result in formation of a planar species. Binding of fluoride to the sensor molecule resulted in increase fluorescence due to the greater planarity of the molecule when bound to fluoride. The lack of a significant shift in fluorescence spectra upon binding to fluoride suggests that the original fluorophore is intact but exhibits greater fluorescence emission.

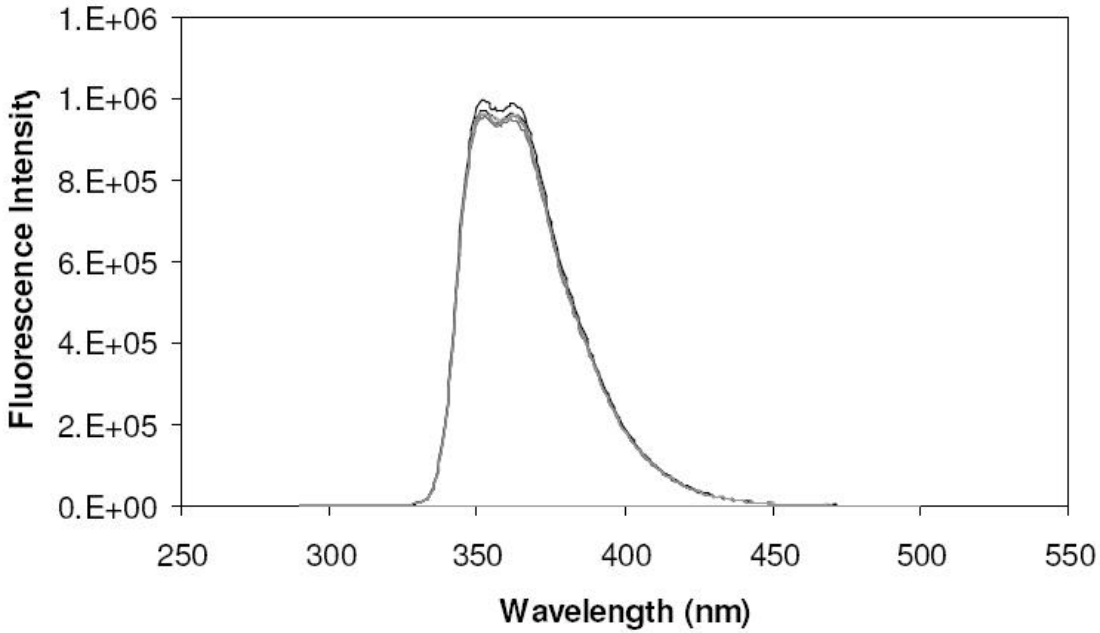

Figure 7.9, Fluorescence spectra of analog 2 upon addition of halides. Initial concentration of analog 2 is 5uM, halides' concentration is 25uM and all from tetrabutylammonium salts. The top spectrum is halide-free. The top second is the one with fluoride, the top third is the one with bromide and the bottom is the one with iodide. Ex=273nm.

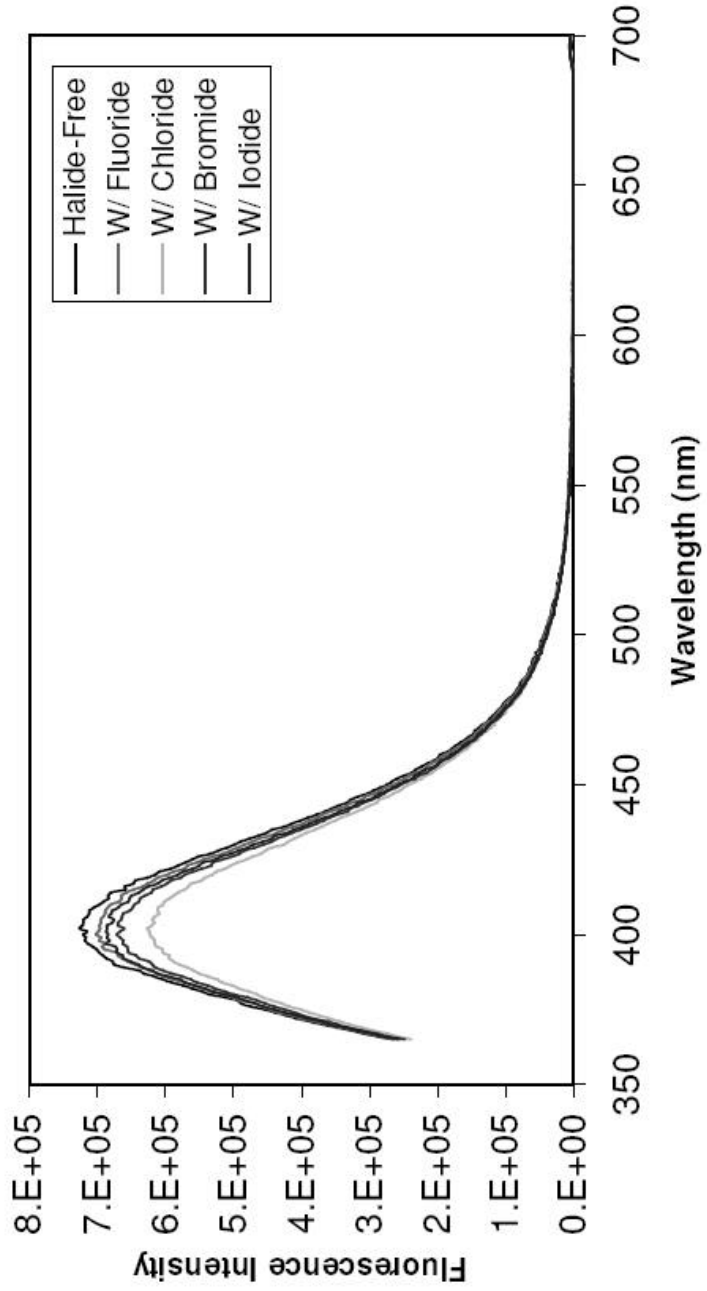

Figure 7.10, Fluorescence spectra of 1,8-diaminonaphthalene with addition of halides. Initial concentration of 1,8-diaminonaphthalene is 5um. The halides' concentration is 25uM. Excitation wavelength is 350nm.

Figure 7.11. Computer modeling on sensor molecule with SPARTAN

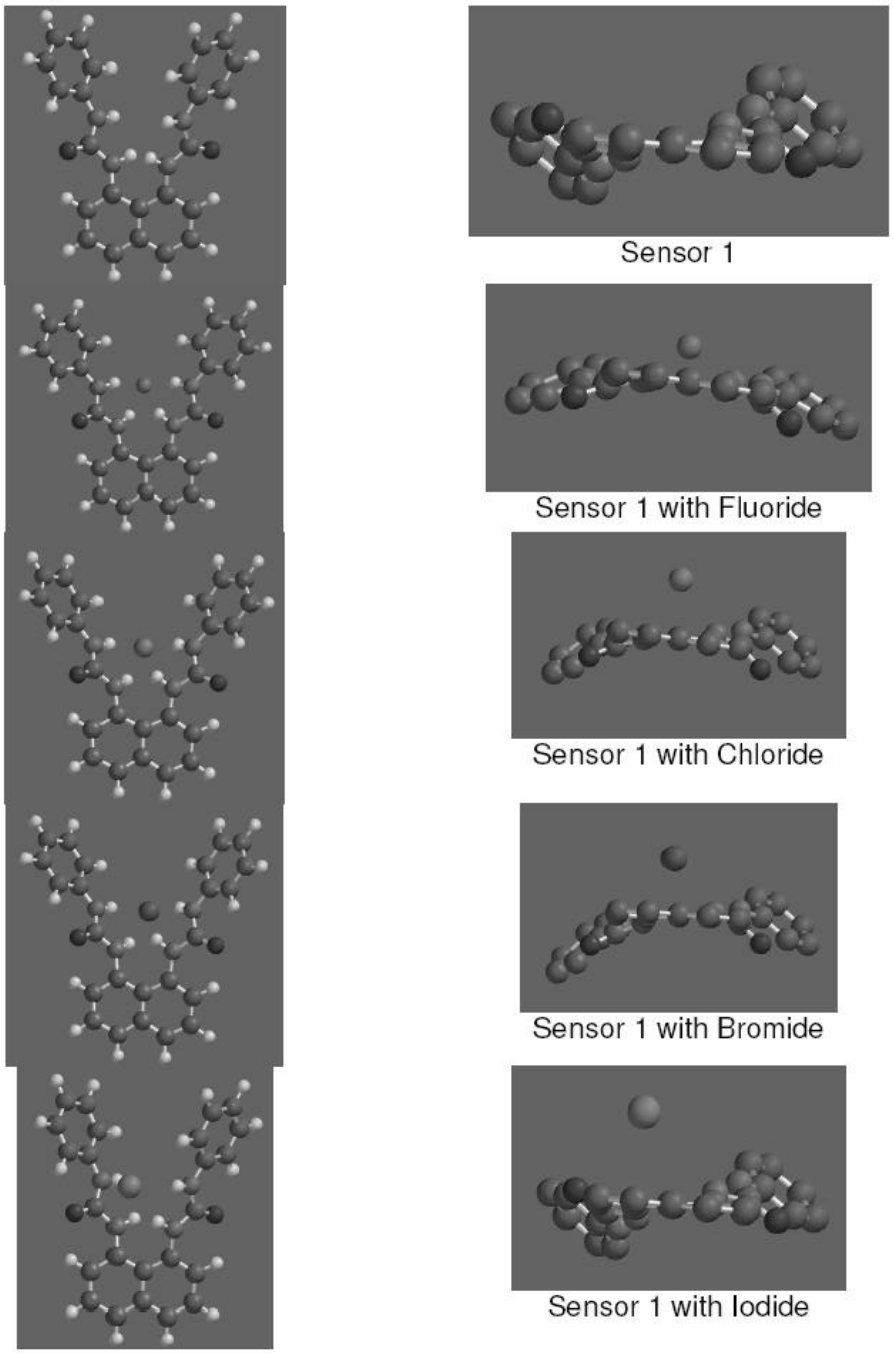

Since sensor 1 and analog 2 have the same functional groups, while the location of the two urea groups is different, the different behavior of these two molecules upon addition of fluoride must result from the different geometries of these molecules. For comparison, Spartan (PC) modeling on analog 2, 2,3-di(phenyl)ureaylnaphthalene, was carried out. As shown in **Fig. 7.12**, the space between two urea groups can accommodate all the halides. If the computer modeling effectively predicts stereochemistry, then a three-ring structure could be formed with 2,3-di(phenyl)ureaylnaphthalene also. While the computer modeling offers the structure with optimal energy minimization, it has little information on binding constant. However, the quenching effect of fluoride on 2,3-di(phenyl)ureaylnaphthalene could indicate that a three-ring structure might not be the direct reason why 1,8-di(phenyl)ureaylnaphthalene has signal enhancement upon addition of fluoride. However, the fluorescence spectra of analog 2 with halides shows only slight signal decreases, which indicates that the two phenylureayl groups are relatively rigid and the interaction between halides and the two urea groups is very weak. In cases of fluorescence cation sensing, almost all the cation sensors have increase signal. TICT, twisted internal charge-transfer, is used to explain that the complex no longer has this radiationless decay route that the initial sensor molecule has.

Further study to find out what factor(s) is/are dominant or even determinant is extremely desirable. The space between the two urea groups is surely critical in this case. It only accommodates fluoride rather than any other halides. The stereo-arrangement of the two benzene rings might play an important role. Recently an X-ray

Figure 7.12. Computer modeling on analog 2 with SPARTAN

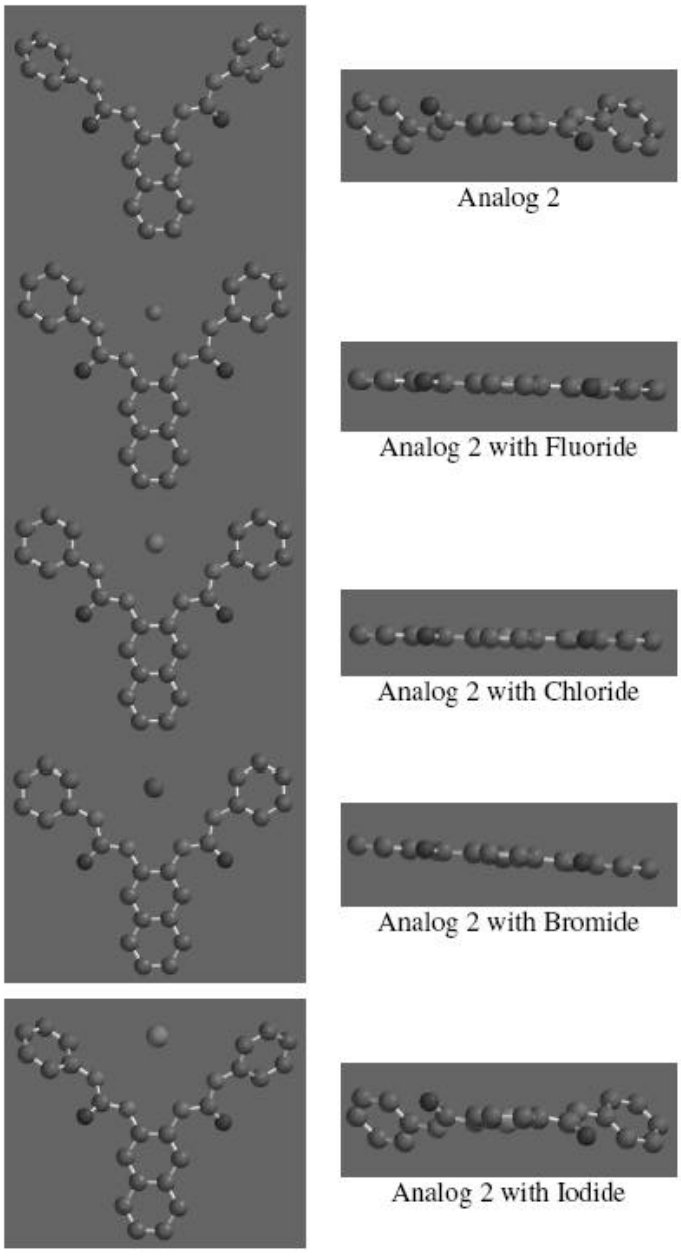

crystal structure of a fluoride-induced amide receptor was reported [102]. An X-ray crystal structure of sensor molecule 1 would be extremely desired. Study of these factors could lead to design of fluorescence-increasing sensor molecules for chloride, which is biological prevalent and important.

CONCLUSIONS

Phenoxyacetic acid second order reaction rate constants with hydroxyl radical are $(3.88 \pm 0.13) \times 10^9$ $M^{-1}s^{-1}$, $(3.62 \pm 0.10) \times 10^9$ $M^{-1}s^{-1}$, $(3.60 \pm 0.08) \times 10^9$ $M^{-1}s^{-1}$, and $(2.54 \pm 0.10) \times 10^9$ $M^{-1}s^{-1}$ for 2,4,5-T, 3,4-D, 2,4-D and 4-CPA respectively. The presence of HA and FA inhibits degradations and the inhibition is proportional to the amount of HA/FA applied and the hydrophobicity of the target pollutant. The expected inhibition of degradation calculated from binding constants and water/octanol partition coefficients are significantly lower than the experimental values, indicating the inhibition cannot be simply explained by binding to HA/FA. These phenomena were observed with other hydrophobic species, PAHs. The reasonable explanation of these observations is the physical isolation of Fe(II), the hydroxyl radical generation site, from the target species since Fe(II) is prone to bind to hydrophilic sites of HA/FA and pollutants are prone to bind to hydrophobic sites of HA/FA.

In contrast, CMßCD brings pollutants closer to Fe(II) by entrapping a pollutant into its cavity and chelating Fe(II) with its carbomethyl groups. Degradation enhancement is significant even with the presence of HA/FA in the system. Though the improvement is proportional to the amount of CMßCD added, the improvement could have upper limits since CMßCD acts a scavenger at the same time. Given the fact that

CMßCD can remove hydrophobic pollutants from contaminated sites, there is a potential to apply this approach to remediation in real systems. This potential was initially confirmed with degradation of PCBs in a simple water/sand two-phase system. However, the same success with PAHs has not been achieved. Further studies in the process of dissolution and mass balance are necessary for further improvement in two-phase systems.

A novel halide sensor (1,8-diphenylureaylnaphthalene), which performs with increasing fluorescence with fluoride and decreasing fluorescence with all other halides, was synthesized and reported. Studies using NMR and computer modeling with SPARTAN were carried out, including comparison with an analog molecule, 2,3-diphenylureaylnaphthalene. Both studies indicated that only fluoride can be accommodated in the space between the urea groups. Furthermore, fluoride strongly interacts with the protons of the urea groups. While the size between the two urea groups and the molecular rearrangement upon addition of halides could contribute to this novel phenomenon, further study such as X-ray crystallography would be beneficial. Additional development could lead to fluorescence-increasing sensor for chloride, which is biologically prevalent and important. Such a sensor would overcome limitations with current fluorescence-quenching anion sensors.

References

[1] Hutzinger, G.W. and Dixon, J.B., 1989, Sources and Emissions of PCDD and PCDF, Chemosphere, 18,23

[2] Thomas, J.M. and Ward, C. H., 1989, *In situ* Biorestoration of Organic Contaminants in the Subsurface. Environ. Sci. Technol. 23, 760

[3] Bigda, R., J. Chem. Eng. Prog., 1995, 91(12), 62-66

[4] Wardman, Peter; Candeias, L.P.; Radiat. Res., 1996, 145(5), 523-531

[5] Haber, F.; Weiss, J. Proceedings of the Royal Society, Series A, Mathematical and Physical Sciences, 1934, 147(861), 332-351

[6] Tomita, M.; Okuyama, T.; Watanabe, S.; Watanabe, H. Arch. Toxicol. 1994, 68, 428-433

[7] Haag, W.R.; Hoigne, J. Chemosphere 1985, 14, 1659-1671

[8] J. J. Pignatello, Environ. Sci. Technol. 1992, 26, 944 – 951

[9] Y. Sun and J.J. Pignattello, J. Agric. Food Chem., 40, 322-27(1992) & 41, 308-12(1993)

[10] Tedder, D.W. and Pohland, F. G., ACS Symposium Series, # 518, 1993, 343-356

[11] Croft, S.; Gillbert, C.; Smith J.R.L., Stell J.K. and Sanderson W.R. J. Chem. Soc. Perkin Trans. 2 153-160 (1992)

[12] Watts, R.J.; Udell, M.D. and Monsen R.M. Water Environ. Res. 65, 839-844 (1993)

[13] Vella, P.A. and Munder, J.A. Toxic Pollutant Destruction, In Emerging technologies in Hazardous Waste Management III. pp 85-105, ACS, Washington (1993)

[14] Lemley A.T. and Dowling K.C., J. Environ. Sci. Health, B30(5), 585-604, (1995)

[15] J. Phy. Chem. Ref. Data, 1988, Vol. 17, No. 2, pp513-886

[16] Klein, G. W.; Bhatia, K.; Madhavan, V.; Schuler, R. H. J. Phys. Chem. 1975, 79(17), 1767 – 1774

[17] Kakarla P. Watts R.J., . Environ. Eng., 2003, 307:215-229

[18] Araujo, E. etc. Appl. BioChem BioTechnol., 2002, 97:91-103

[19] Li Y.S.,Liu C.C. and Chern B.R., Bull. Environ. Contam. Toxicol., 1999, 62:336-343

[20] Geo-Cleanse International, Inc. Geo-Cleanse Treatment program. Pensacola, FL: Naval Air Station Pensacola, September 24, 1999

[21] Delle Site, Alessandro., J. Phys. Chem. Ref. Data (2001), 30(1), 187-439

[22] Moran, Mary Ann; Zepp, Richard G., Limnol. Oceanogr. (1997), 42(6), 1307-1316

[23] Vaughan, D.; Lumsdon, D.G.; Linehan, D.J., Chem. Ecol. (1993), 8(3), 185-201

[24] Chiou, C.T. et al. Environ. Sci. Technol. 1986, 20, 502-506

[25] Meredith, C. E.; Radosevich, M. J. Environ. Sci. Health Part B 1998, 33, 17-36

[26] Laor, Y.; Strom, P. F.; Farmer, W. J. J. Biotechnology 1996, 51, 227-234

[27] Humic Substances in the Suwannee River, Georgia: Interactions, Properties, and Processed Structures, U.S. Geo. Survey Water-Supply Paper 2373

[28] Biochemistry Laboratory, Dept. Of Soil, Water, and Climate, University of Minnesota, St. Paul, MN, USA. Values are presented on a moisture-free, ash-free basis, (1996)

[29] Chiou, C.T. et al., Environ. Sci. Technol. 1986, 20, 502-508

[30] James, W.J., French, D., Rundle, R.E., Act. Cyst. 12,385 (1959)

[31] Nickon; Silversmith The Name Game, Pergamon; Elmsford, NY, p 235

[32] Wojcik, J.F. and Rohrbach, R. P., J. Phy. Chem., 79, 2251, (1975)

[33] Cramer, F. Henglein, F.M., Angew. Chem. 68, 649 (1956)

[34] Thakkar, A.L., Demacro, P.V., J. Pharm. Sci., 60, 652(1971)

[35] Wood, D.J. et al, J. Amer. Chem. Soc., 99, 1935(1977)

[36] Otagiri, M. and Uekama, M. Chem. Pharm. Bull., 23, 188(1975)

[37] Blumer, M. 1976, Ploycyclic aromatic compounds in nature, Sci. Am., 234(3):35-45

[38] Harrison, R.M.,Perry, R. and Welling, R.A.; Water Res.,9,(1975) 331-346

[39] Edwards,N.T., J. Environ. Qual., 12 (1983) 427-441

[40] Bollag, J.M. and Kaiser, J.P., Crit. Rev. Environ. Control, 21, (1991) 297-329

[41] Zafiriou, O.C. et al. Environ. Sci. Technol. 18(1984) 358A-371A

[42] Pearlman, R.S. and Yalkowshy, S.H. J. Phys. Chem. Ref. Data, 13(2), 555-562

[43] WSSA, 1983; Farm Chemicals Handbook, 1990

[44] Farm Chem. Handbook, 1975, Meister Publishing Co. Willoughy OH

[45] McConnel, E.E., Moore, J.A. and Dalgard, D.W., Toxicol. Appl. Pharmocol. 43:175-187

[46] Hilerman, B., Chem. and Eng. News, Feb, 2002, pp25

[47] Polychlorinated Biphenyls: A Report, National Research Council. Committee on the Assessment of Polychlorina, National Academy Press; (June 1979)

[48] Deguchi, Y.; Dobashi, S.; Fukuda, N.; Shinoda, K.; Morita, M.; Environ. Sci. Technol.; 2003; 37(20); 4737-4742

[49] Hoekstra, P. F.; Wong, C. S.; O'Hara, T. M.; Solomon, K. R.; Mabury, S. A.; Muir, D. C. G.; Environ. Sci. Technol.; 2002; 36(7); 1419-1425; b) Jackson, L. J.; Carpenter, S. R.; Manchester-Neesvig, J.; Stow, C. A.; Environ. Sci. Technol.; 2001; 35(5); 856-

862; c) Chu, S.; Covaci, A.; Haraguchi, K.; Voorspoels, S.; Van de Vijver, K.; Das, K.; Bouquegneau, J.-M.; De Coen, W.; Blust, R.; Schepens, P.; Environ. Sci. Technol.; 2003; 37(20); 4573-4578

[50] Sather, P. J.; Ikonomou, M. G.; Addison, R. F.; He, T.; Ross, P. S.; Fowler, B.; Environ. Sci. Technol.; 2001; 35(24); 4874-4880; b) Ghosh, U.; Zimmerman, J. R.; Luthy, R. G.; Environ. Sci. Technol.; 2003; 37(10); 2209-2217

[51] Stow, C. A.; Lamon, E. C.; Qian, S. S.; Schrank, C. S.; Environ. Sci. Technol.; 2004; 38(2); 359-363

[52] Gutsche, C. David and Nam, Kye Chun, J. Am. Chem. Soc., 1988, 6153-6162; b) Hanna, T. A.; Liu, L.; Angeles-Boza, A. M.; Kou, X.; Gutsche, C. D.; Ejsmont, K.; Watson, W. H.; Zakharov, L. N.; Incarvito, C. D.; Rheingold, A. L.; J. Am. Chem. Soc.; 2003; 125(20); 6228-6238. c) Dilip V. Khasnis, Michael Lattman, C. David Gutsche; J. Am. Chem. Soc.; 1990; 112(25); 9422-9423

[53] Diamond, D.; McKervey, M.A., Chem. Soc. Rev. 1996, 15-24; Diamond, D.; Nolan, K., Anal. Chem. 2001, 73(1), 22-29A.

[54] Grady, T.; Harris, S.J.; Smyth, M.R.; Diamond, D., Anal. Chem. 1996, 68, 3775; b) Grady, T.; Joyce, T.; Smyth, M.R.; Harris, S.J.; Diamond, D., Anal. Comm. 1998, 35(4), 123-125

[55] Hutchinson, S.; Kearney, G.A.; Horne, E.; Lynch, B.; Glennon, J.D.; McKervey, M.A.; Harris, S.J., Anal. Chim. Acta 1994, 291(3), 269-75.

[56] Glennon, J.D.; Horne, E.; O'Connor, K.; Kearney, G.A.; Harris, S.J.; McKervey,M.A., Anal Proc. 1994, 31, 33

[57] C. David Gutsche, Lorenz J. Bauer; J. Am. Chem. Soc.; 1985; 107(21); 6052-6059; b) C. David Gutsche, Lorenz J. Bauer; J. Am. Chem. Soc.; 1985; 107(21); 6059-6063

[58] A. Soi, W. Bauer, H. Mauser, C. Moll, F. Hampel, A. Hirsch, J. Chem. Soc., Perkin Trans. II (1998) 1471.

[59] Christian, G.G. Analytical Chemistry, 5th Ed. Pp711-714, John Weily and Sons, New York(1994)

[60] X. Zhou and K. Mopper, Mar. Chem., 1990, 30, 71-78

[61] Lindsey, M.E. and Tarr, M.A., Chemosphere, 2000, 41, 409-417

[62] Holm Ellegehausen, Christian D'Hondt and Richard Fuerer, Pesti. Sci., 1981, 12, 219-227

[63] M.E. Lindsey, G. Xu, Jia Lu and M.A. Tarr, The Science of the Total Environment, 307 (2003), 215-229

[64] Brezonik, P. L.; Fulkerson-Brekken, J. Environ. Sci. Technol. 1998, 32, 3004-3010

[65] Voelker, B.M.; Suizberger, B. Environ. Sci. Technol., 1996, 30, 1106-1114

[66] Lindsey, M.; Tarr, M.A. Environ. Sci. Technol. 2000, 34, 444-449

[67] James, W.J., French, D. Rundle, R.E., Act. Cyst., 12, 385(1959)

[68] Chin, Y.P.; Aiken, G.R.; Danielsen, K.M. Environ. Sci. Technol. 1997, 31, 1630-1635; b) Chin. Y.P.; Gschwend, P.M. Environ. Sci. Technol. 1992, 26, 1621-1626

[69] Bender, Myron L.; Komiyama, M., Cyclodextrin Chemistry, 1978, Springer, Berlin, Ger.

[70] Chin, Y.P.; Gschwend, P.M.; Environ. Sci. Technol., 1992, 26, 1621-1626

[71] Davies, G.; Fataftah, A.; Cherkasskiy, A.; Ghabbour, E. A.; Radwan, A.; Jansen, S. A.; Kolla, S.; Pacoolla, M. D.; Sein, L. T.; Buermann, W.; Balasubramanian, M.;

Budnick, J.; Xing, B. J. Chem Soc., Dalton Trans. 1997, 4047-4060; b) Sein, L. T. Jr.; Varnum, J. M.; Jansen, S. A. Environ. Sci. Technol. 1999, 33, 546-552

[72] Sterling, Theodor D. Science (1971), 174(4016), 1358-9

[73] Almeida, Waldemar F. Toxicological aspects of the herbicides, 2,4-D and 2,4,5-T. Biologico (1974), 40(2), 44-51

[74] J. Yu, R.C. Flagan and J.H. Seinfeld, Environ. Sci. and Technol., 32(16), 2357-2370

[75] M. Ojala, T. Kotiaho, J. Siirila and M.L. Sihvonen, Talanta, 8, 1297-1309

[76] Cary T. Chiou, Ronald L Malcoim, Terry I. Brinton and Daniel E. Kile, Environ. Sci. Technol, 1986, 20, 502-508

[77] Li, Nanqin; Lee, Hian Kee Anal. Chem. (2000), 72(21), 5272-5279

[78] Hawthorne, Steven B. and Grabanski, Carol B. ,Environ. Sci. Technol. (2000), 34(20), 4348-4353

[79] Li, Nanqin; Lee, Hian Kee. Anal. Chem. (2000), 72(21)

[80] A. Munoz De La Pena, T. Ndou, J. B. Zung and I.M. Warner, J. Phys. Chem., 1991, 95, 3330-3334

[81] Hashmoto, S.; Thomas, J.K. J. Am. Chem. Soc., 1985, 107, 4662; Hamai, S.J., J. Phys. Chem., 1989, 93, 2074-2078

[82] Shixiang, Gao; Liansheng, Wang; Qingguo, Huang; Sukui, Han., Chemosphere (1998), 37(7), 1299-1305

[83] Evans, Christopher H.; Partyka, Morgan; Van Stam, Jan., J. Inclusion Phenom. Macrocyclic Chem. (2000), 38(1-4), 381-396; b) Avakyan, V. G.; Nazarov, V. B.; Alfimov, M. V.; Bagaturyants, A. A. Russ. Chem. Bull. (1999), 48(10), 1833-1844

[84] Mohseni, R.M. and Hurtubise, R.J., J. Chromatography, 1990, 499, 395-410

[85] Chin, Y.P. and Gschwend, P.W., Environ. Sci. Technol., 1992, 26(8),1621-1626

[86] Thompson, R.B., 1997, Advances in Fluorescence Sensing Technology III Proc. SPIE 1980. b) UndenFriend, S., 1969, Fluorecence Assay In Biology and medicine, Vol. II, Academics Press, New York.

[87] (a) P. D. Gale, Angew. Chem., Int. Ed., 2001, 40, 486; (b) F. P. Schmidtchen and M. Berger, Chem. Rev., 1997, 97, 1609; (c) T. S. Snowden and E. V. Anslyn, Chem. Biol., 1999, 3, 740

[88] L. Fabbrizzi, H. Faravelli, G. Franzese, M. Licchelli, A. Perotti and A. Taglietti, Chem. Commun., 1998, 971–972; b) Kieslinger, D., Draxler, S., Trznadel, K. and Lippitsch,M.E., 1997, Sensors Actuators B, 38-39:300-304; c) H. Miyaji, P. Anzenbacher, Jr, J. Sessler, E. R. Bleasdale and P. A. Gale, Chem. Commun., 1999, 1723–1724; d) P. Anzenbacher, Jr., K. Jursikova and J. L. Sessler, J. Am. Chem. Soc., 2000, 122, 9350–9351

[89] Lakowwicz,J.R., 1995, Fluorescence Spectroscopy of Biomeolecules, VCH Publishers, New York, pp 294-306

[90] Haugland, R.P., 1996, Handbook of Fluorescent Probes and Research Chemicals, Molecular Probes, Inc., Eugene, Oregon

[91] Weber,G., 1951, Biochem. J., 51:155-167

[92] a) Kautsky, H., 1939, Trans. Faraday Soc. 35:216-219; b) Knibbe, H., Rehm, D., and Weller, A., 1968, Ber. Bunsenges, Phys. Chem., 72:257-263; c) Eftink, M.R. and Ghiron, C., 1981, Anal. Biochem. 114:199-227; d) Eftink, M.R., 1991, Fluorescence

Quenching: Theory and Application, in Topics in Fluorescence Spectroscopy, Vol.,2, Principles, J.R. Lakowicz(ed.), Plenum Press, New York, pp 53-126

[93] Eftink, M.R. and Ghiron, C.A., 1976, J. Phys. Chem., 80:486-493

[94] Lakowicz, J.R. and Weber, G., 1973, Biochem., 12:4161-4170

[95] Forster, Th., 1948, Ann. Phys. 2:55-75; b) Stryer, L., 1978, Annu. Rev. Biochem., 47:819-846; c) Clegg, R.M., 1996, Fluorescence Resonance Energy Transfer, in Fluorescence Imaging Spectroscopy and Microscopy, X.F. Wang and B. Herman (ed.), John Wiley and Sons, New York, pp 179-252

[96] Bacon, J.R. and Demas, J.N., 1987, Anal. Chem., 59:2780-2785; b) Wolfbeis,O.S., 1991, Oxygen Sensors, in Fiber Optic Chemical Sensors and Biosensors, Vol. II, O.S. Wolfbeis(ed.), CRC Press, Boca Raton, Florida, pp 19-53

[97] Biwersi, J., Tulk, B. and Verkman, A.S., 1994, Anal. Biochem., 219:139-143; b) Illsley, N.P. and Verkman,A.S., 1987, Biochem. 26:1215-1219; c) Verkman, A.S., Sellers, M.C., Chao, A.C., Leung,T. and Ketcham, R., 1989, Anal. Biochem., 178:355-361

[98] Trace Element in Medicine, Vol. 11, No. 3(1994) 104-108

[99] a) Hoston, M.E., Akkaya, E.U. and Czarnik, A.W., 1989, J. Am. Chem. Soc., 111:8735-8737; b) Pederson, C. J., 1967, J. Am. Chem. Soc. 89:7017-7036; c) Pederson, C. J., 1988, Science, 241:536-540; d) Crossley, R., Goolamali, Z., and Sammes, P.G., 1994, J. Chem. Soc., Perkin Trans., 1994, 1615-1623; e) Minta, A. and Tsien, R. Y., 1989, J. Biol., Chem. 264:19449-19457

[100] Rettig, W. and Lapouyade, R. 1994, Fluorescence probes based on twisted intramolecule charge transfer (TICT) states and other adiabatic photoreactions, in

Topics in Fluorescence Spectroscopy, Vol. 4, Probe Design and Chemical Sensing, J.R. Lakowicz, etc, Plenum Press, New York, pp109-149

[101] PC Spartan Plus, User's Guide (2nd version), Wavefunction, Inc., 1999.

[102] Simon J. Coles, etc.; Chem. Comm. 2003, 568-569

VITA

The author, Guoxiang Xu, was born in DongYang, Zhejing, China in February 1976. He grew up and spent most time at his southern hometown until he joined Nankai University, TianJin, China, where he got first cultivation in Chemistry and research and his B.S. in Chemistry. Later he continued study there until he joined University of New Orleans to pursue further study in Chemistry. He joined M.A. Tarr's group and mainly worked on environment-related analysis.